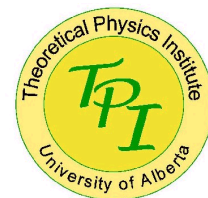


Phys XXX: Superconductivity March 2013
University of Camerino

Superconductivity and Strongly Correlated Electrons

F. Marsiglio

fm3@ualberta.ca



PACS (Physics and Astronomy Classification Scheme)

- 10**—The Physics of Elementary Particles and Fields
- 20**—Nuclear Physics
- 30**—Atomic and Molecular Physics
- 40**—Electromagnetism, Optics, Acoustics, Heat Transfer, Classical Mechanics, and Fluid Dynamics
- 50**—Physics of Gases, Plasmas, and Electric Discharges
- 60**—Condensed Matter: Structural, Mechanical and Thermal Properties
- 70**—Condensed Matter: Electronic Structure, Electrical, Magnetic, and Optical Properties
- 80**—Interdisciplinary Physics and Related Areas of Science and Technology
- 90**—Geophysics, Astronomy, and Astrophysics

PACS (Physics and Astronomy Classification Scheme)

- 10**—The Physics of Elementary Particles and Fields
- 20**—Nuclear Physics
- 30**—Atomic and Molecular Physics
- 40**—Electromagnetism, Optics, Acoustics, Heat Transfer, Classical Mechanics, and Fluid Dynamics
- 50**—Physics of Gases, Plasmas, and Electric Discharges
- 60**—Condensed Matter: Structural, Mechanical and Thermal Properties
- 70**—Condensed Matter: Electronic Structure, Electrical, Magnetic, and Optical Properties
- 80**—Interdisciplinary Physics and Related Areas of Science and Technology
- 90**—Geophysics, Astronomy, and Astrophysics

60—Condensed Matter: Structural, Mechanical and Thermal Properties

[61. Structure of solids and liquids; crystallography](#)

[62. Mechanical and acoustical properties of condensed matter](#)

[63. Lattice dynamics](#)

[64. Equations of state, phase equilibria, and phase transitions](#)

[65. Thermal properties of condensed matter](#)

[66. Nonelectronic transport properties of condensed matter](#)

[67. Quantum fluids and solids](#)

[68. Surfaces and interfaces; thin films and nanosystems \(structure and nonelectronic properties\)](#)

70—Condensed Matter: Electronic Structure, Electrical, Magnetic, and Optical Properties

[71. Electronic structure of bulk materials](#)

[72. Electronic transport in condensed matter](#)

[73. Electronic structure and electrical properties of surfaces, interfaces, thin films, and low-dimensional structures](#)

[74. Superconductivity](#)

[75. Magnetic properties and materials](#)

[76. Magnetic resonances and relaxations in condensed matter, Mössbauer effect](#)

[77. Dielectrics, piezoelectrics, and ferroelectrics and their properties](#)

[78. Optical properties, condensed-matter spectroscopy and other interactions of radiation and particles with condensed matter](#)

[79. Electron and ion emission by liquids and solids; impact phenomena](#)

74. Superconductivity (*for superconducting devices, see 85.25.-j*)

74.10.+v Occurrence, potential candidates

74.20.-z Theories and models of superconducting state

74.20.De Phenomenological theories (two-fluid, Ginzburg-Landau, etc.)

74.20.Fg BCS theory and its development

74.20.Mn Nonconventional mechanisms

74.20.Pq Electronic structure calculations (*for methods of electronic structure calculations, see 71.15.-m*)

74.20.Rp Pairing symmetries (other than s-wave)

74.25.-q Properties of superconductors

74.25.Bt Thermodynamic properties

74.25.Dw Superconductivity phase diagrams

74.25.F- Transport properties

74.25.fc *Electric and thermal conductivity*

74.25.fg *Thermoelectric effects*

74.25.Gz Optical properties

74.25.Ha Magnetic properties including vortex structures and related phenomena (*for vortices, magnetic bubbles, and magnetic domain structure, see 75.70.Kw*)

74.25.Jb Electronic structure (photoemission, etc.)

74.25.Kc Phonons

74.25.Ld Mechanical and acoustical properties, elasticity, and ultrasonic attenuation (*see also 43.35.Cg Ultrasonic velocity, dispersion, scattering, diffraction, and attenuation in solids; elastic constants—in Acoustics Appendix*)

74.25.N- Response to electromagnetic fields

74.25.nd *Raman and optical spectroscopy*

74.25.nj *Nuclear magnetic resonance*

74.25.nn *Surface impedance*

74.25.Op Mixed states, critical fields, and surface sheaths

74.25.Sv Critical currents

74.25.Uv Vortex phases (includes vortex lattices, vortex liquids, and vortex glasses)

74.25.Wx Vortex pinning (includes mechanisms and flux creep)

74.40.-n Fluctuation phenomena

74.40.De Noise and chaos (*see also 05.45.-a Nonlinear dynamics and chaos; for noise in general studies of fluctuation phenomena, see 05.40.Ca*)

74.40.Gh Nonequilibrium superconductivity

74.40.Kb Quantum critical phenomena

74.45.+c Proximity effects; Andreev reflection; SN and SNS junctions

74.50.+r Tunneling phenomena; Josephson effects (*for SQUIDs, see 85.25.Dq; for Josephson devices, see 85.25.Cp; for Josephson junction arrays, see 74.81.Fa*)

74.55.+v Tunneling phenomena: single particle tunneling and STM

74.62.-c Transition temperature variations, phase diagrams

74.62.Bf Effects of material synthesis, crystal structure, and chemical composition (*for methods of materials synthesis, see 81.20.-n*)

74.62.Dh Effects of crystal defects, doping and substitution (*for specific crystal defects, see 61.72.-y*)

74.62.En Effects of disorder

74.62.Fj Effects of pressure

74.62.Yb Other effects

74.70.-b Superconducting materials other than cuprates (*for cuprates, see 74.72.-h; for superconducting films, see 74.78.-w*)

74.70.Ad Metals; alloys and binary compounds (including Al₅, MgB₂, etc.)

74.70.Dd Ternary, quaternary, and multinary compounds (including Chevrel phases, borocarbides, etc.)

74.70.Kn Organic superconductors

74.70.Pq Ruthenates

74.70.Tx Heavy-fermion superconductors (*for heavy-fermion systems in magnetically ordered materials, see 75.30.Mb; see also 71.27.+a Strongly correlated electron systems, heavy fermions*)

74.70.Wz Carbon-based superconductors

74.70.Xa Pnictides and chalcogenides

74.72.-h Cuprate superconductors

74.72.Cj Insulating parent compounds

74.72.Ek Electron-doped

74.72.Gh Hole-doped

74.72.Kf Pseudogap regime

74.78.-w Superconducting films and low-dimensional structures

74.78.Fk Multilayers, superlattices, heterostructures

74.78.Na Mesoscopic and nanoscale systems

74.81.-g Inhomogeneous superconductors and superconducting systems, including electronic inhomogeneities

74.81.Bd Granular, melt-textured, amorphous, and composite superconductors

74.81.Fa Josephson junction arrays and wire networks (*see also 85.25.Cp Josephson devices*)

74.90.+n Other topics in superconductivity (restricted to new topics in section 74)

The basic elements

PERIODIC TABLE OF THE ELEMENTS

<http://www.ktf-split.hr/periodni/en/>

PERIODIC TABLE OF THE ELEMENTS

<http://www.ktf-split.hr/periodni/en/>

GROUP	1	2											13	14	15	16	17	18		
	IA	IIA											IIIA	IVA	VA	VIA	VIIA	VIIIA		
PERIOD	1	2											3	4	5	6	7	8	9	10
1	1 1.0079 H HYDROGEN												5 10.811 B BORON	6 12.011 C CARBON	7 14.007 N NITROGEN	8 15.999 O OXYGEN	9 18.998 F FLUORINE	10 20.180 Ne NEON		
2	3 6.941 Li LITHIUM	4 9.0122 Be BERYLLIUM																		
3	11 22.990 Na SODIUM	12 24.305 Mg MAGNESIUM																		
4	19 39.098 K POTASSIUM	20 40.078 Ca CALCIUM	21 44.956 Sc SCANDIUM	22 47.867 Ti TITANIUM	23 50.942 V VANADIUM	24 51.996 Cr CHROMIUM	25 54.938 Mn MANGANESE	26 55.845 Fe IRON	27 58.933 Co COBALT	28 58.693 Ni NICKEL	29 63.546 Cu COPPER	30 65.39 Zn ZINC	31 69.723 Ga GALLIUM	32 72.64 Ge GERMANIUM	33 74.922 As ARSENIC	34 78.96 Se SELENIUM	35 79.904 Br BROMINE	36 83.80 Kr KRYPTON		
5	37 85.468 Rb RUBIDIUM	38 87.62 Sr STRONTIUM	39 88.906 Y YTTRIUM	40 91.224 Zr ZIRCONIUM	41 92.906 Nb NIOBIUM	42 95.94 Mo MOLYBDENUM	43 (98) Tc TECHNETIUM	44 101.07 Ru RUTHENIUM	45 102.91 Rh RHODIUM	46 106.42 Pd PALLADIUM	47 107.87 Ag SILVER	48 112.41 Cd CADMIUM	49 114.82 In INDIUM	50 118.71 Sn TIN	51 121.76 Sb ANTIMONY	52 127.60 Te TELLURIUM	53 126.90 I IODINE	54 131.29 Xe XENON		
6	55 132.91 Cs CAESIUM	56 137.33 Ba BARIUM	57-71 La-Lu Lanthanide	72 178.49 Hf HAFNIUM	73 180.95 Ta TANTALUM	74 183.84 W TUNGSTEN	75 186.21 Re RHENIUM	76 190.23 Os OSMIUM	77 192.22 Ir IRIDIUM	78 195.08 Pt PLATINUM	79 196.97 Au GOLD	80 200.59 Hg MERCURY	81 204.38 Tl THALLIUM	82 207.2 Pb LEAD	83 208.98 Bi BISMUTH	84 (209) Po POLONIUM	85 (210) At ASTATINE	86 (222) Rn RADON		
7	87 (223) Fr FRANCIUM	88 (226) Ra RADIUM	89-103 Ac-Lr Actinide	104 (261) Rf RUTHERFORDIUM	105 (262) Db DUBNIUM	106 (266) Sg SEABORGIUM	107 (264) Bh BOHRIUM	108 (277) Hs HASSIUM	109 (268) Mt MEITNERIUM	110 (281) Uun UNUNNIUM	111 (272) Uuu UNUNUNIUM	112 (285) Uub UNUNBIUM		114 (289) Uuq UNUNQUADIUM						

RELATIVE ATOMIC MASS (1)

GROUP IUPAC

GROUP CAS

ATOMIC NUMBER

SYMBOL

ELEMENT NAME

Metal

Semimetal

Nonmetal

1 Alkali metal

2 Alkaline earth metal

Transition metals

Lanthanide

Actinide

16 Chalcogens element

17 Halogens element

18 Noble gas

STANDARD STATE (25 °C; 101 kPa)

Ne - gas

Ga - liquid

Fe - solid

Tc - synthetic

LANTHANIDE

57 138.91 La LANTHANUM	58 140.12 Ce CERIUM	59 140.91 Pr PRASEODYMIUM	60 144.24 Nd NEODYMIUM	61 (145) Pm PROMETHIUM	62 150.36 Sm SAMARIUM	63 151.96 Eu EUROPIUM	64 157.25 Gd GADOLINIUM	65 158.93 Tb TERBIUM	66 162.50 Dy DYSPROSIUM	67 164.93 Ho HOLMIUM	68 167.26 Er ERBIUM	69 168.93 Tm THULIUM	70 173.04 Yb YTTERBIUM	71 174.97 Lu LUTETIUM
-------------------------------------	----------------------------------	--	-------------------------------------	-------------------------------------	------------------------------------	------------------------------------	--------------------------------------	-----------------------------------	--------------------------------------	-----------------------------------	----------------------------------	-----------------------------------	-------------------------------------	------------------------------------

ACTINIDE

89 (227) Ac ACTINIUM	90 232.04 Th THORIUM	91 231.04 Pa PROTACTINIUM	92 238.03 U URANIUM	93 (237) Np NEPTUNIUM	94 (244) Pu PLUTONIUM	95 (243) Am AMERICIUM	96 (247) Cm CURIUM	97 (247) Bk BERKELIUM	98 (251) Cf CALIFORNIUM	99 (252) Es EINSTEINIUM	100 (257) Fm FERMIUM	101 (258) Md MENDELEVIUM	102 (259) No NOBELIUM	103 (262) Lr LAWRENCIUM
-----------------------------------	-----------------------------------	--	----------------------------------	------------------------------------	------------------------------------	------------------------------------	---------------------------------	------------------------------------	--------------------------------------	--------------------------------------	-----------------------------------	---------------------------------------	------------------------------------	--------------------------------------

(1) Pure Appl. Chem., 73, No. 4, 667-683 (2001)

Relative atomic mass is shown with five significant figures. For elements having no stable nuclides, the value enclosed in brackets indicates the mass number of the longest-lived isotope of the element.

However three such elements (Th, Pa, and U) do have a characteristic terrestrial isotopic composition, and for these an atomic weight is tabulated.

Editor: Aditya Vardhan (adivar@netlinx.com)

Copyright © 1998-2003 EniG. (eni@ktf-split.hr)

Periodic Table of Superconductivity

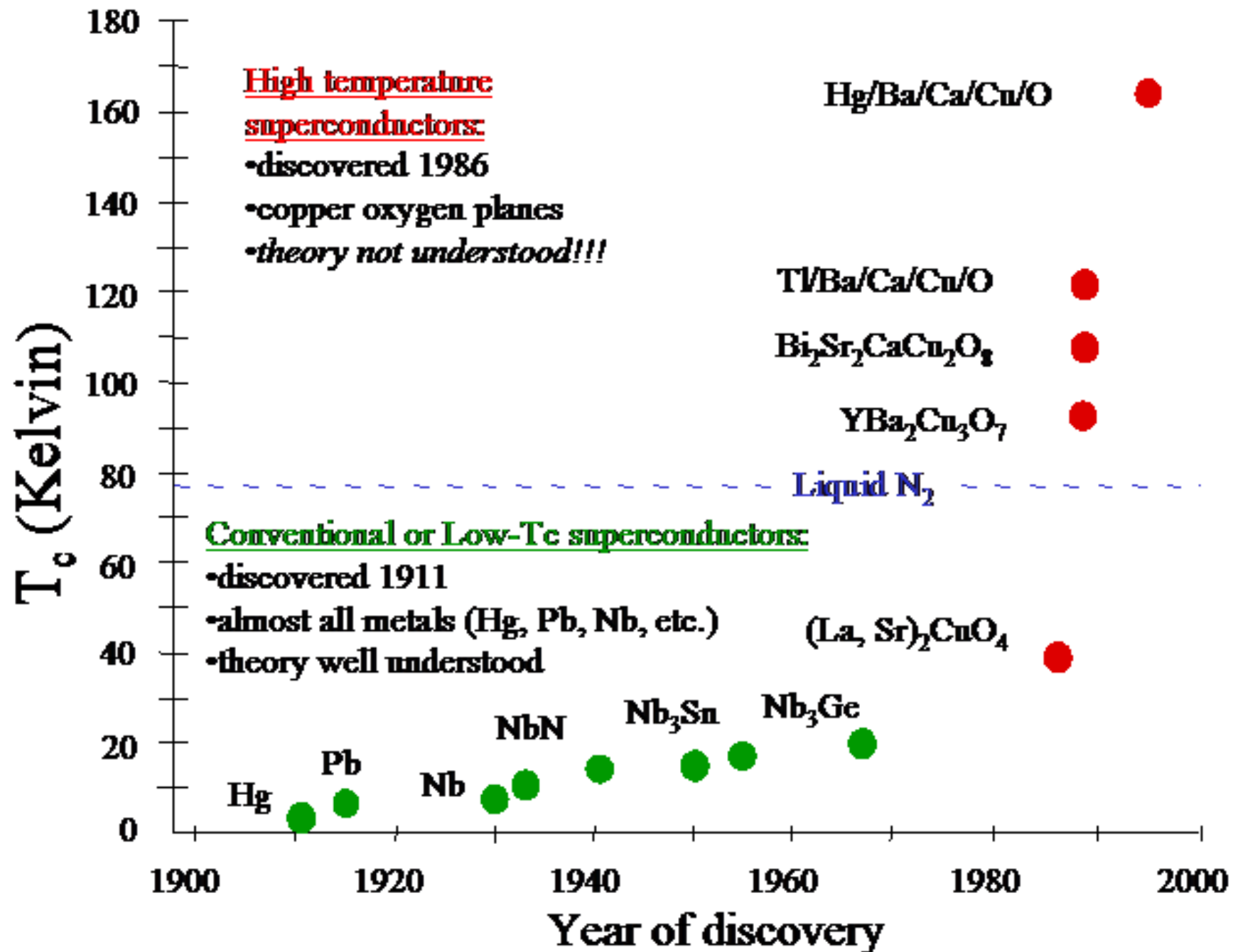
(dedicated to the memory of Bernd Matthias)

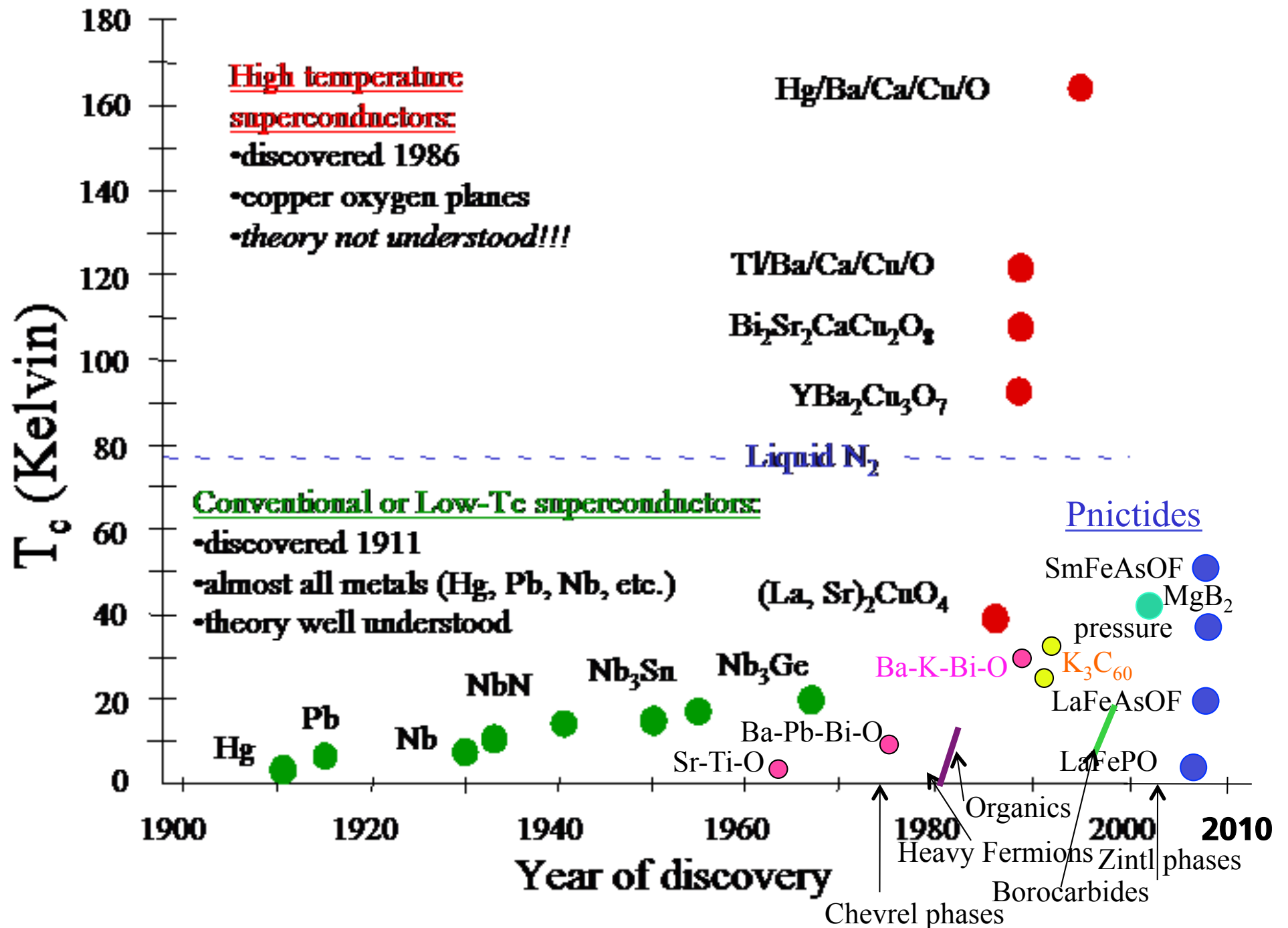
30 elements superconduct at ambient pressure, 23 more superconduct at high pressure.

H		ambient pressure superconductor										high pressure superconductor					He			
<div>Li0.0004 14 30</div>		<div>Be0.026</div>		<div>T_c(K) T_c^{max}(K) P(GPa)</div>					<div>T_c^{max}(K) P(GPa)</div>					<div>B11 250</div>		C	N	<div>O0.6 100</div>	F	Ne
Na		Mg																	Ar	
K		<div>Ca25 161</div>	<div>Sc19.6 106</div>	<div>Ti0.39 3.35 56.0</div>	<div>V5.38 16.5 120</div>	Cr	Mn	<div>Fe2.1 21</div>	Co	Ni	Cu	<div>Zn0.875</div>	<div>Ga1.091 7 1.4</div>	<div>Ge5.35 11.5</div>	<div>As2.4 32</div>	<div>Se8 150</div>	<div>Br1.4 100</div>	Kr		
Rb		<div>Sr7 50</div>	<div>Y19.5 115</div>	<div>Zr0.546 11 30</div>	<div>Nb9.50 9.9 10</div>	<div>Mo0.92</div>	<div>Tc7.77</div>	<div>Ru0.51</div>	<div>Rh.00033</div>	Pd	Ag	<div>Cd0.56</div>	<div>In3.404</div>	<div>Sn3.722 5.3 11.3</div>	<div>Sb3.9 25</div>	<div>Te7.5 35</div>	<div>I1.2 25</div>	Xe		
Cs		<div>Ba5 18</div>	<div>insert La-Lu</div>	<div>Hf0.12 8.6 62</div>	<div>Ta4.483 4.5 43</div>	<div>W0.012</div>	<div>Re1.4</div>	<div>Os0.655</div>	<div>Ir0.14</div>	Pt	Au	<div>Hg-α4.153</div>	<div>Tl2.39</div>	<div>Pb7.193</div>	<div>Bi8.5 9.1</div>	Po	At	Rn		
Fr		Ra	<div>insert Ac-Lr</div>	Rf	Ha															
		<div>La-fcc6.00 13 15</div>	<div>Ce1.7 5</div>	Pr	Nd	Pm	Sm	<div>Eu2.75 142</div>	Gd	Tb	Dy	Ho	Er	Tm	Yb	<div>Lu12.4 174</div>				
		Ac	<div>Th1.368</div>	<div>Pa1.4</div>	<div>U0.8(β) 2.4(α) 1.2</div>	Np	Pu	<div>Am0.79 2.2 6</div>	Cm	Bk	Cf	Es	Fm	Md	No	Lr				

N.W. Ashcroft, Nature
News and Views, 2002

H 1																	He 2	
Li 3	Be 4											B 5	C 6	N 7	O 8	F 9	Ne 10	
Na 11	Mg 12											Al 13	Si 14	P 15	S 16	Cl 17	Ar 18	
K 19	Ca 20	Sc 21	Ti 22	V 23	Cr 24	Mn 25	Fe 26	Co 27	Ni 28	Cu 29	Zn 30	Ga 31	Ge 32	As 33	Se 34	Br 35	Kr 36	
Rb 37	Sr 38	Y 39	Zr 40	Nb 41	Mo 42	Tc 43	Ru 44	Rh 45	Pd 46	Ag 47	Cd 48	In 49	Sn 50	Sb 51	Te 52	I 53	Xe 54	
Cs 55	Ba 56	La 57	Hf 72	Ta 73	W 74	Re 75	Os 76	Ir 77	Pt 78	Au 79	Hg 80	Tl 81	Pb 82	Bi 83	Po 84	At 85	Rn 86	
Fr 87	Ra 88	Ac 89	Ru 104	Ha 105	Unh 106	Uns 107	Uno 108	Une 109										
			Ce 58	Pr 59	Nd 60	Pm 61	Sm 62	Eu 63	Gd 64	Tb 65	Dy 66	Ho 67	Er 68	Tm 68	Yb 70	Lu 71		
			Th 90	Pa 91	U 92	Np 93	Pu 94	Am 95	Cm 96	Bk 97	Cf 98	Es 99	Fm 100	Md 101	No 102	Lr 103		



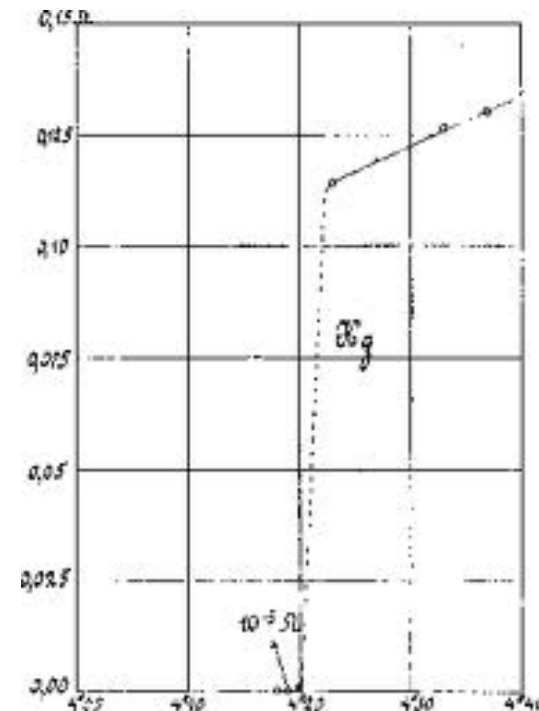


Superconductivity

Kamerlingh Onnes, H.,
"The Superconductivity of Mercury."
Comm. Phys. Lab. Univ. Leiden; Nos.
122 and 124, 1911.

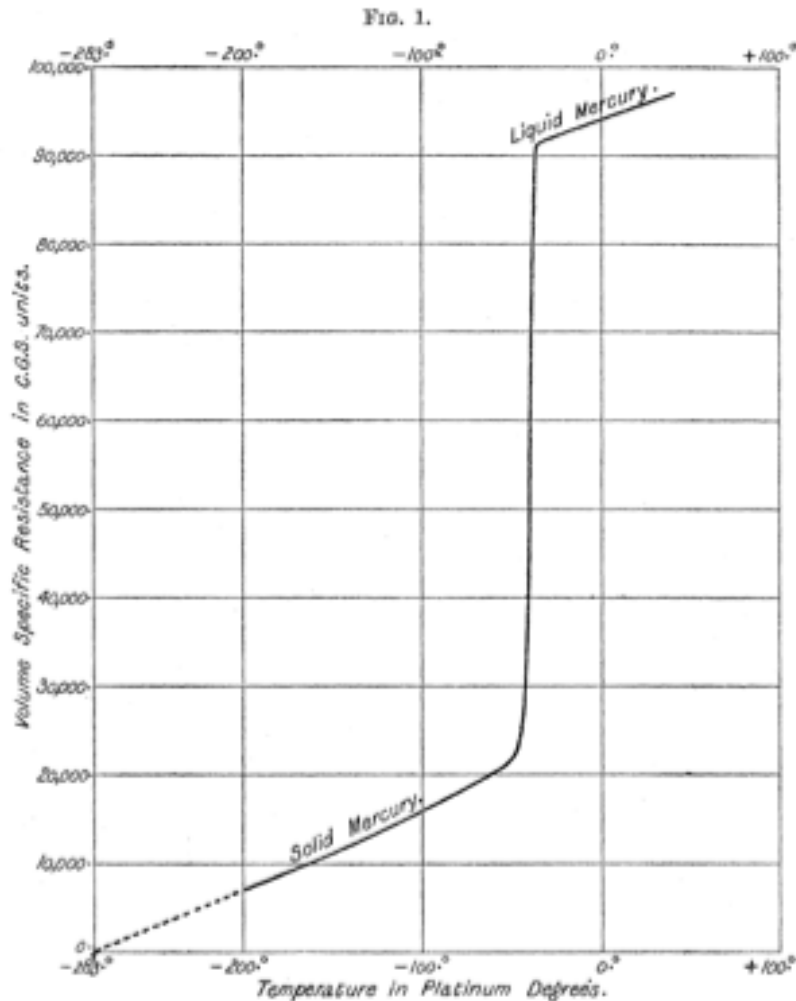


Heike Kamerlingh Onnes



Superconductivity

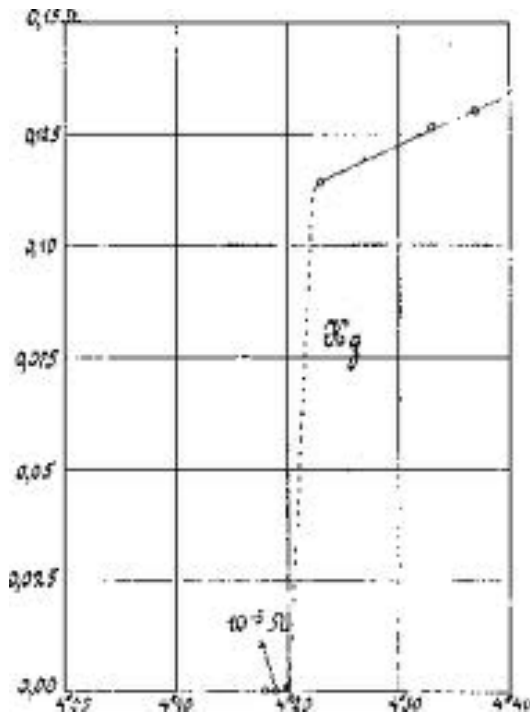
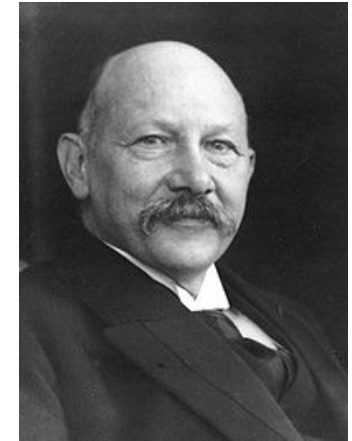
On the Electrical Resistivity of Pure Mercury at the Temperature of Liquid Air James Dewar and J. A. Fleming



Proceedings of the Royal Society of London,
Vol. 60 (1896 – 1897), pp. 76-81

...but, Lord Kelvin....

Aside: **Gilles Holst**, the student



- Really the discoverer of superconductivity
- Founding director of Philips labs in Netherlands
 - Holst Memorial Lectures, started 1977
- Acknowledged by Kamerlingh-Onnes in papers, and in a letter for membership in Royal Dutch Academy

“As a research director at Philips, according to Casimir, Holst would never insist on being coauthor, let alone sole author of papers based essentially on the work of others.”

As quoted from Casimir, in Dahl: *Superconductivity*

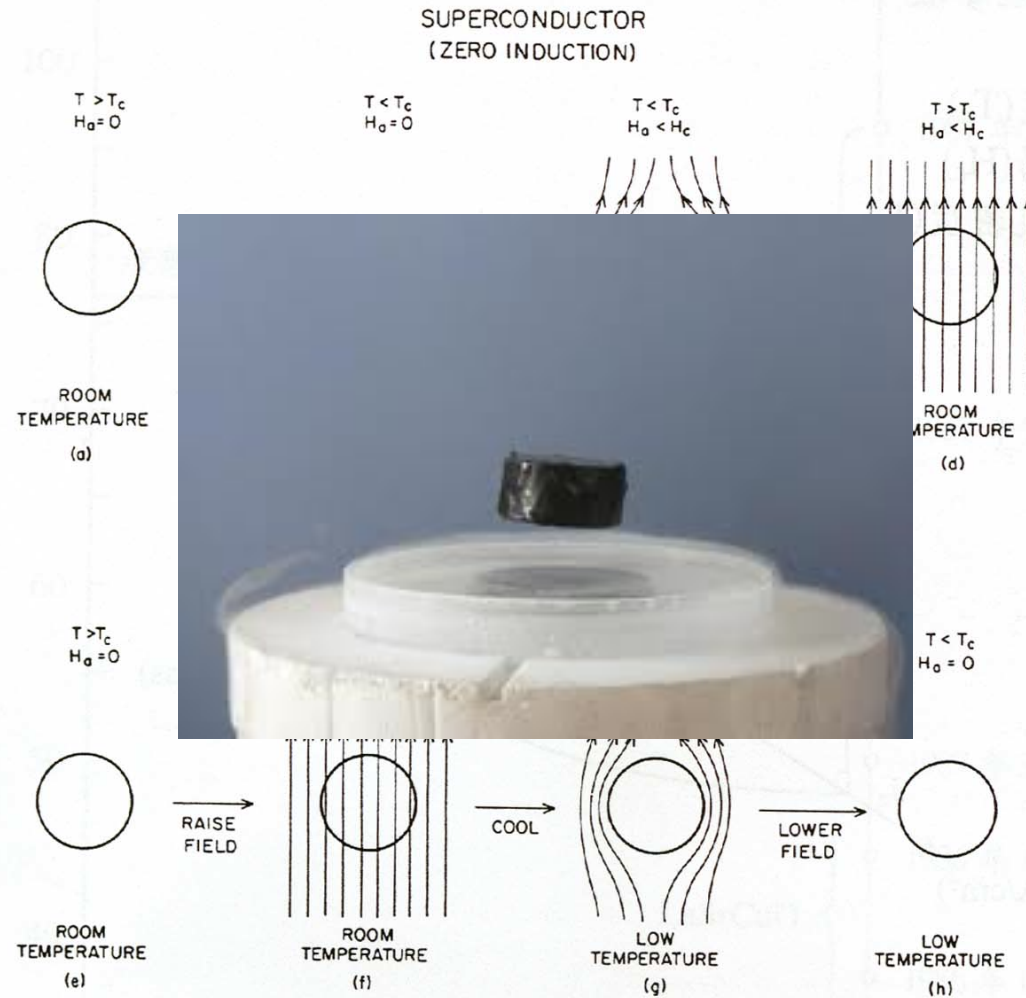


Walther Meißner
1882 - 1974

Meissner-Ochsenfeld Effect



Robert Ochsenfeld
1901 - 1993



Flux exclusion
(no big deal)

Flux expulsion
(big deal !)

Dahl, p.180

What else happened between 1933 and the 'modern era'?

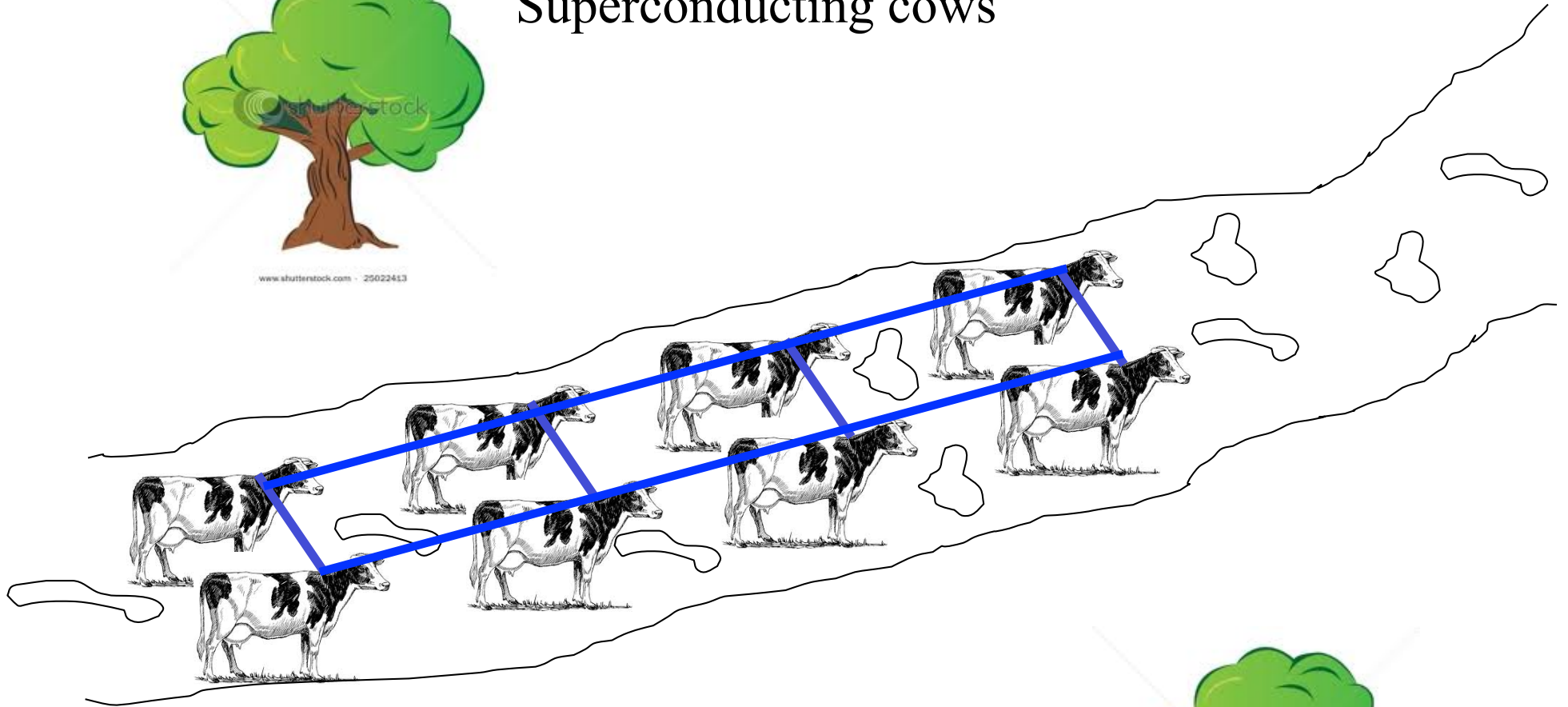
Heinz and Fritz London, 1935



Superconducting cows



www.shutterstock.com · 25022413



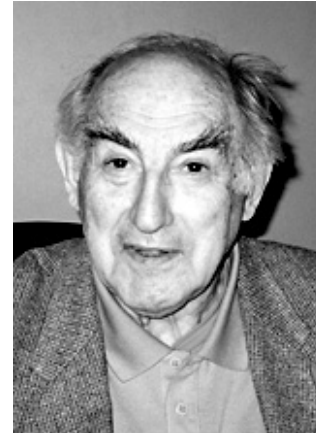
www.shutterstock.com · 25022413

What else happened between 1933 and the 'modern era'?

Heinz and Fritz London, 1935



Vitaly Ginzburg and



Lev Landau, 1950



Alexei A. Abrikosov 1956



Brian Josephson 1962

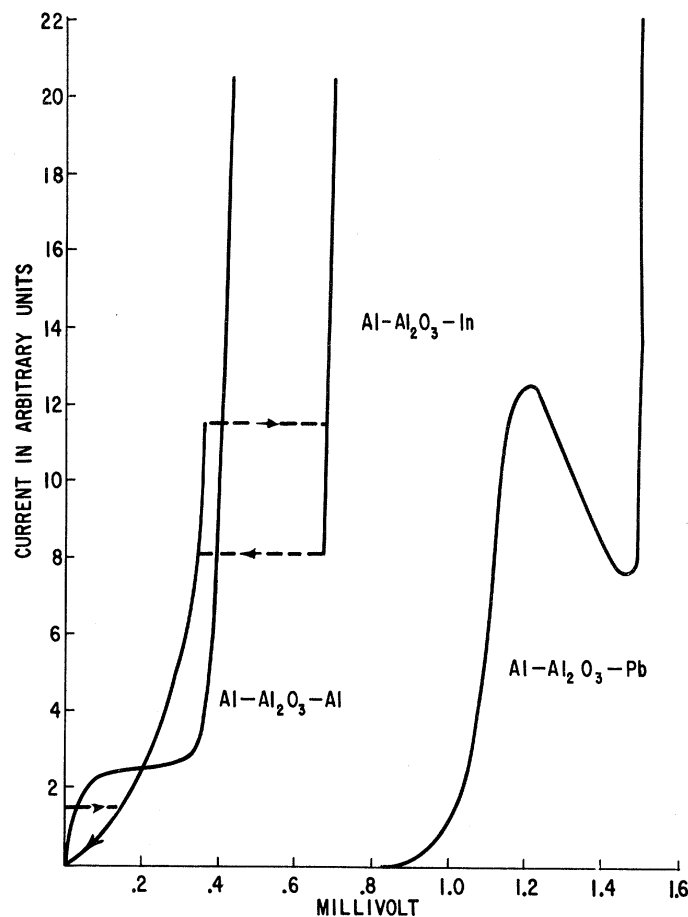


ELECTRON TUNNELING BETWEEN TWO SUPERCONDUCTORS

Ivar Giaever

General Electric Research Laboratory, Schenectady, New York

(Received October 31, 1960)



Then
er
rs.

was not traced out. Also, as is apparent from the low-current behavior of this sample, the oxide film is pierced by a superconductive bridge. When the current is increased the bridge goes normal, and its conductivity is too low to affect the general characteristics of the tunneling. When the current is decreased, the bridge remains normal at a lower current due to Joule heating.

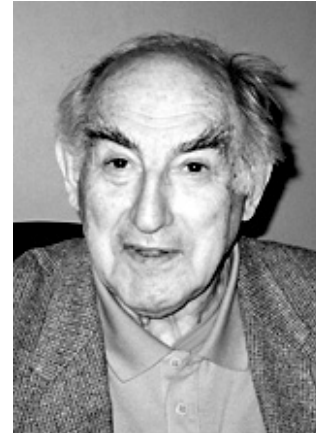
ANALOGOUS TEAM DISCUSSION

What else happened between 1933 and the 'modern era'?

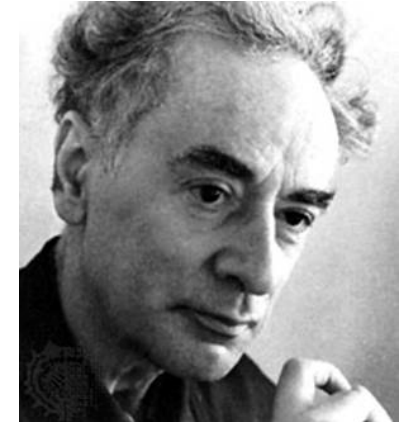
Heinz and Fritz London, 1935



Vitaly Ginzburg and



Lev Landau, 1950



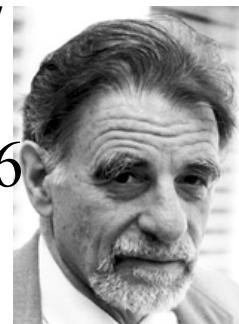
Alexei A. Abrikosov 1956



J. Bardeen L.N. Cooper J.R. Schrieffer
1957



1986



J. Georg Bednorz K. Alexander Müller

Brian Josephson 1962



**How we view
electronic properties
in
Condensed Matter**

The Theory of Everything

R. B. Laughlin* and David Pines^{†‡§}



Bob Laughlin



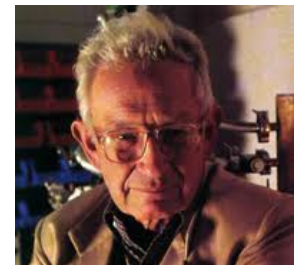
David Pines

28–31 PNAS January 4, 2000 vol. 97 no. 1

$$i\hbar \frac{\partial}{\partial t} |\Psi\rangle = \mathcal{H} |\Psi\rangle \quad [1]$$

See also, P.W. Anderson's 'More is Different' in Science, 1972

$$\begin{aligned} \mathcal{H} = & - \sum_j^{N_e} \frac{\hbar^2}{2m} \nabla_j^2 - \sum_\alpha^{N_i} \frac{\hbar^2}{2M_\alpha} \nabla_\alpha^2 \\ & - \sum_j^{N_e} \sum_\alpha^{N_i} \frac{Z_\alpha e^2}{|\vec{r}_j - \vec{R}_\alpha|} + \sum_{j \ll k}^{N_e} \frac{e^2}{|\vec{r}_j - \vec{r}_k|} + \sum_{\alpha \ll \beta}^{N_j} \frac{Z_\alpha Z_\beta e^2}{|\vec{R}_\alpha - \vec{R}_\beta|}. \end{aligned} \quad [2]$$



“
We have succeeded in reducing all of ordinary physical behavior to a simple, correct Theory of Everything only to discover that it has revealed exactly nothing about many things of great importance.”

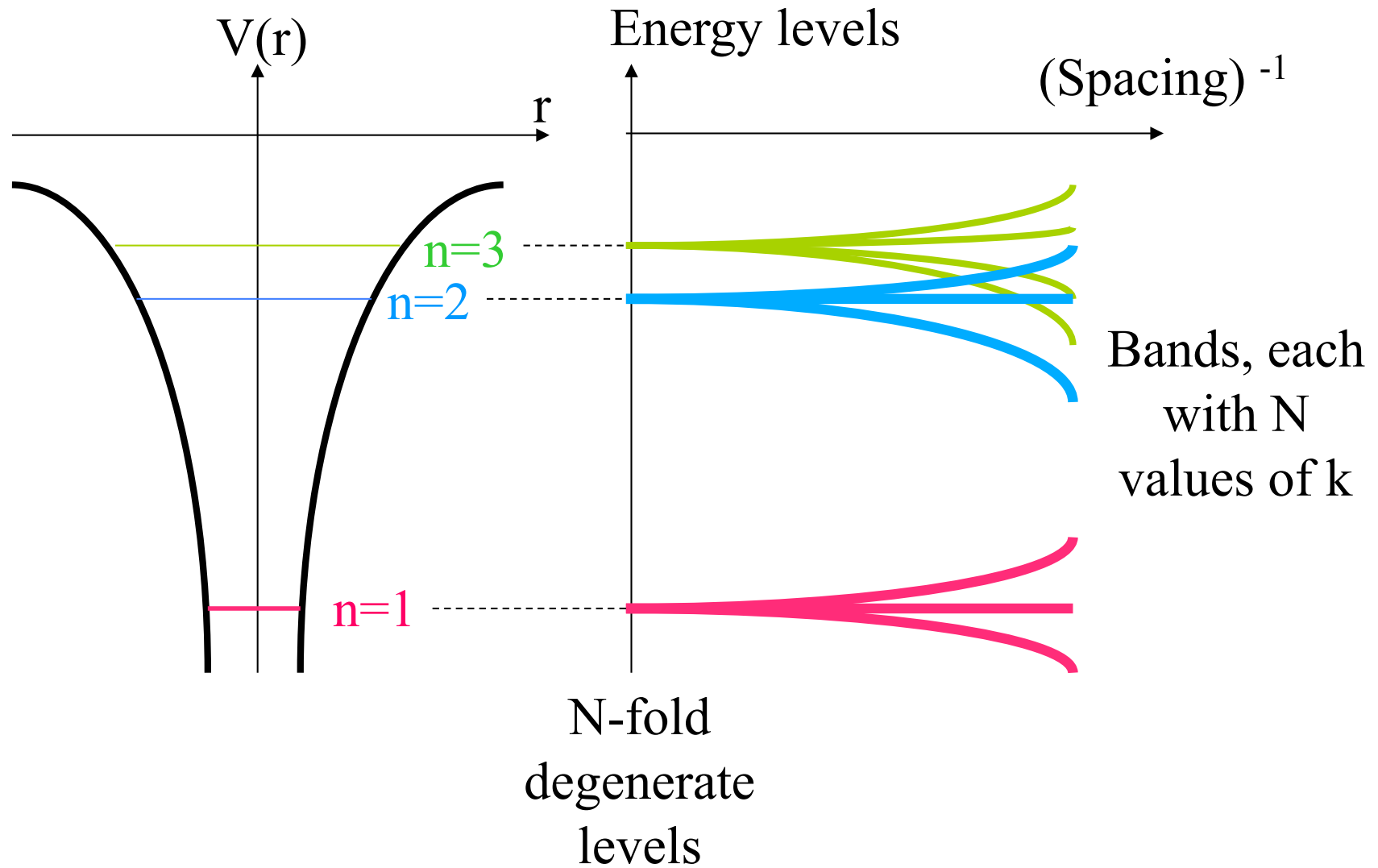
A big “rug”: Fermi Liquid Theory

nothing very exceptional about the
normal state of electrons in a metal
(pretend they don't interact)

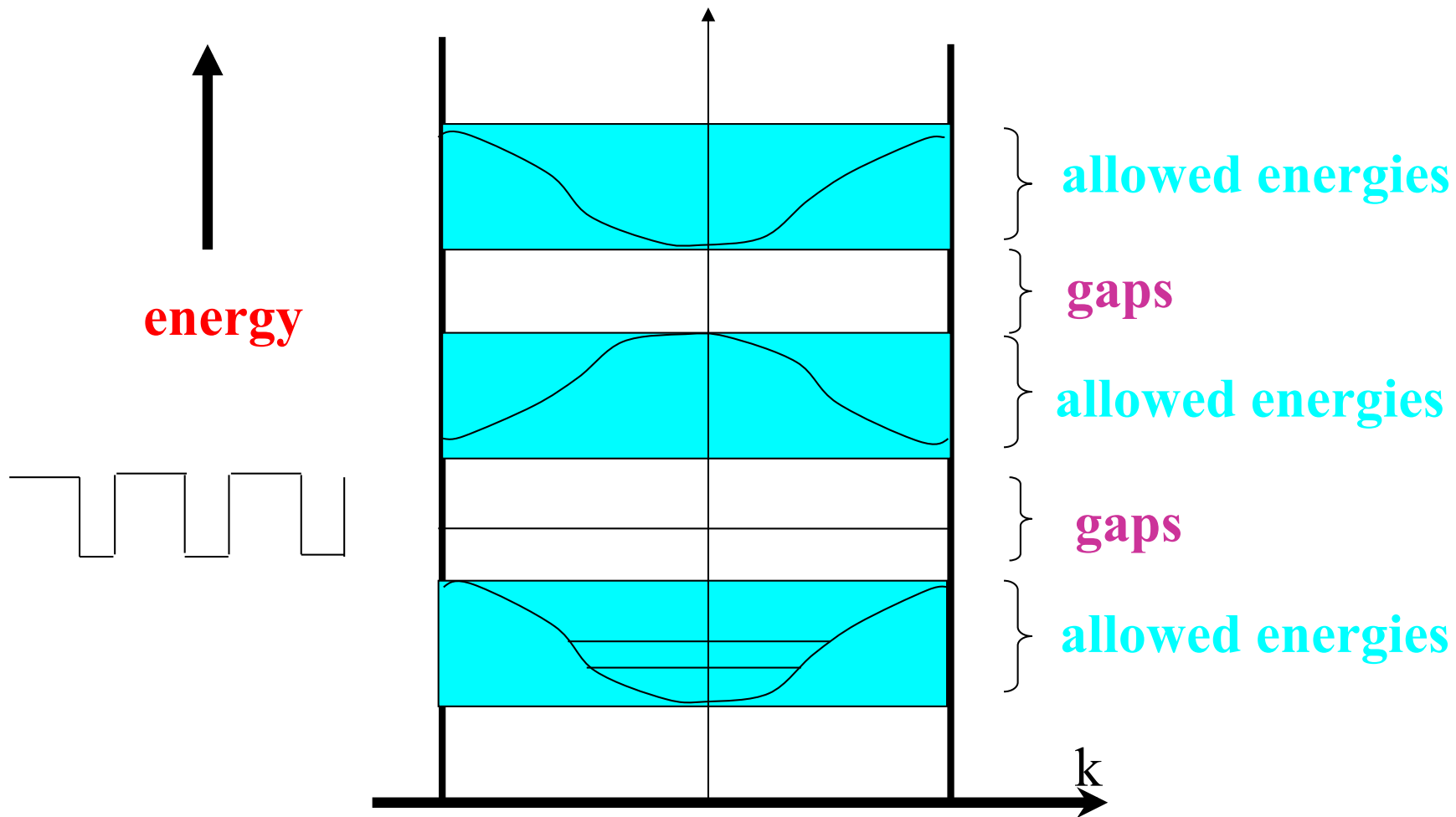
... a premise for ‘conventional’ superconductivity



Band theory of metals

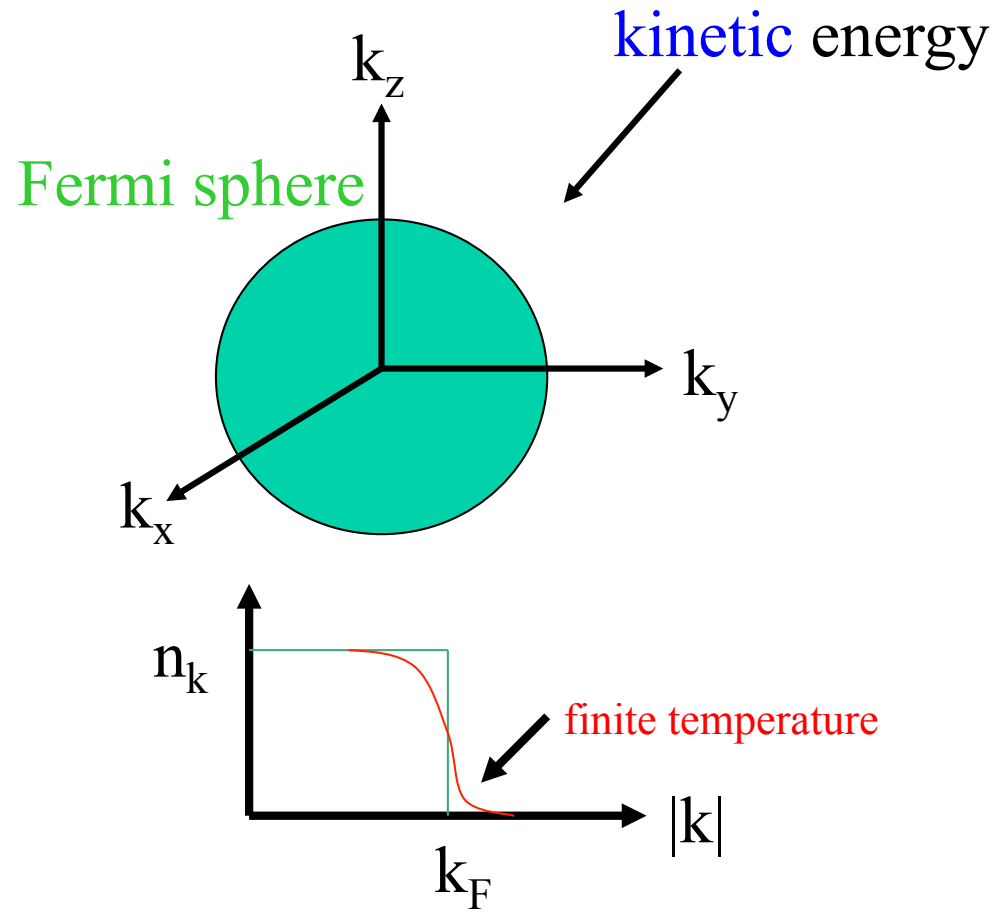


Band theory of metals



Everything is governed by Boltzmann ($e^{-E/k_B T}$) and Pauli

Electrons in solids



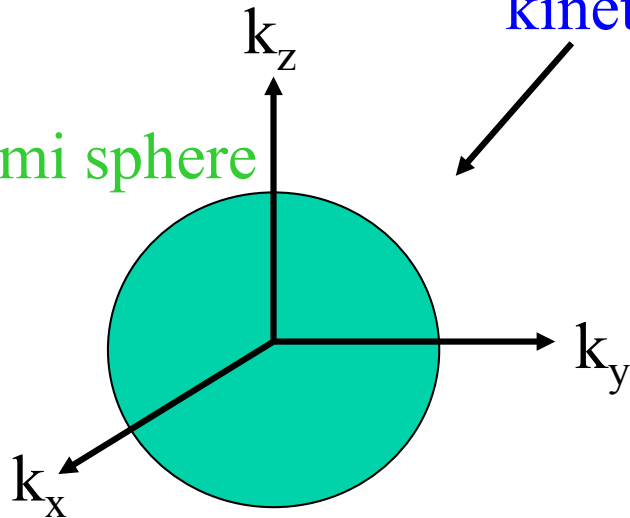
$$E_{\text{kin}} = 2 \sum \epsilon_k n_k$$

Electrons in solids

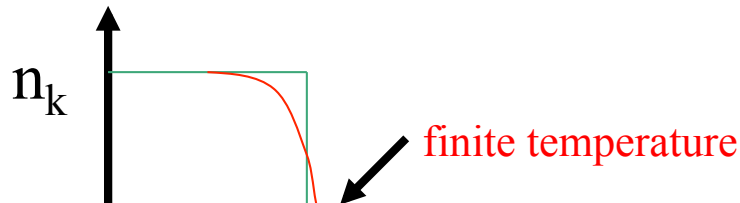
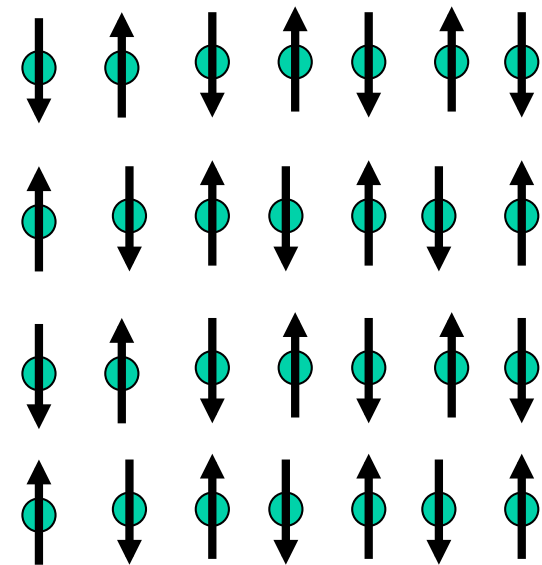


kinetic vs. potential energy

Fermi sphere



Mott insulator



Introduce frustration, doping, and so on, and one can stabilize a spin liquid: maybe even a Resonating Valence Bond (RVB) state; lower the temperature, and one gets a high T_c superconductor! (P.W. Anderson)

Spontaneous spinning of a magnet levitating over a superconductor

J.E. Hirsch^{a,*}, D.J. Hirsch^b

^a *Department of Physics, University of California, San Diego, La Jolla, CA 92093-0319, USA*

^b *Carmel Valley Middle School, San Diego, CA 92130, USA*

Received 9 April 2003; received in revised form 7 May 2003; accepted 13 May 2003

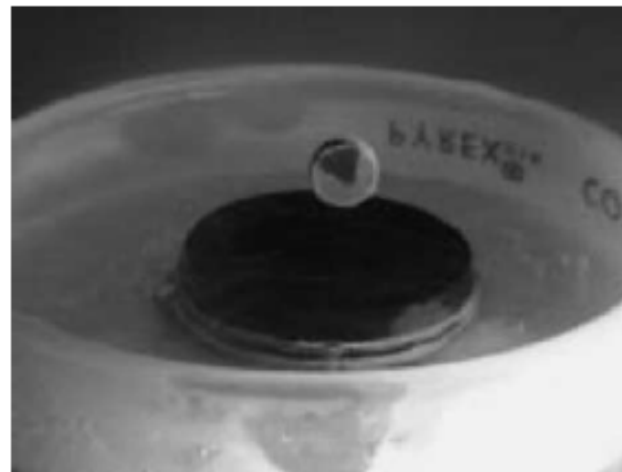


Fig. 1. Photograph of experimental setup. A YBCO disk rests on a metal base that is submerged in liquid N_2 . A $Nd_2Fe_{14}B$ magnet levitates on top of the superconductor.

Ultrathin films

Onset of Superconductivity in the Two-Dimensional Limit

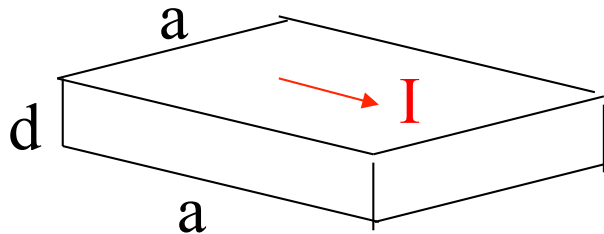
D. B. Haviland, Y. Liu, and A. M. Goldman

School of Physics and Astronomy, University of Minnesota, Minneapolis, Minnesota 55455

(Received 2 February 1989)

$$R = \rho L / A$$

$$R_s = \rho a / (ad) = \rho / d$$



sheet resistance
resistance/sheet

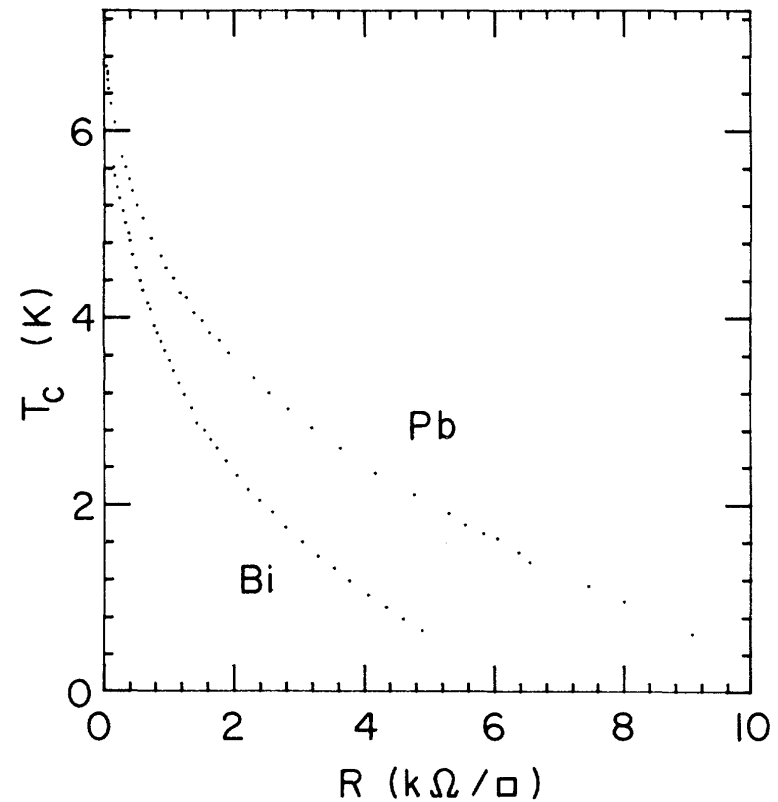
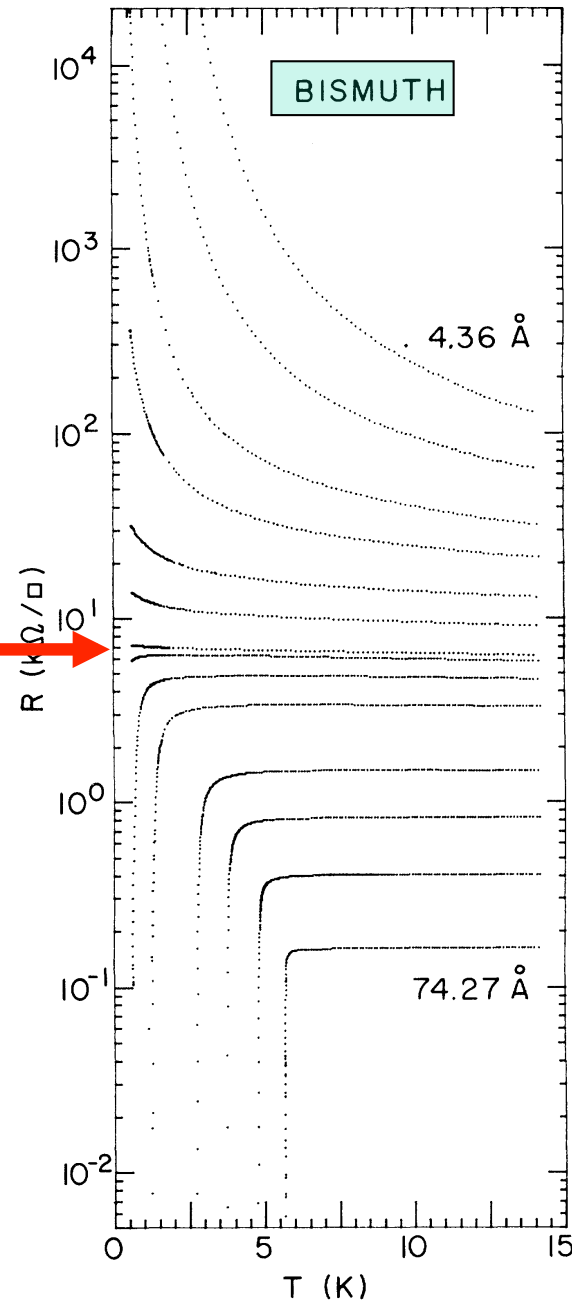


FIG. 3. Dependence of the mean-field transition temperature of Bi and Pb films on sheet resistance.

$$\frac{h}{4e^2} = 6.45 \text{ k}\Omega$$



not as close in Pb



decreasing
film
thickness

FIG. 1. Evolution of the temperature dependence of the sheet resistance $R(T)$ with thickness for a Bi film deposited onto Ge. Fewer than half of the traces actually acquired are shown. Film thicknesses shown range from 4.36 to 74.27 Å.

Interfaces

http://www.jst.go.jp/sicp/ws2009_ge3rd/presentation/14.pdf



Two Dimensional Electron Gases at Oxide Interfaces

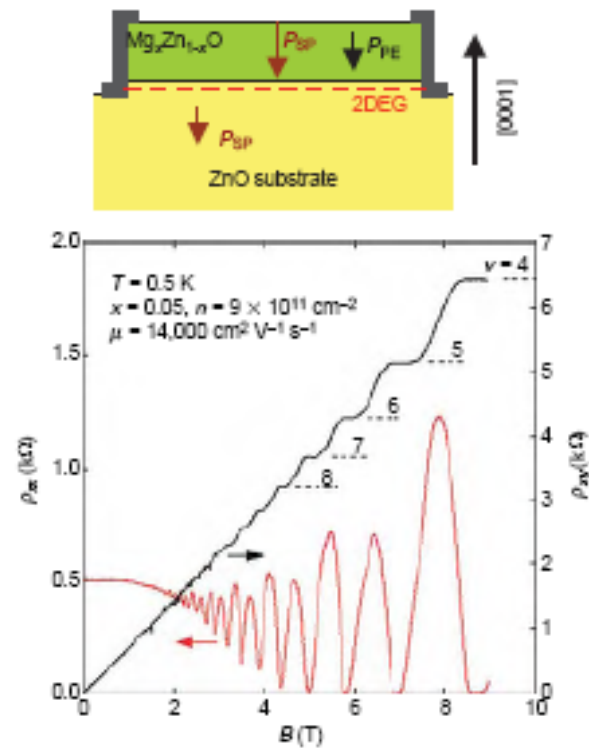
Jochen Mannhart

Center for Electronic Correlations and Magnetism

University of Augsburg

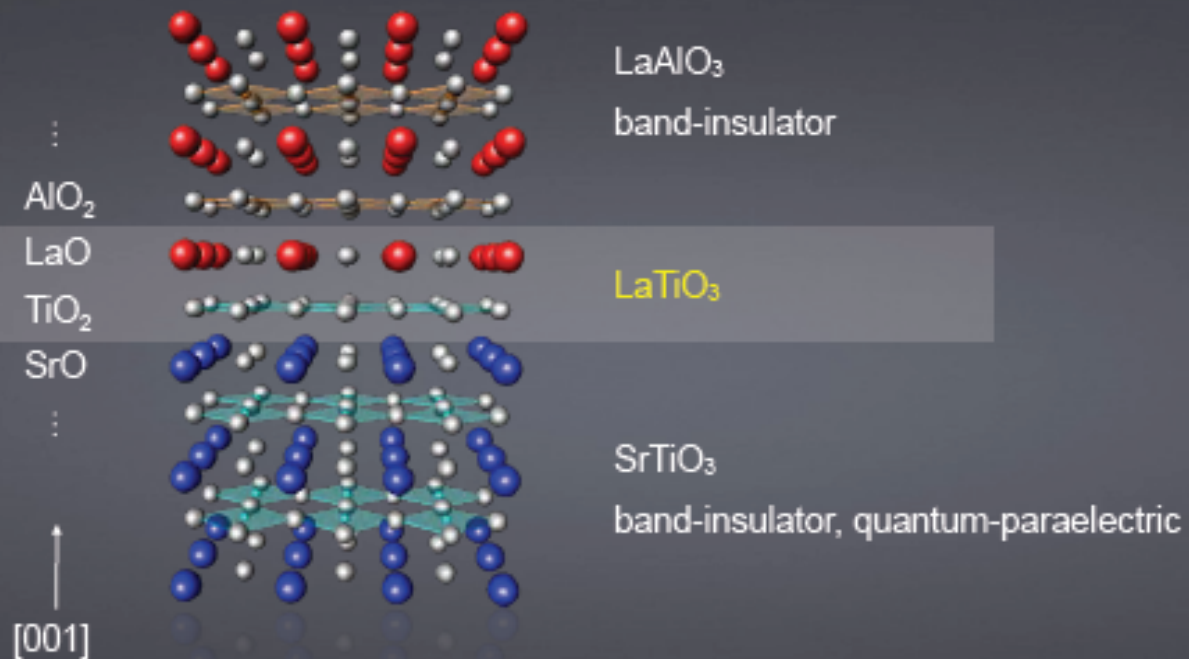
JST-DFG Workshop on Nanoelectronics, Kyoto, Jan. 21, 2009

2-DEGs Can Be Realized in Oxides



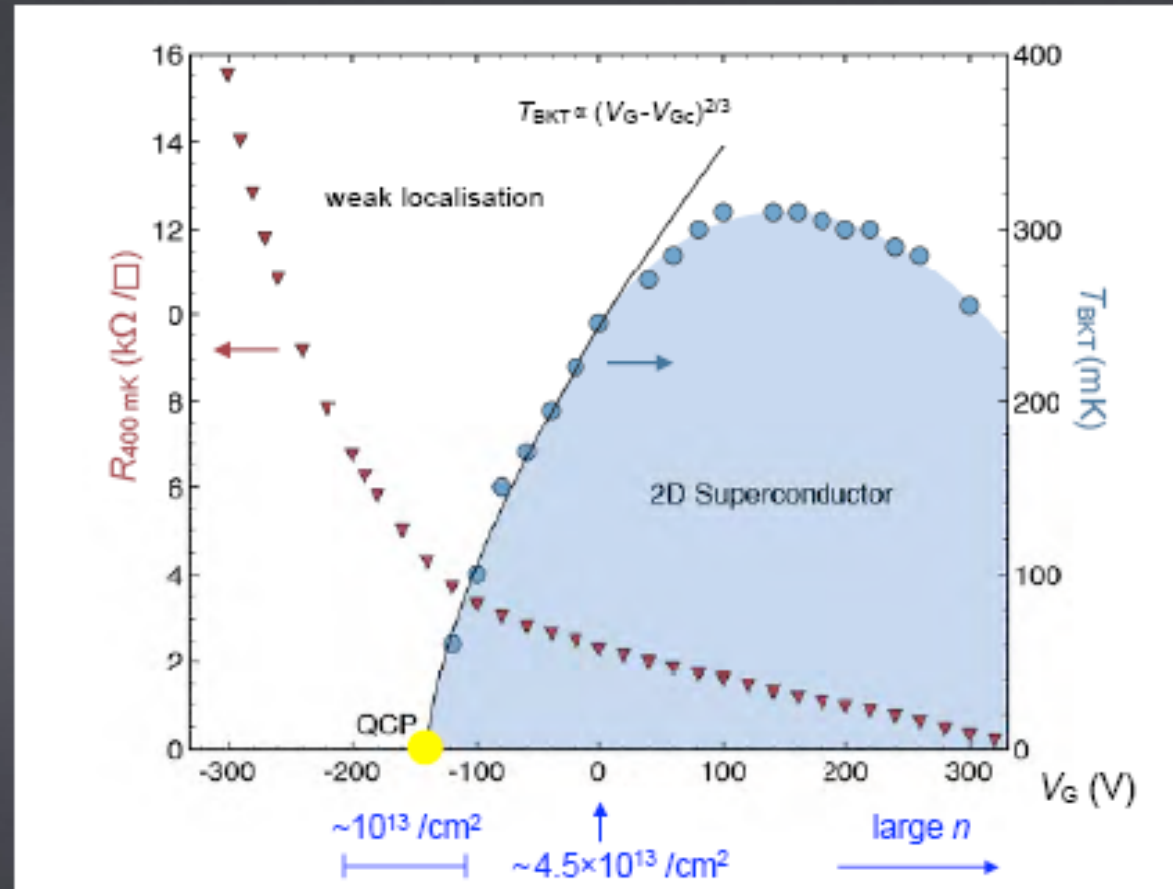
A. Tsukazaki et al., Science (2007)

The *n*-type LaAlO_3 / SrTiO_3 Interface



A. Ohtomo, H. Hwang, Nature 427, 423 (2004)

Measured Phase Diagram of the LaAlO₃/SrTiO₃ Interface

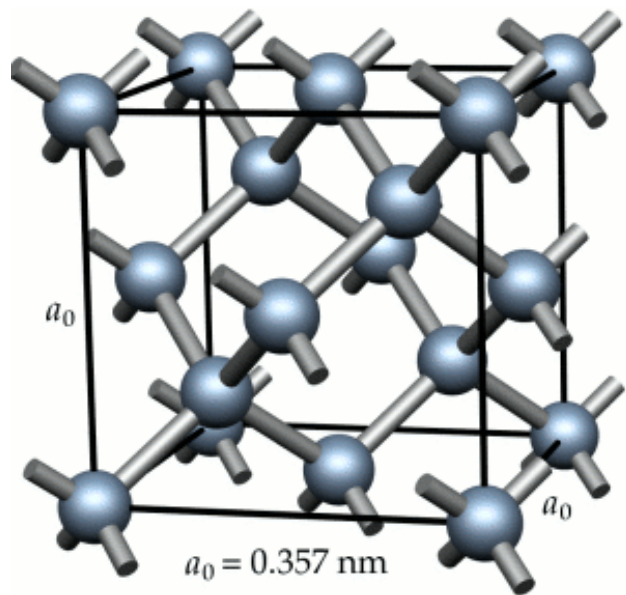


A.D. Caviglia *et al.*, nature 2008

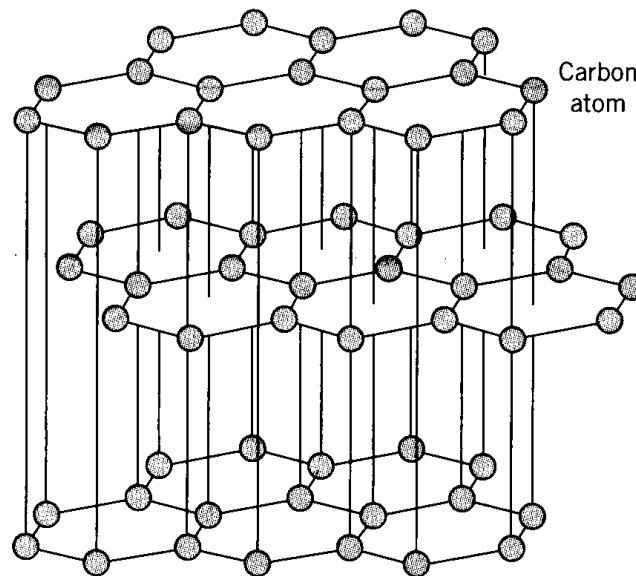
Fun with Carbon

Allotropes of Carbon

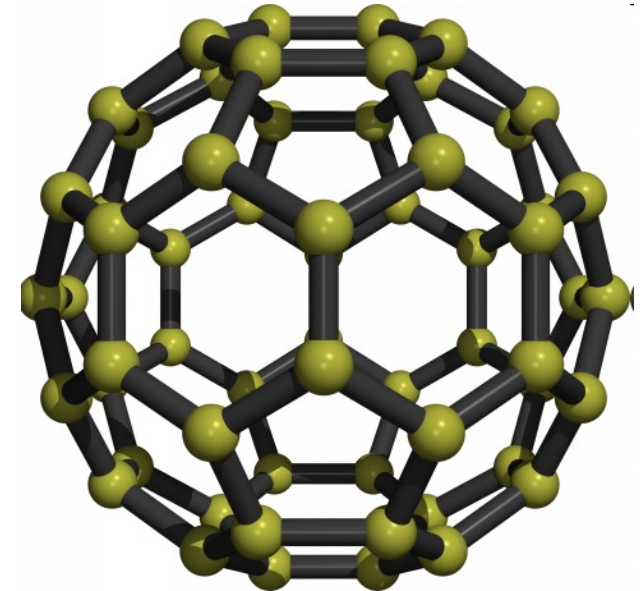
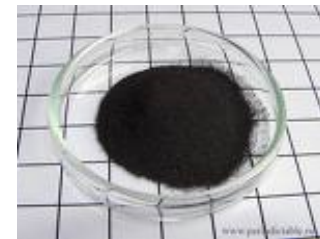
diamond



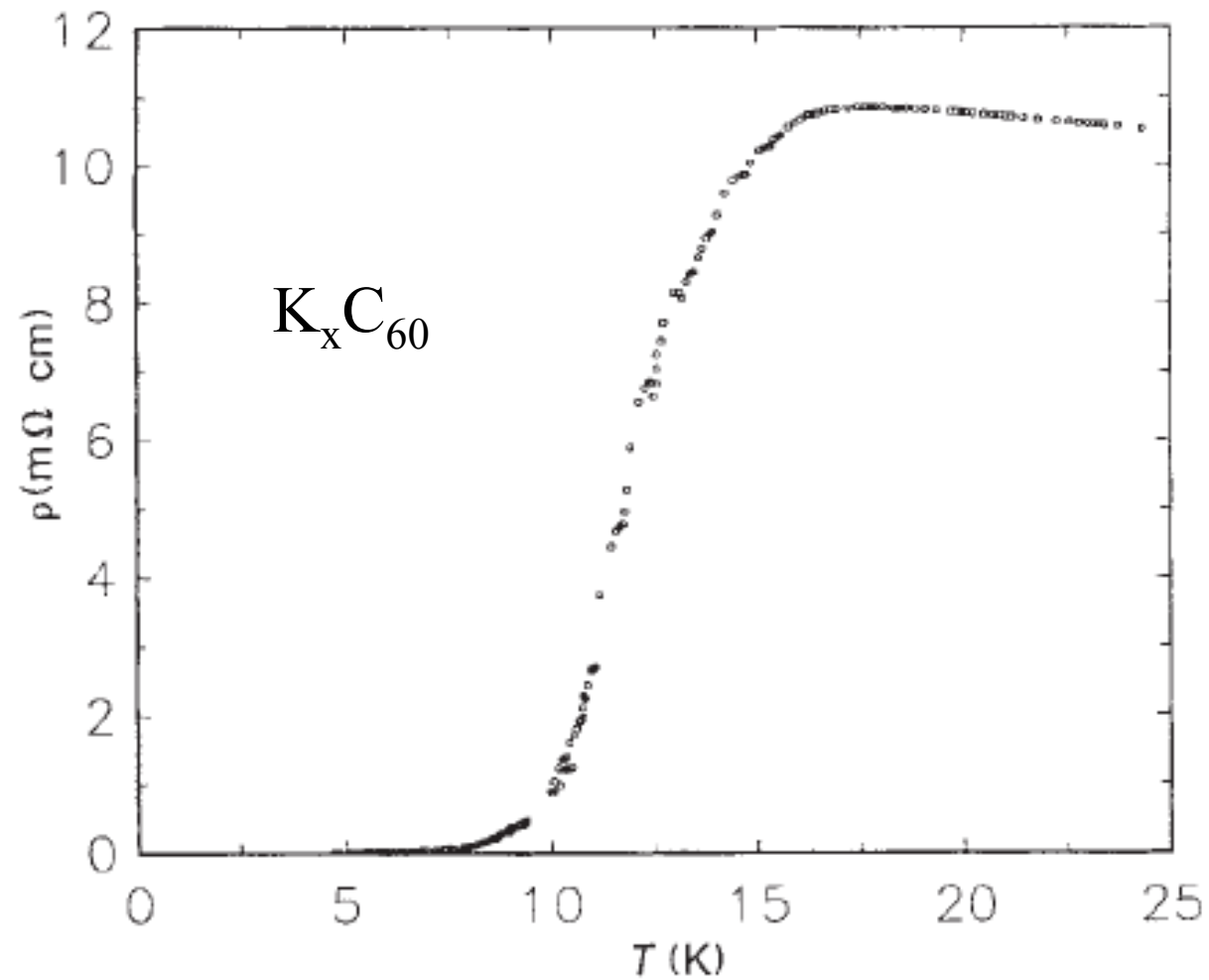
graphite



Buckminster fullerene

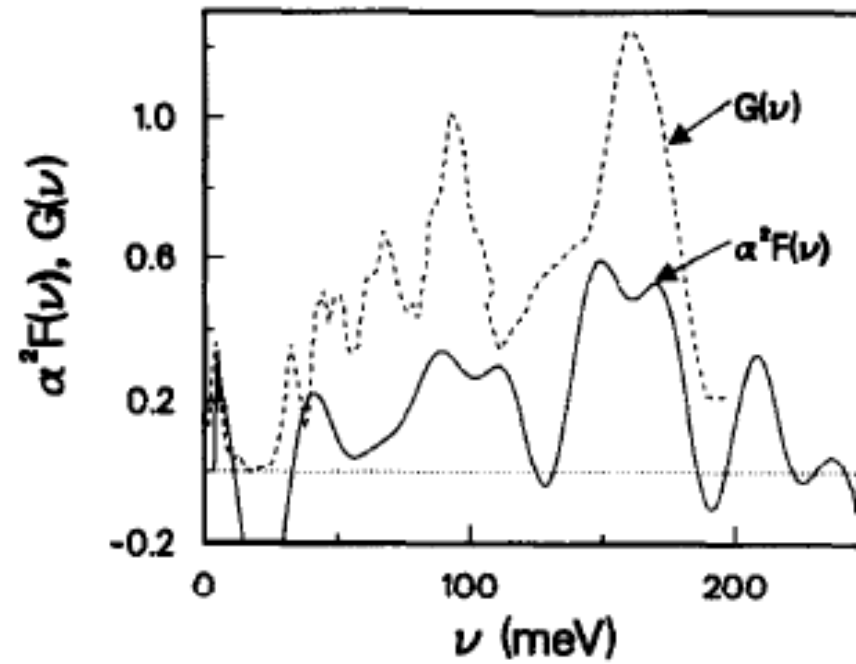


A.F. Hebard et al. Nature 350, 600 (1991)



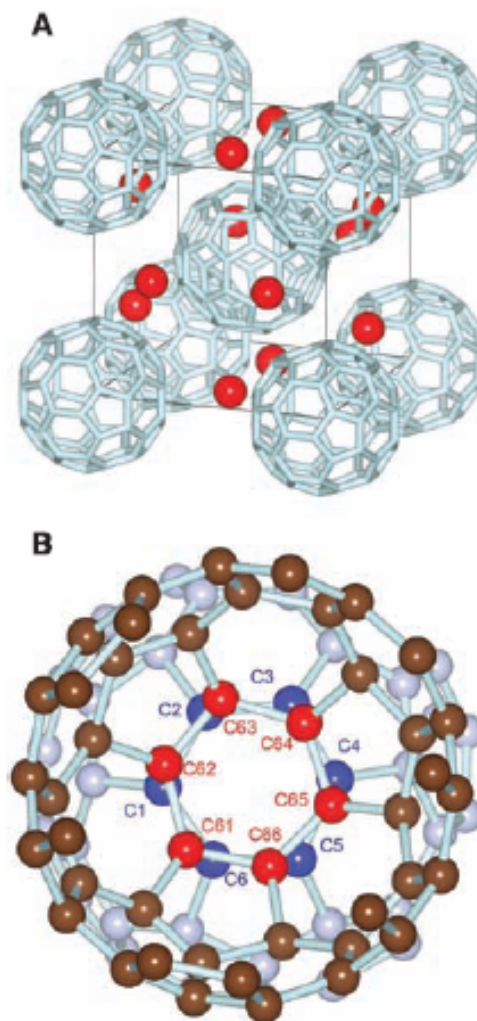
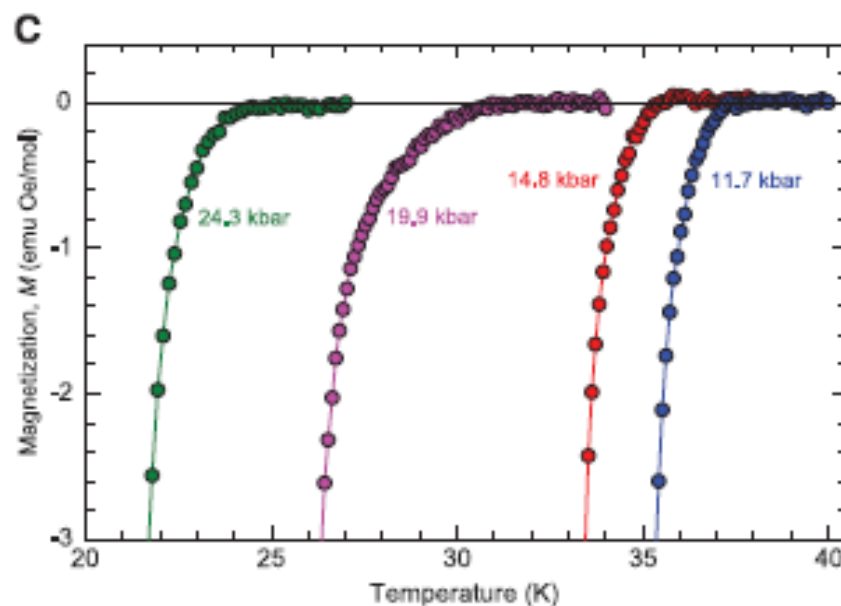
Electron-phonon driven...?

F. Marsiglio et al. / Physics Letters



The Disorder-Free Non-BCS Superconductor Cs_3C_{60} Emerges from an Antiferromagnetic Insulator Parent State

Yasuhiro Takabayashi,^{1*} Alexey Y. Ganin,^{2*} Peter Jeglič,³ Denis Arčon,^{3,4} Takumi Takano,⁵ Yoshihiro Iwasa,⁵ Yasuo Ohishi,⁶ Masaki Takata,^{6,7} Nao Takeshita,⁸ Kosmas Prassides,^{1†} Matthew J. Rosseinsky^{2†}



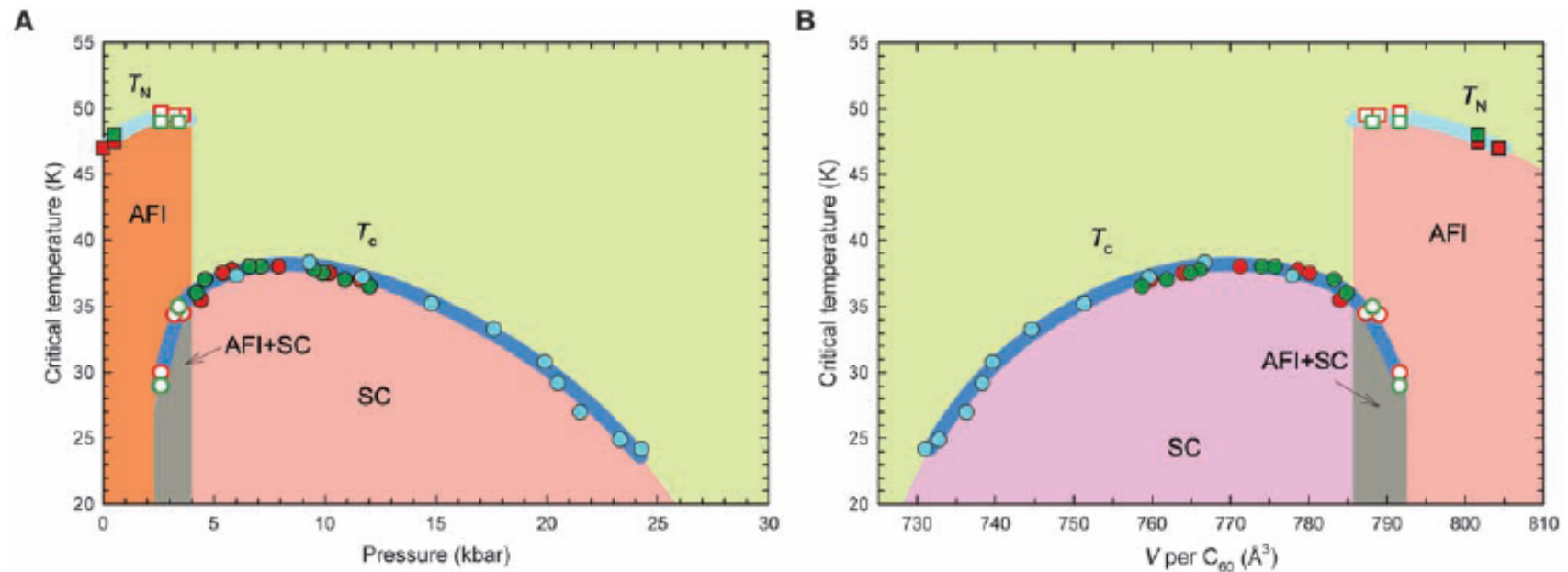


Fig. 4. Electronic phase diagram of A15 Cs_3C_{60} showing the evolution of the Néel temperature T_N (squares) and the superconducting transition temperature T_c (circles), and thus the isosymmetric transition from the ambient-pressure AFI state to the high-pressure superconducting state, (A) with change in pressure and (B) as a function of volume occupied per fulleride anion, V , at 14.6 K for A15

Cs_3C_{60} . Different symbol colors represent data obtained for different sample batches. Open symbols represent data in the AFI-superconductor coexistence regime. T_N is defined as the temperature at which the 20 Oe FC temperature-dependent magnetization M begins to increase; T_c is defined as the temperature at which the 20 Oe ZFC temperature-dependent M begins to decrease.

Just like high temperature cuprate superconductors !!!

Graphene

Speaking of carbon....

Electric Field Effect in Atomically Thin Carbon Films

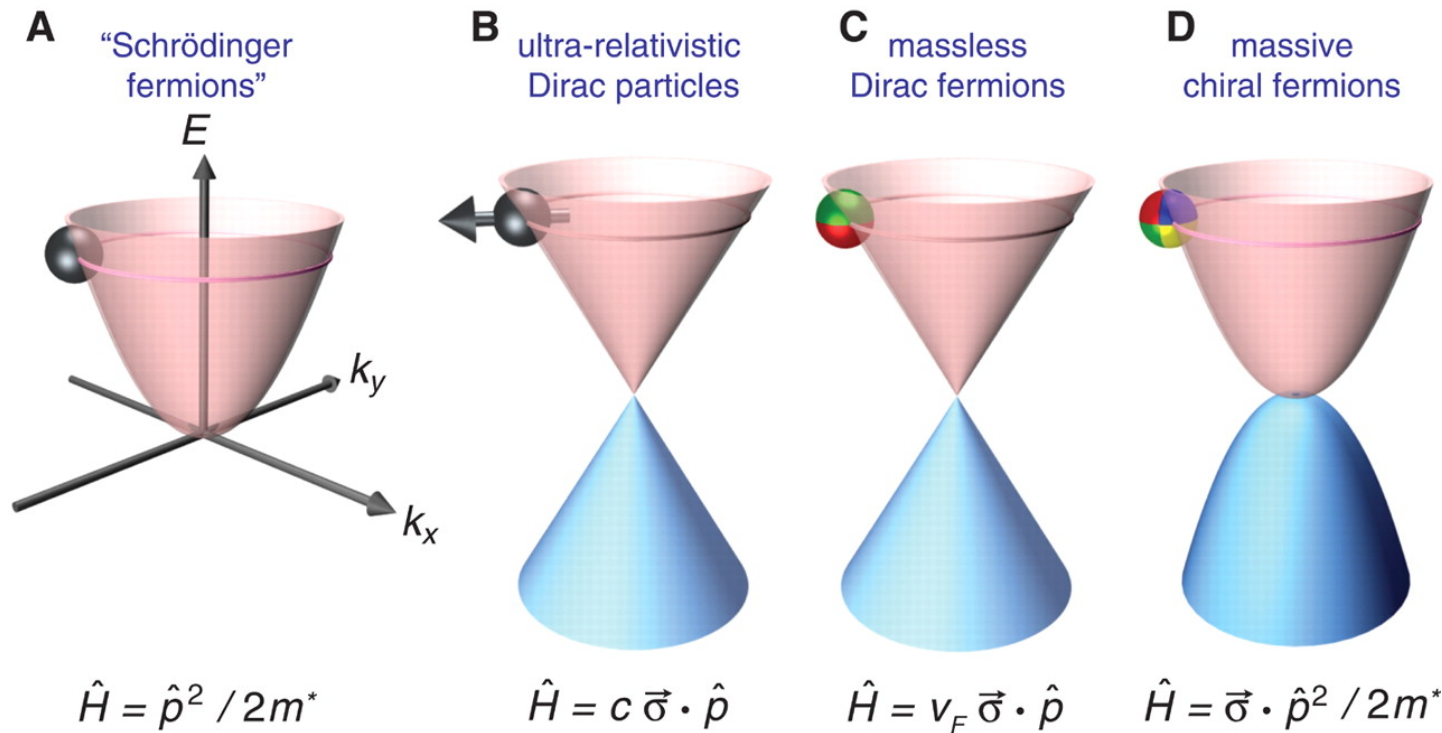
K. S. Novoselov,¹ A. K. Geim,^{1*} S. V. Morozov,² D. Jiang,¹
Y. Zhang,¹ S. V. Dubonos,² I. V. Grigorieva,¹ A. A. Firsov²

666

22 OCTOBER 2004 VOL 306 SCIENCE www.sciencemag.org

Welcome to graphene!

Fig. 2 Quasi-particle zoo



A. K. Geim Science 324, 1530 -1534 (2009)

Fig. 2 Quasi-particle zoo. (A) Charge carriers in condensed matter physics are normally described by the Schrödinger equation with an effective mass m^* different from the free electron mass (\hat{p} is the momentum operator). (B) Relativistic particles in the limit of zero rest mass follow the Dirac equation, where c is the speed of light and $\vec{\sigma}$ is the Pauli matrix. (C) Charge carriers in graphene are called massless Dirac fermions and are described by a 2D analog of the Dirac equation, with the Fermi velocity $v_F \approx 1 \times 10^6$ m/s playing the role of the speed of light and a 2D pseudospin matrix describing two sublattices of the honeycomb lattice (3). Similar to the real spin that can change its direction between, say, left and right, the pseudospin is an index that indicates on which of the two sublattices a quasi-particle is located. The pseudospin can be indicated by color (e.g., red and

The electronic properties of graphene

A. H. Castro Neto

Department of Physics, Boston University, 590 Commonwealth Avenue, Boston, Massachusetts 02215, USA

F. Guinea

Instituto de Ciencia de Materiales de Madrid, CSIC, Cantoblanco, E-28049 Madrid, Spain

N. M. R. Peres

Center of Physics and Department of Physics, Universidade do Minho, P-4710-057, Braga, Portugal

K. S. Novoselov and A. K. Geim

Department of Physics and Astronomy, University of Manchester, Manchester, M13 9PL, United Kingdom

(Published 14 January 2009)

This article reviews the basic theoretical aspects of graphene, a one-atom-thick allotrope of carbon, with unusual two-dimensional Dirac-like electronic excitations. The Dirac electrons can be controlled by application of external electric and magnetic fields, or by altering sample geometry and/or topology. The Dirac electrons behave in unusual ways in tunneling, confinement, and the integer quantum Hall effect. The electronic properties of graphene stacks are discussed and vary with stacking order and number of layers. Edge (surface) states in graphene depend on the edge termination (zigzag or armchair) and affect the physical properties of nanoribbons. Different types of disorder modify the Dirac equation leading to unusual spectroscopic and transport properties. The effects of electron-electron and electron-phonon interactions in single layer and multilayer graphene are also presented.

DOI: [10.1103/RevModPhys.81.109](https://doi.org/10.1103/RevModPhys.81.109)

PACS number(s): 81.05.Uw, 73.20.-r, 03.65.Pm, 82.45.Mp

CONTENTS

I. Introduction	110	B. Topological lattice defects	136
II. Elementary Electronic Properties of Graphene	112	C. Impurity states	137
A. Single-layer, two-dimensional graphene	112	D. Localized states near edges, cracks, and voids	137
B. Bilayer and multilayer graphene	113	E. Self-doping	138
C. Graphene nanoribbons	114	F. Vector potential and gauge field disorder	139

by application of external electric and magnetic fields, or by altering sample geometry and/or topology. The Dirac electrons behave in unusual ways in tunneling, confinement, and the integer quantum Hall effect. The electronic properties of graphene stacks are discussed and vary with stacking order and number of layers. Edge (surface) states in graphene depend on the edge termination (zigzag or armchair) and affect the physical properties of nanoribbons. Different types of disorder modify the Dirac equation leading to unusual spectroscopic and transport properties. The effects of electron-electron and electron-phonon interactions in single layer and multilayer graphene are also presented.

DOI: [10.1103/RevModPhys.81.109](https://doi.org/10.1103/RevModPhys.81.109)

PACS number(s): 81.05.Uw, 73.20.-r, 03.65.Pm, 82.45.Mp

CONTENTS

I. Introduction	110	B. Topological lattice defects	136
II. Elementary Electronic Properties of Graphene	112	C. Impurity states	137
A. Single layer: Tight-binding approach	112	D. Localized states near edges, cracks, and voids	137
1. Cyclotron mass	113	E. Self-doping	138
2. Density of states	114	F. Vector potential and gauge field disorder	139
B. Dirac fermions	114	1. Gauge field induced by curvature	140
1. Chiral tunneling and Klein paradox	115	2. Elastic strain	140
2. Confinement and <i>Zitterbewegung</i>	117	3. Random gauge fields	141
C. Bilayer graphene: Tight-binding approach	118	G. Coupling to magnetic impurities	141
D. Epitaxial graphene	119	H. Weak and strong localization	142
E. Graphene stacks	120	I. Transport near the Dirac point	143
1. Electronic structure of bulk graphite	121	J. Boltzmann equation description of dc transport in doped graphene	144
F. Surface states in graphene	122	K. Magnetotransport and universal conductivity	145
G. Surface states in graphene stacks	124	1. The full self-consistent Born approximation (FSBA)	146
H. The spectrum of graphene nanoribbons	124	V. Many-Body Effects	148
1. Zigzag nanoribbons	125	A. Electron-phonon interactions	148
2. Armchair nanoribbons	126	B. Electron-electron interactions	150
I. Dirac fermions in a magnetic field	126	1. Screening in graphene stacks	152
J. The anomalous integer quantum Hall effect	128	C. Short-range interactions	152
K. Tight-binding model in a magnetic field	128	1. Bilayer graphene: Exchange	153
L. Landau levels in graphene stacks	130	2. Bilayer graphene: Short-range interactions	154
M. Diamagnetism	130	D. Interactions in high magnetic fields	154
N. Spin-orbit coupling	131	VI. Conclusions	154
III. Flexural Phonons, Elasticity, and Crumpling	132	Acknowledgments	155
IV. Disorder in Graphene	134	References	155
A. Ripples	135		

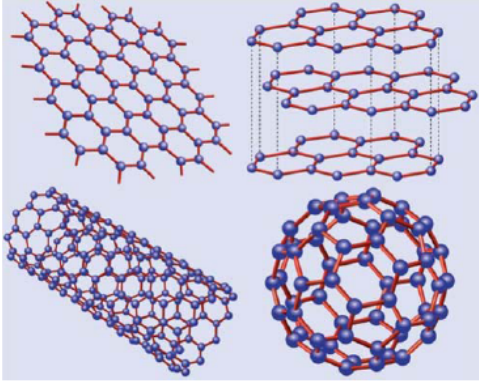


FIG. 1. (Color online) Graphene (top left) is a honeycomb lattice of carbon atoms. Graphite (top right) can be viewed as a stack of graphene layers. Carbon nanotubes are rolled-up cylinders of graphene (bottom left). Fullerenes (C_{60}) are molecules consisting of wrapped graphene by the introduction of pentagons on the hexagonal lattice. From [Castro Neto *et al.*, 2006a](#).

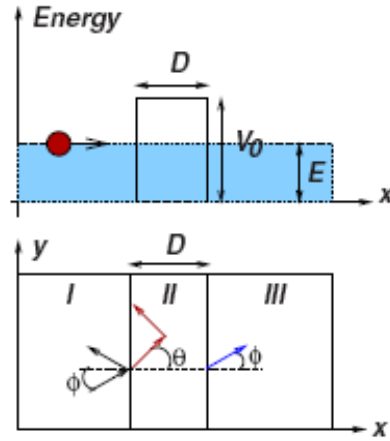


FIG. 6. (Color online) Klein tunneling in graphene. Top: schematic of the scattering of Dirac electrons by a square potential. Bottom: definition of the angles ϕ and θ used in the scattering formalism in regions I, II, and III.

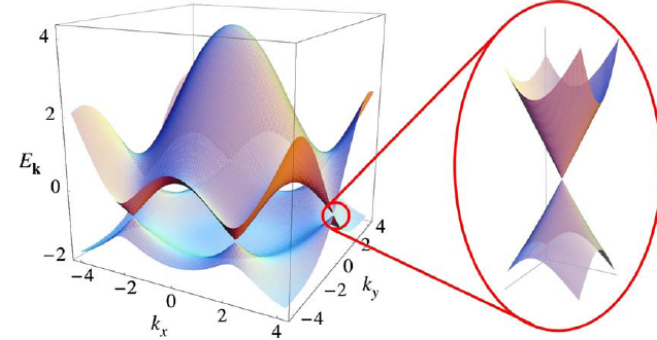


FIG. 3. (Color online) Electronic dispersion in the honeycomb lattice. Left: energy spectrum (in units of t) for finite values of t and t' , with $t=2.7$ eV and $t'=-0.2t$. Right: zoom in of the energy bands close to one of the Dirac points.

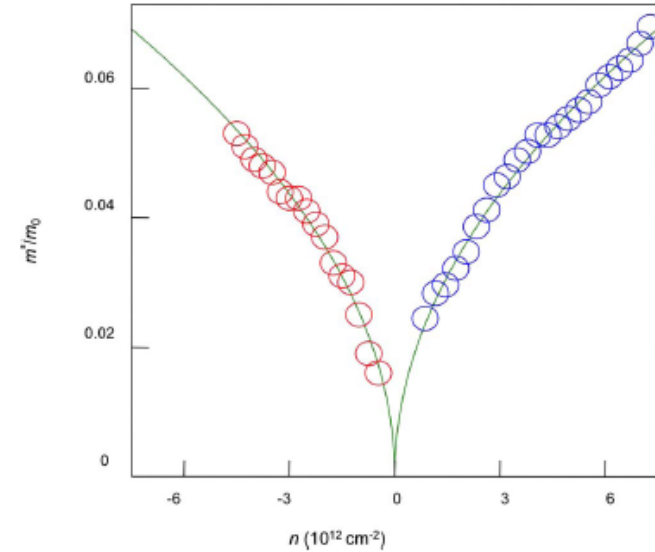
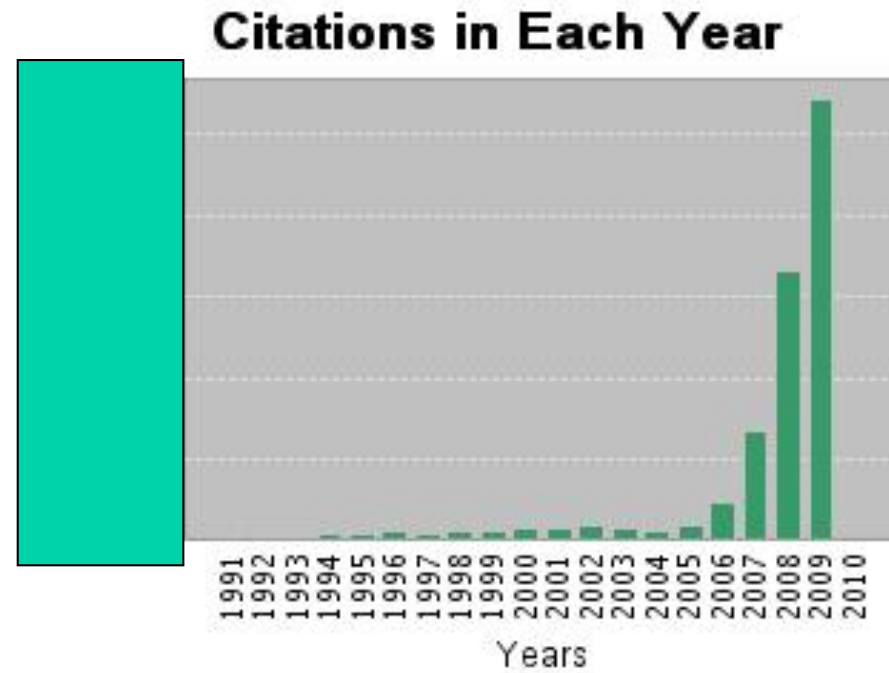


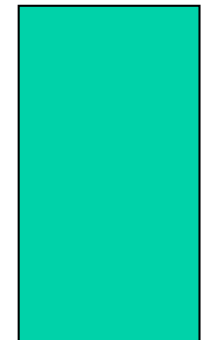
FIG. 4. (Color online) Cyclotron mass of charge carriers in graphene as a function of their concentration n . Positive and negative n correspond to electrons and holes, respectively. Symbols are the experimental data extracted from the temperature dependence of the SdH oscillations; solid curves are the best fit by Eq. (13). m_0 is the free-electron mass. Adapted from [Novoselov, Geim, Morozov, *et al.*, 2005](#).

A.K. Geim



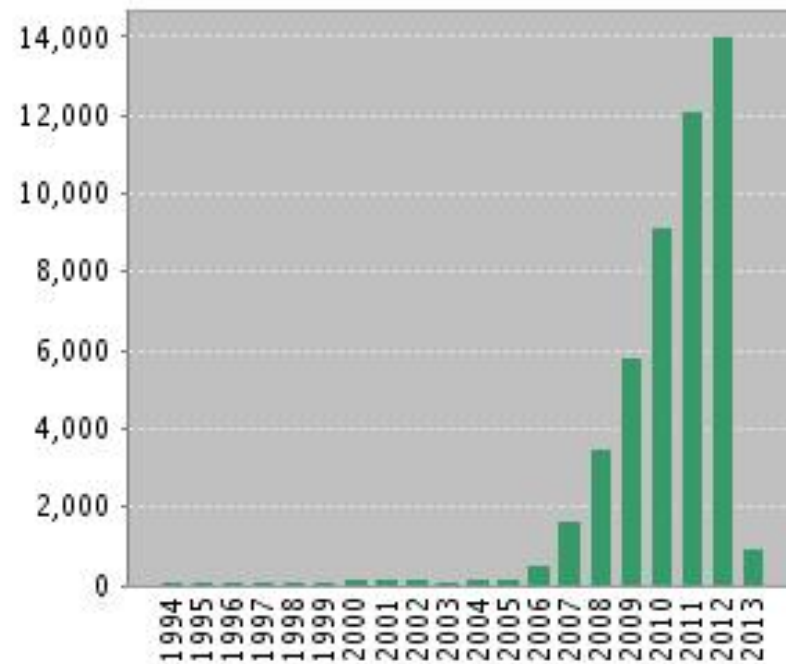
citations

2004 Science paper:
2005 Nature paper:
2007 Nature Materials:
2009 Rev. Mod. Phys:



A.K. Geim

Citations in each year



citations

2004 Science paper:	9479
2005 Nature paper:	5249
2007 Nature Materials:	6670
2009 Rev. Mod. Phys:	3079

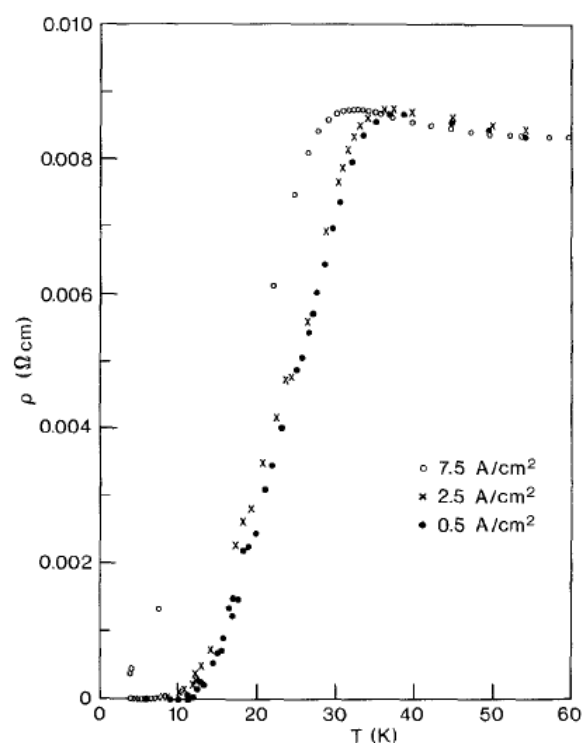
High Temperature Superconductivity

Possible High T_c Superconductivity in the Ba - La - Cu - O System

J.G. Bednorz and K.A. Müller

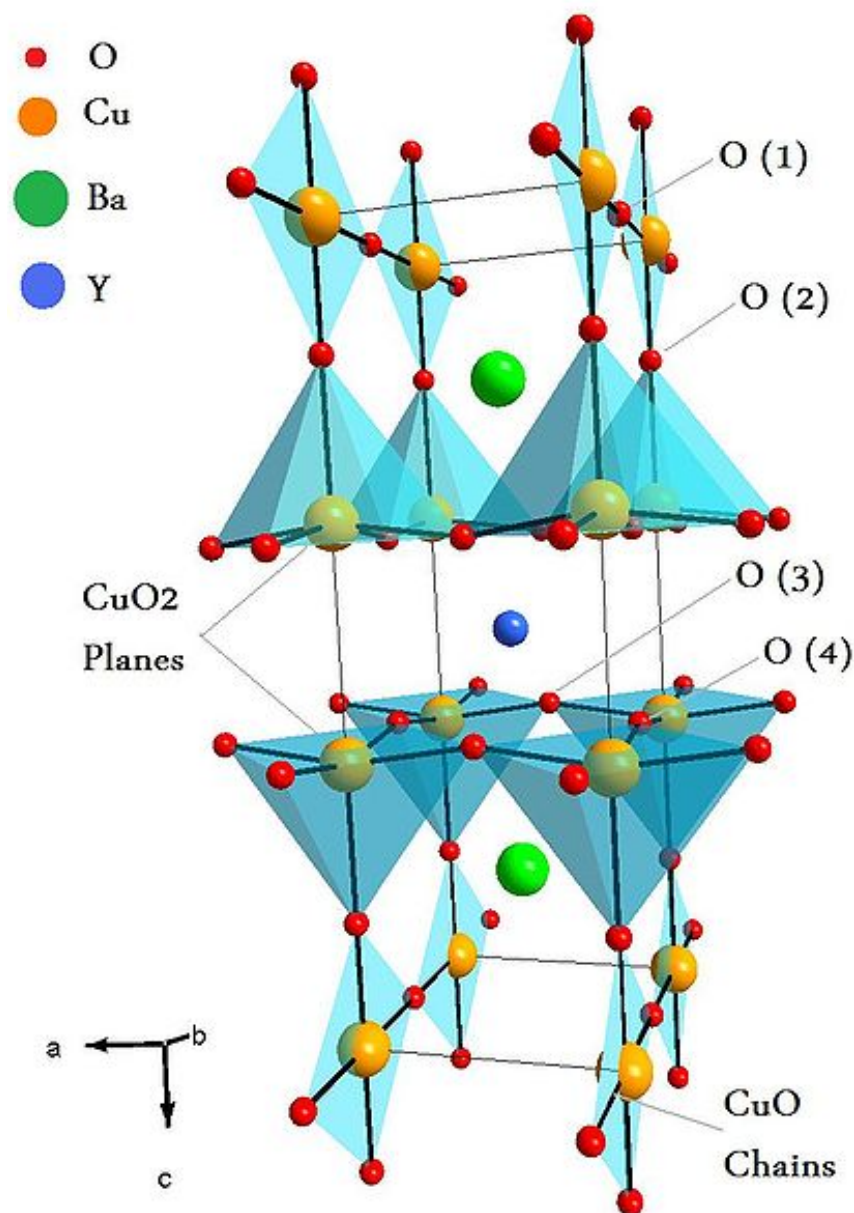
IBM Zürich Research Laboratory, Rüschlikon, Switzerland

Received April 17, 1986



an-
und

Fig. 3. Low-temperature resistivity of a sample with $x(\text{Ba})=0.75$, recorded for different current densities



Superconductivity at 93 K in a New Mixed-Phase Y-Ba-Cu-O Compound System at Ambient Pressure

M. K. Wu, J. R. Ashburn, and C. J. Torng

Department of Physics, University of Alabama, Huntsville, Alabama 35899

and

P. H. Hor, R. L. Meng, L. Gao, Z. J. Huang, Y. Q. Wang, and C. W. Chu^(a)

Department of Physics and Space Vacuum Epitaxy Center, University of Houston, Houston, Texas 77004

(Received 6 February 1987; Revised manuscript received 18 February 1987)

A stable and reproducible superconductivity transition between 80 and 93 K has been unambiguously observed both resistively and magnetically in a new Y-Ba-Cu-O compound system at ambient pressure. An estimated upper critical field $H_{c2}(0)$ between 80 and 180 T was obtained.

PACS numbers: 74.70.Ya

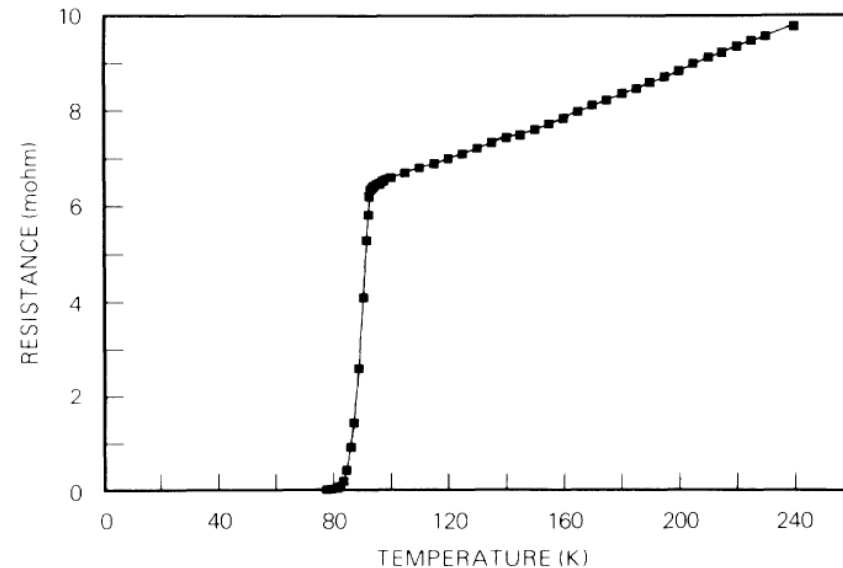
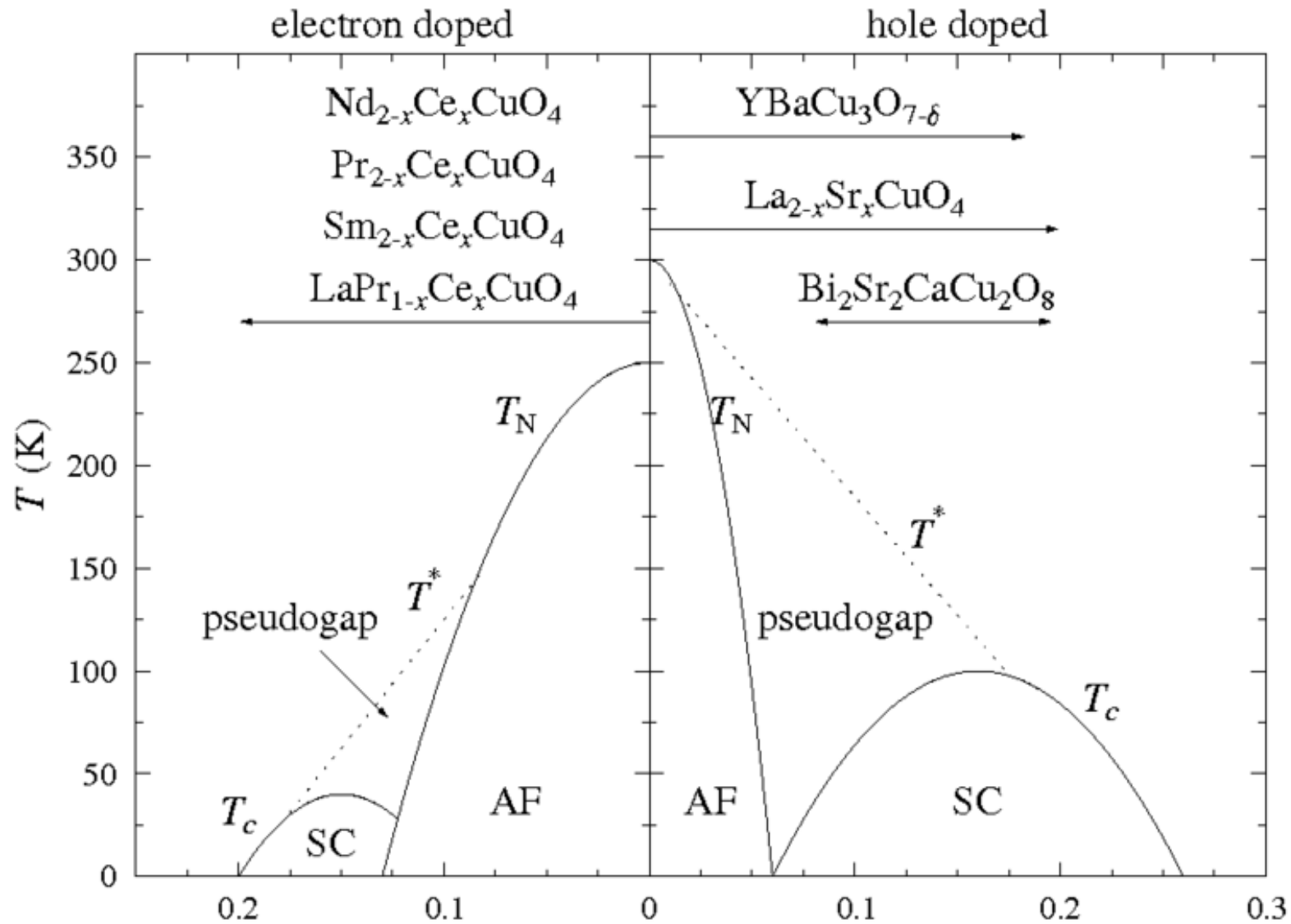


FIG. 3. Magnetic field effect on resistance.

Phase diagram for cuprate materials



<http://www.unine.ch/n/phys/theocond/Research/supra/PhaseDiagramCuprates.gif>

<http://en.wikipedia.org/wiki/File:Cuphasediag.png>

PERIODIC TABLE OF THE ELEMENTS

<http://www.ktf-split.hr/periodni/en/>

PERIODIC TABLE OF THE ELEMENTS

<http://www.ktf-split.hr/periodni/en/>

GROUP

1 **IA**

2 **IIA**

13 **IIIA**

14 **IVA**

15 **VA**

16 **VIA**

17 **VIIA**

18 **VIIIA**

PERIOD

1

2

3

4

5

6

7

RELATIVE ATOMIC MASS (1)

GROUP IUPAC

GROUP CAS

ATOMIC NUMBER

SYMBOL

ELEMENT NAME

Metal
 Semimetal
 Nonmetal

1 Alkali metal
 16 Chalcogens element

2 Alkaline earth metal
 17 Halogens element

 Transition metals
 18 Noble gas

 Lanthanide
 Actinide

STANDARD STATE (25 °C; 101 kPa)

Ne - gas **Fe** - solid

Ga - liquid **Tc** - synthetic

1 1.0079 H HYDROGEN																	2 4.0026 He HELIUM	
3 6.941 Li LITHIUM	4 9.0122 Be BERYLLIUM																	10 20.180 Ne NEON
11 22.990 Na SODIUM	12 24.305 Mg MAGNESIUM	13 10.811 B BORON	14 12.011 C CARBON	15 14.007 N NITROGEN	16 15.999 O OXYGEN	17 18.998 F FLUORINE	18 39.948 Ar ARGON											
19 39.098 K POTASSIUM	20 40.078 Ca CALCIUM	21 44.956 Sc SCANDIUM	22 47.867 Ti TITANIUM	23 50.942 V VANADIUM	24 51.996 Cr CHROMIUM	25 54.938 Mn MANGANESE	26 55.845 Fe IRON	27 58.933 Co COBALT	28 58.693 Ni NICKEL	29 63.546 Cu COPPER	30 65.39 Zn ZINC	31 69.723 Ga GALLIUM	32 72.64 Ge GERMANIUM	33 74.922 As ARSENIC	34 78.96 Se SELENIUM	35 79.904 Br BROMINE	36 83.80 Kr KRYPTON	
37 85.468 Rb RUBIDIUM	38 87.62 Sr STRONTIUM	39 88.906 Y YTTRIUM	40 91.224 Zr ZIRCONIUM	41 92.906 Nb NIOBIUM	42 95.94 Mo MOLYBDENUM	43 (98) Tc TECHNETIUM	44 101.07 Ru RUTHENIUM	45 102.91 Rh RHODIUM	46 106.42 Pd PALLADIUM	47 107.87 Ag SILVER	48 112.41 Cd CADMIUM	49 114.82 In INDIUM	50 118.71 Sn TIN	51 121.76 Sb ANTIMONY	52 127.60 Te TELLURIUM	53 126.90 I IODINE	54 131.29 Xe XENON	
55 132.91 Cs CAESIUM	56 137.33 Ba BARIUM	57-71 La-Lu Lanthanide	72 178.49 Hf HAFNIUM	73 180.95 Ta TANTALUM	74 183.84 W TUNGSTEN	75 186.21 Re RHENIUM	76 190.23 Os OSMIUM	77 192.22 Ir IRIDIUM	78 195.08 Pt PLATINUM	79 196.97 Au GOLD	80 200.59 Hg MERCURY	81 204.38 Tl THALLIUM	82 207.2 Pb LEAD	83 208.98 Bi BISMUTH	84 (209) Po POLONIUM	85 (210) At ASTATINE	86 (222) Rn RADON	
87 (223) Fr FRANCIUM	88 (226) Ra RADIUM	89-103 Ac-Lr Actinide	104 (261) Rf RUTHERFORDIUM	105 (262) Db DUBNIUM	106 (266) Sg SEABORGIUM	107 (264) Bh BOHRNIUM	108 (277) Hs HASSIUM	109 (268) Mt MEITNERIUM	110 (281) Uun UNUNNIUM	111 (272) Uuu UNUNUNIUM	112 (285) Uub UNUNBIUM	114 (289) Uuq UNUNQUADIUM						

LANTHANIDE

57 138.91 La LANTHANUM	58 140.12 Ce CERIUM	59 140.91 Pr PRASEODYMIUM	60 144.24 Nd NEODYMIUM	61 (145) Pm PROMETHIUM	62 150.36 Sm SAMARIUM	63 151.96 Eu EUROPIUM	64 157.25 Gd GADOLINIUM	65 158.93 Tb TERBIUM	66 162.50 Dy DYSPROSIUM	67 164.93 Ho HOLMIUM	68 167.26 Er ERBIUM	69 168.93 Tm THULIUM	70 173.04 Yb YTTERBIUM	71 174.97 Lu LUTETIUM
-------------------------------------	----------------------------------	--	-------------------------------------	-------------------------------------	------------------------------------	------------------------------------	--------------------------------------	-----------------------------------	--------------------------------------	-----------------------------------	----------------------------------	-----------------------------------	-------------------------------------	------------------------------------

ACTINIDE

89 (227) Ac ACTINIUM	90 232.04 Th THORIUM	91 231.04 Pa PROTACTINIUM	92 238.03 U URANIUM	93 (237) Np NEPTUNIUM	94 (244) Pu PLUTONIUM	95 (243) Am AMERICIUM	96 (247) Cm CURIUM	97 (247) Bk BERKELIUM	98 (251) Cf CALIFORNIUM	99 (252) Es EINSTEINIUM	100 (257) Fm FERMIUM	101 (258) Md MENDELEVIUM	102 (259) No NOBELIUM	103 (262) Lr LAWRENCIUM
-----------------------------------	-----------------------------------	--	----------------------------------	------------------------------------	------------------------------------	------------------------------------	---------------------------------	------------------------------------	--------------------------------------	--------------------------------------	-----------------------------------	---------------------------------------	------------------------------------	--------------------------------------

(1) Pure Appl. Chem., 73, No. 4, 667-683 (2001)

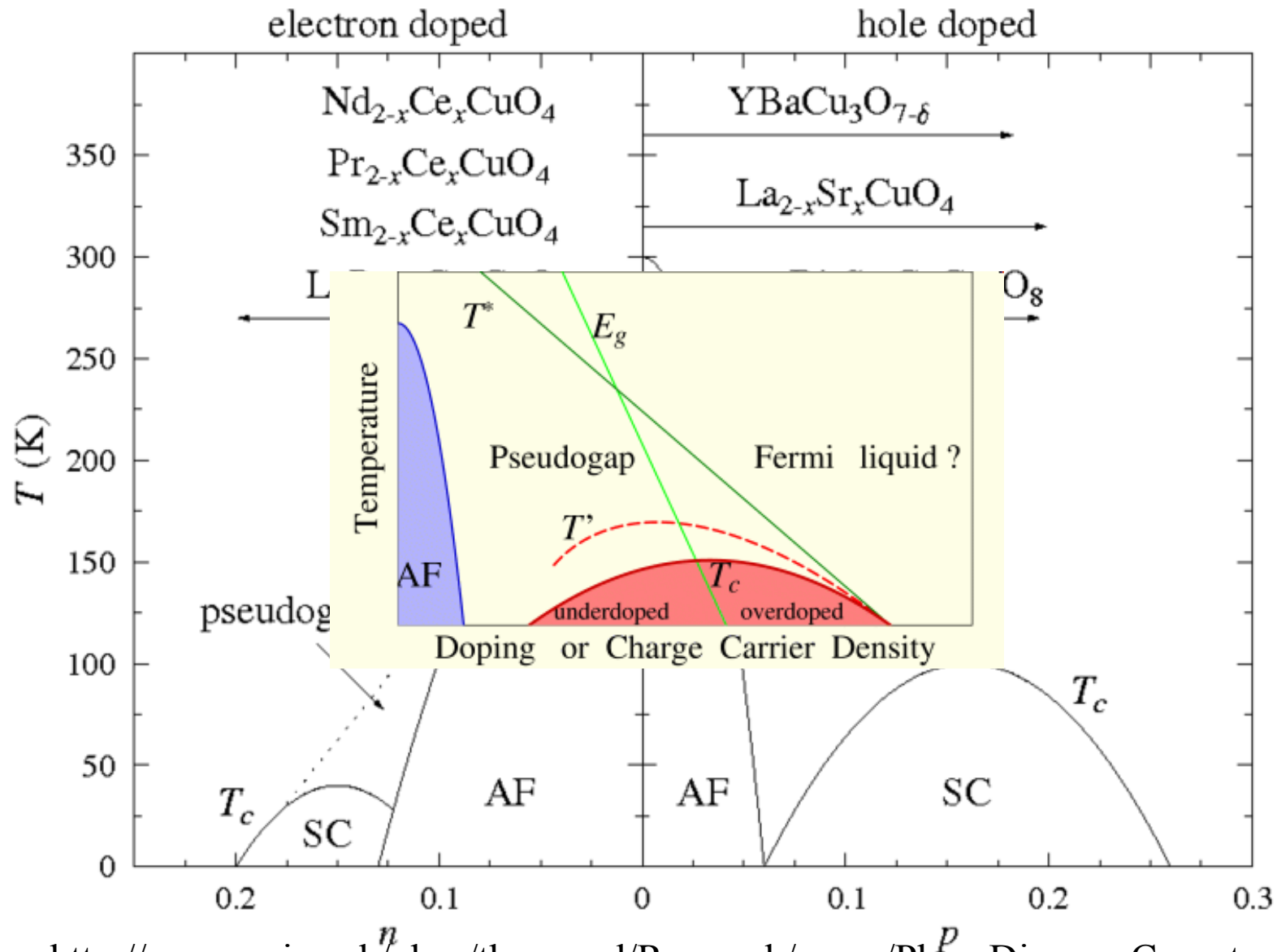
Relative atomic mass is shown with five significant figures. For elements having no stable nuclides, the value enclosed in brackets indicates the mass number of the longest-lived isotope of the element.

However three such elements (Th, Pa, and U) do have a characteristic terrestrial isotopic composition, and for these an atomic weight is tabulated.

Editor: Aditya Vardhan (adivar@netlinx.com)

Copyright © 1998-2003 EniG. (eni@ktf-split.hr)

Phase diagram for cuprate materials



<http://www.unine.ch/phys/theocond/Research/supra/PhaseDiagramCuprates.gif>

<http://en.wikipedia.org/wiki/File:Cuphasediag.png>

BCS formalism vs. Pairing Mechanism

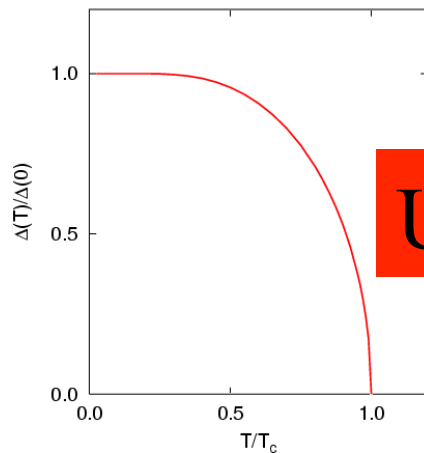
$$\Delta = |V| \frac{1}{N} \sum_k \frac{\Delta}{2E_k}$$

T_c equation (useless)

$$\frac{2\Delta}{k_B T_c} = 3.53$$

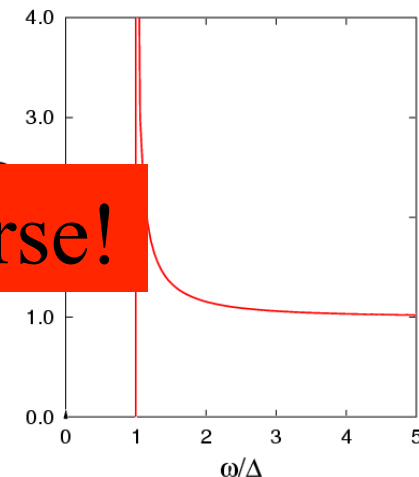
Universality

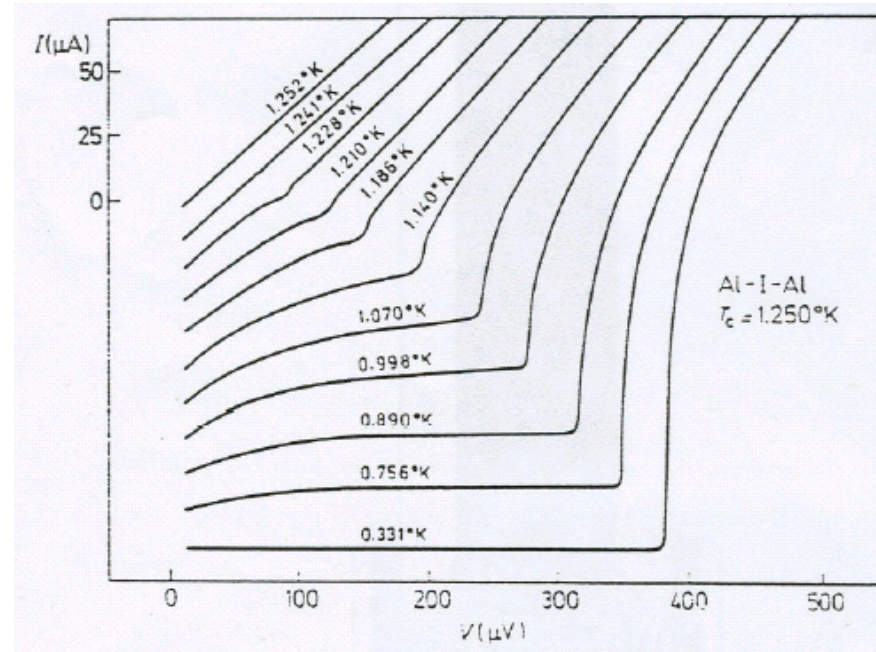
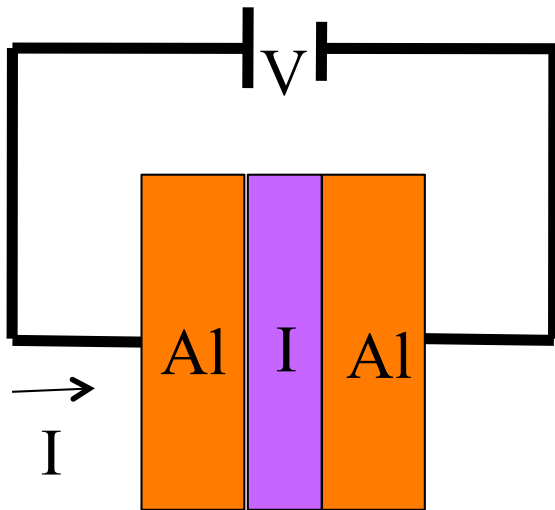
$$\frac{\Delta C}{\gamma T_c} = 1.43$$



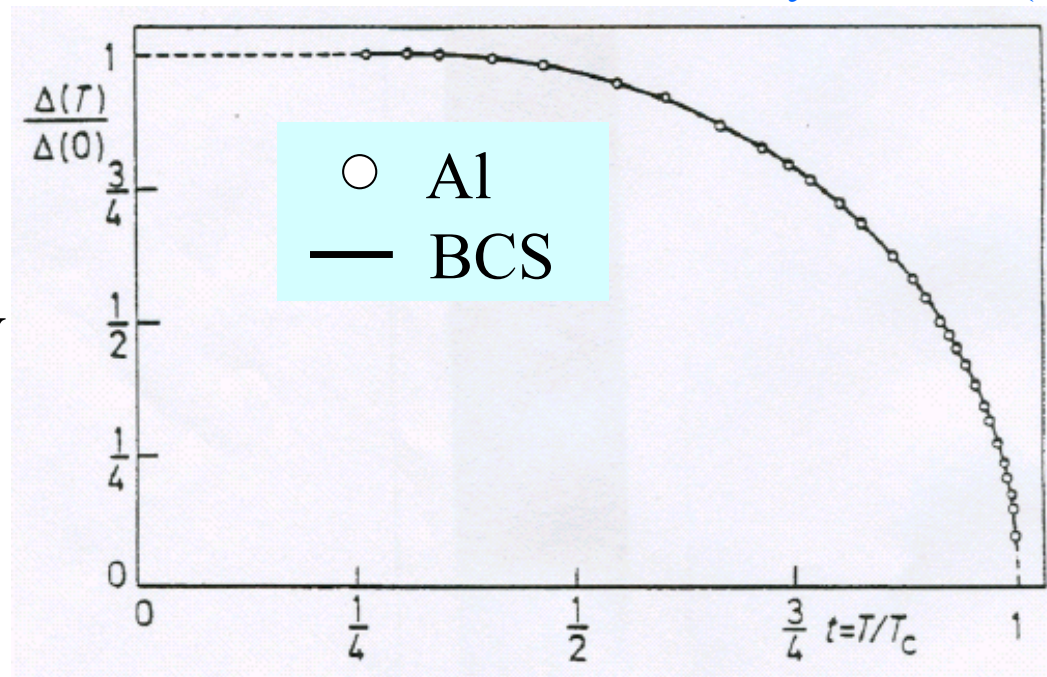
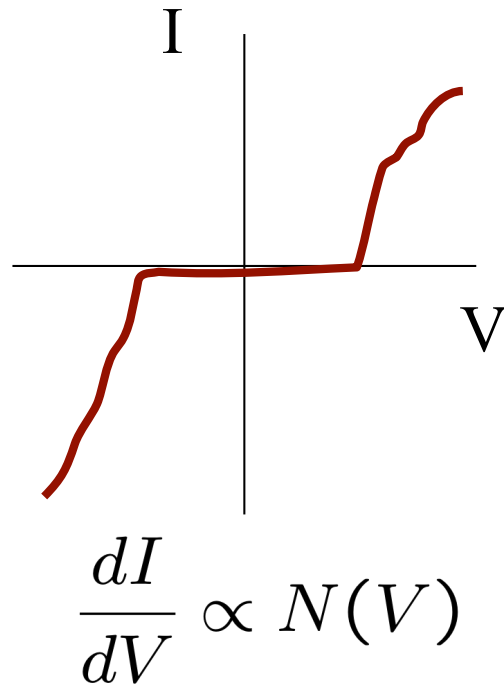
Universality is wonderful

Universality is a curse!



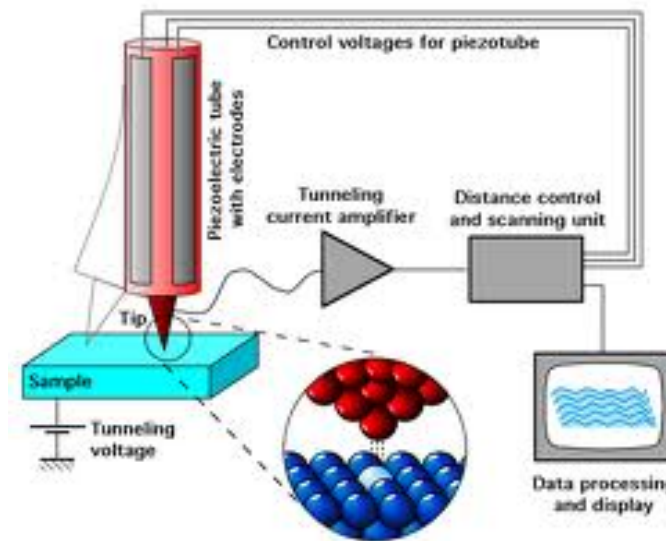


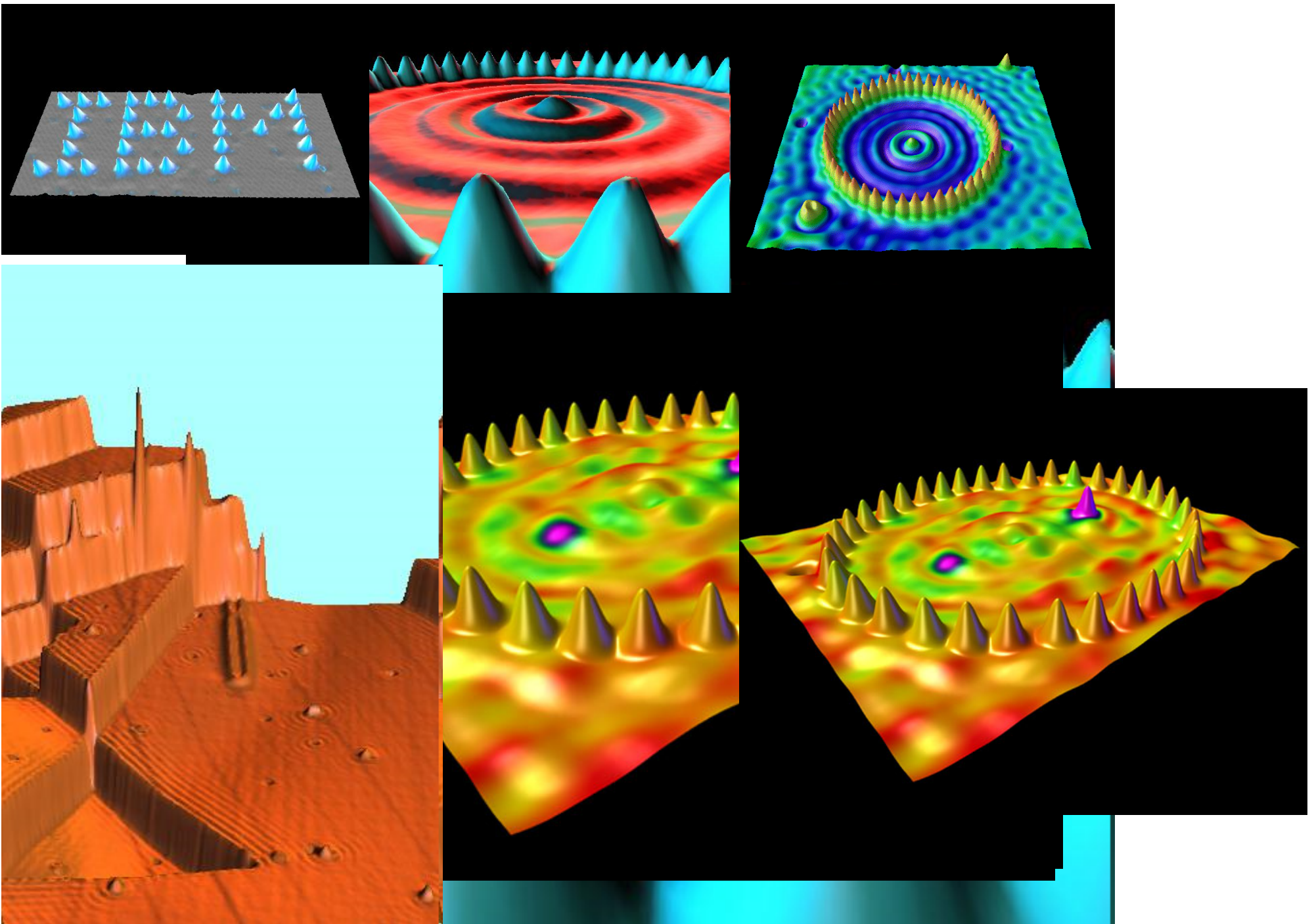
B.L. Blackford and R.H. March, Can. J. Phys. 46, 141 (1968)



Nowadays...

Scanning Tunneling Microscope (STM)





Crommie, Lutz, and Eigler <http://www.almaden.ibm.com/vis/index.html>

Pseudogap Precursor of the Superconducting Gap in Under- and Overdoped $\text{Bi}_2\text{Sr}_2\text{CaCu}_2\text{O}_{8+\delta}$

Ch. Renner,¹ B. Revaz,¹ J.-Y. Genoud,¹ K. Kadowaki,² and Ø. Fischer¹

¹DPMC, Université de Genève, 24, Quai Ernest-Ansermet, 1211 Genève 4, Switzerland

²University of Tsukuba, Institute of Materials Science, Tsukuba, 305 Ibaraki, Japan

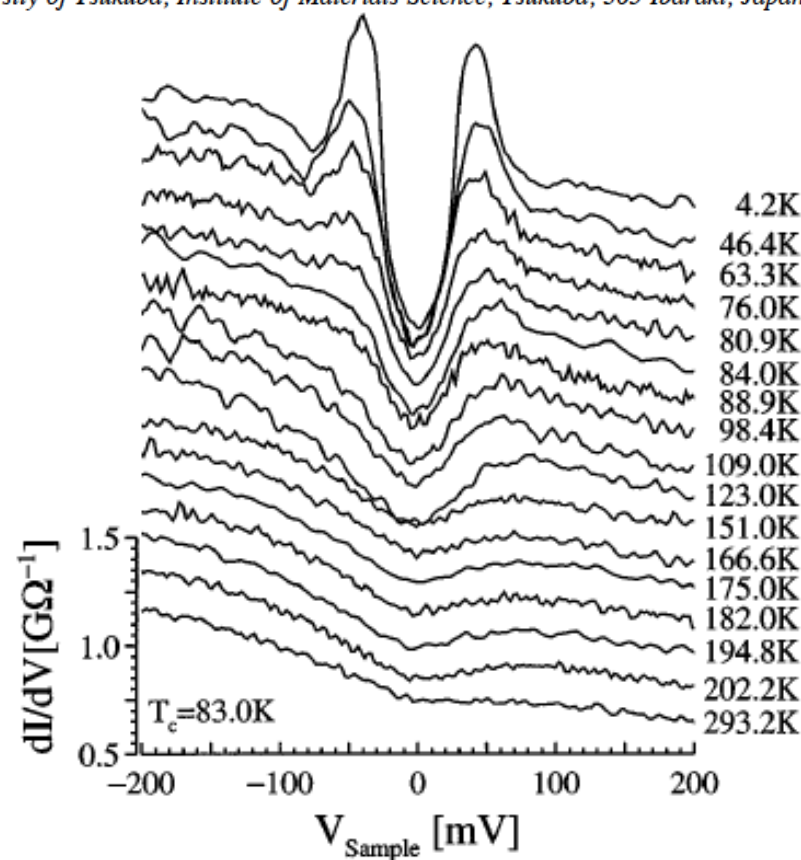


FIG. 2. Tunneling spectra measured as a function of temperature on underdoped Bi2212. The conductance scale corresponds to the 293 K spectrum, the other spectra are offset vertically for clarity.

Coincidence of Checkerboard Charge Order and Antinodal State Decoherence in Strongly Underdoped Superconducting $\text{Bi}_2\text{Sr}_2\text{CaCu}_2\text{O}_{8+\delta}$

K. McElroy,^{1,2,3} D.-H. Lee,^{1,2} J. E. Hoffman,⁴ K. M. Lang,⁵ J. Lee,³ E. W. Hudson,⁶ H. Eisaki,⁷
S. Uchida,⁸ and J. C. Davis^{3,*}

TABLE I. The average p

Figure 1	T_c	p (%)
(a)	89K OD	19 ± 1
(b)	79K UD	15 ± 1
(c)	75K UD	13 ± 1
(d)	65K UD	11 ± 1

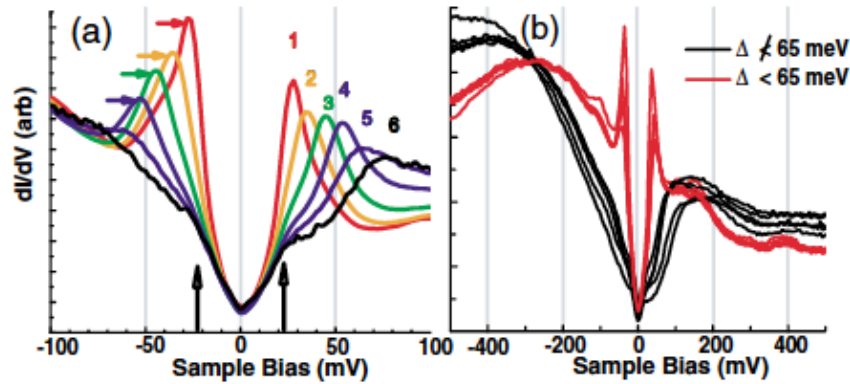


FIG. 2 (color). (a) The average spectrum, $g(E)$, associated with each gap value in a given FOV (field of view) from 1. These were extracted from 1(b) but the equivalent analysis for $g(\vec{r}, V)$ at all dopings yields results which are indistinguishable. The coherence peaks are seen spectra 1–4. (b) Characteristic spectra from the two regions $\Delta < 65$ (red) and $\Delta > 65$ (black). It

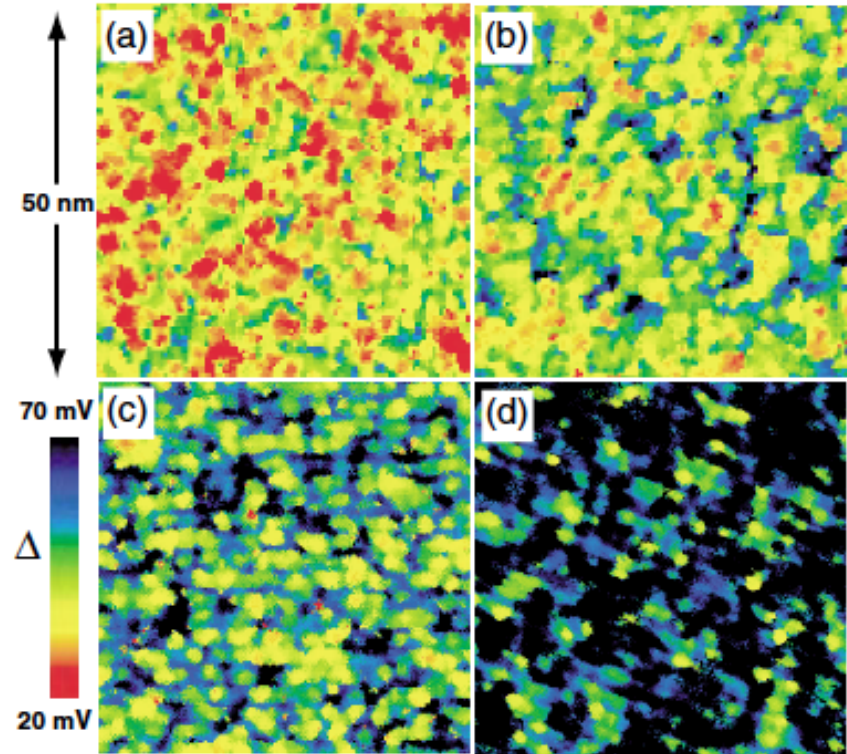
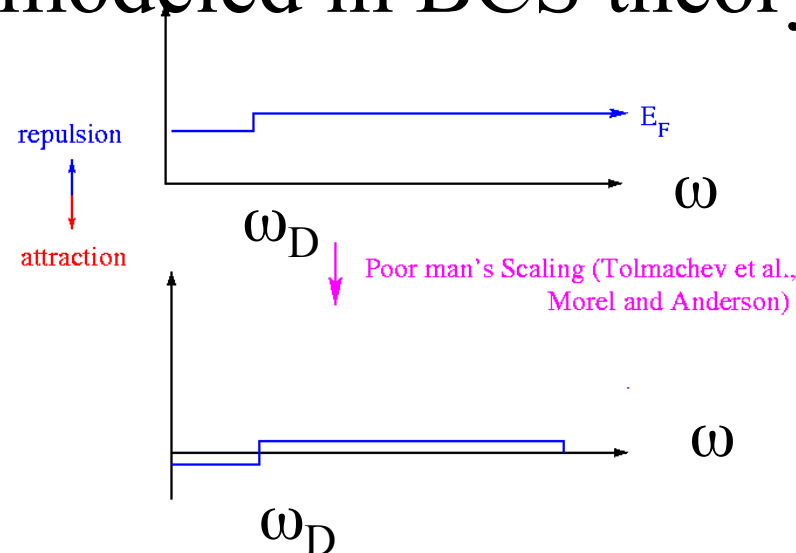


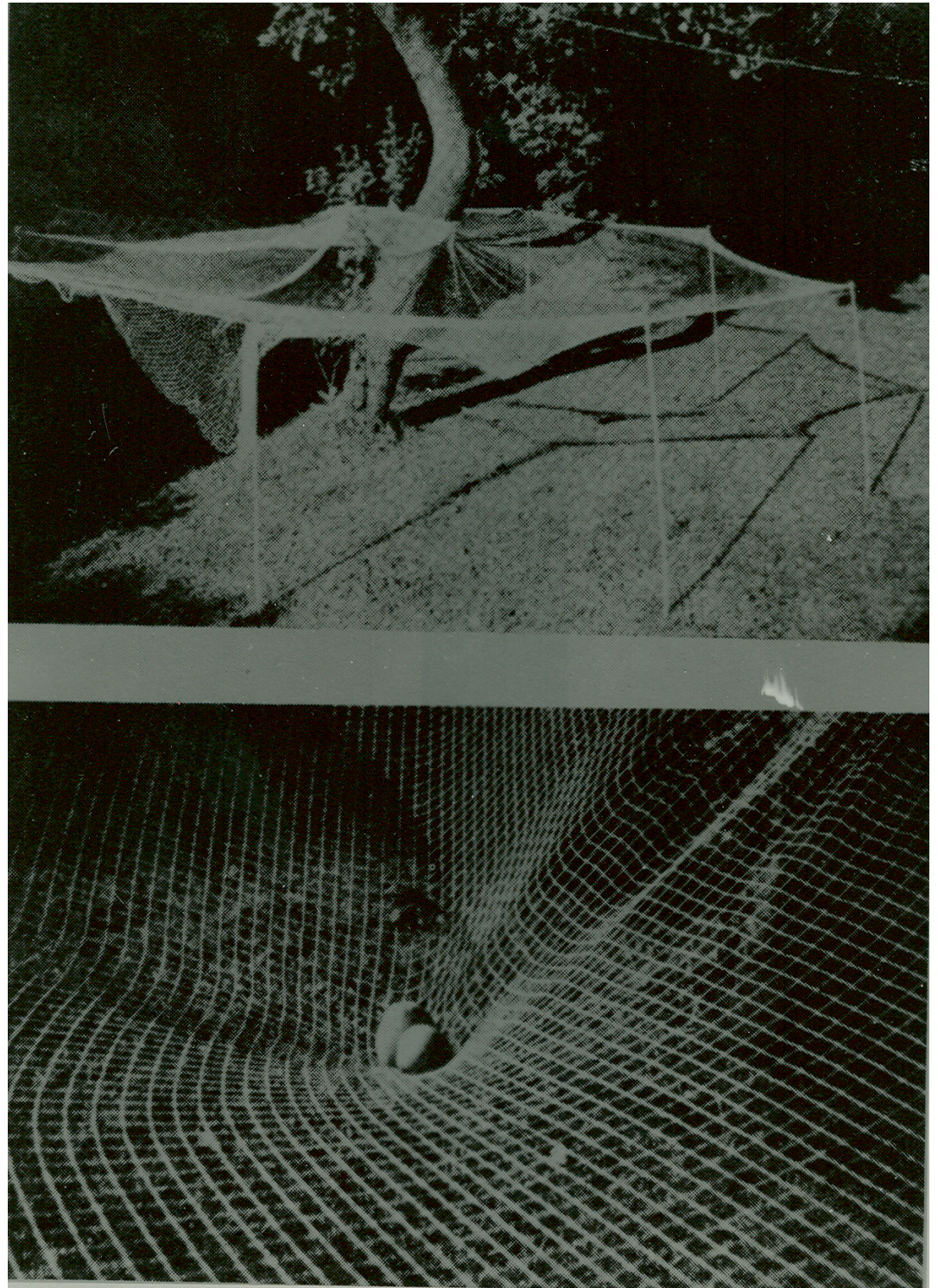
FIG. 1 (color). (a)–(d) Measured $\Delta(\vec{r})$, gap maps, for the four different hole-doping levels listed in I. Color scales identical.

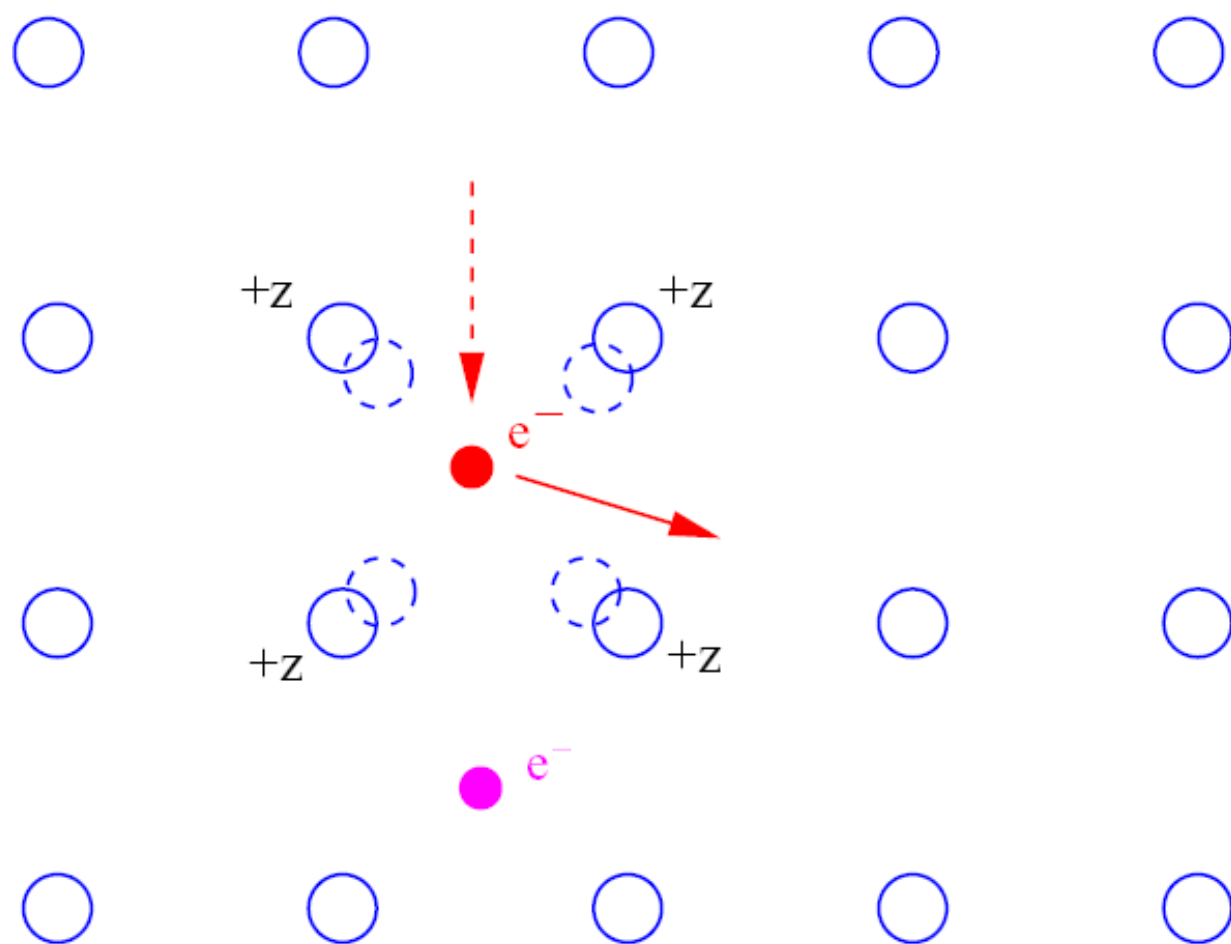
Eliashberg Theory

- Extension of BCS formalism to include dynamical electron-phonon interaction
- builds on Migdal theory in the normal state
- loosely modeled in BCS theory

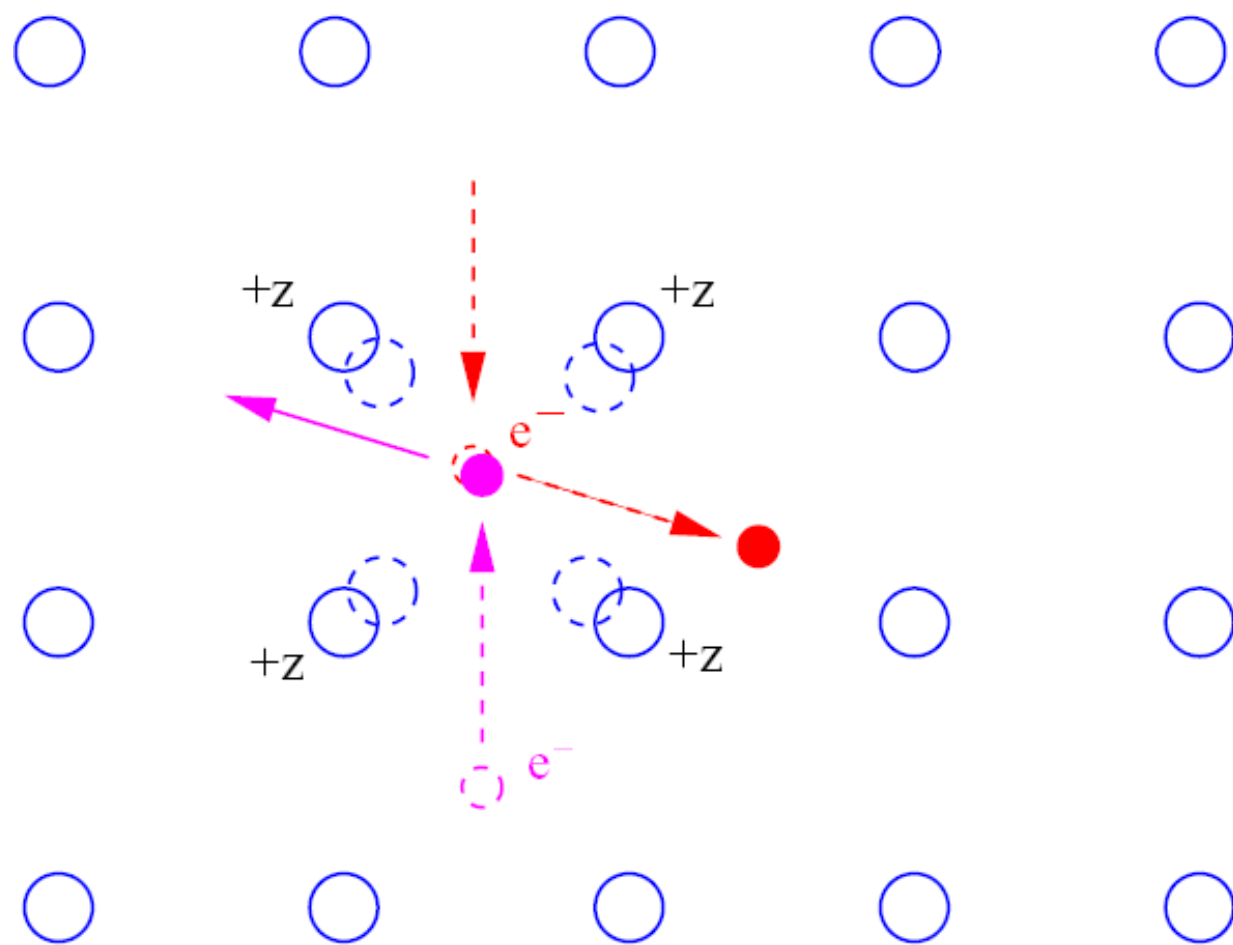


One electron
“attracts” the
second electron





effective attraction



effective attraction

Eliashberg Theory

$$\Delta(\textcolor{red}{k}, \textcolor{blue}{\omega}) = \mathcal{F}[V_{\textcolor{red}{k}, \textcolor{red}{k}'}(\textcolor{blue}{\omega}, \textcolor{blue}{\omega}')]]$$

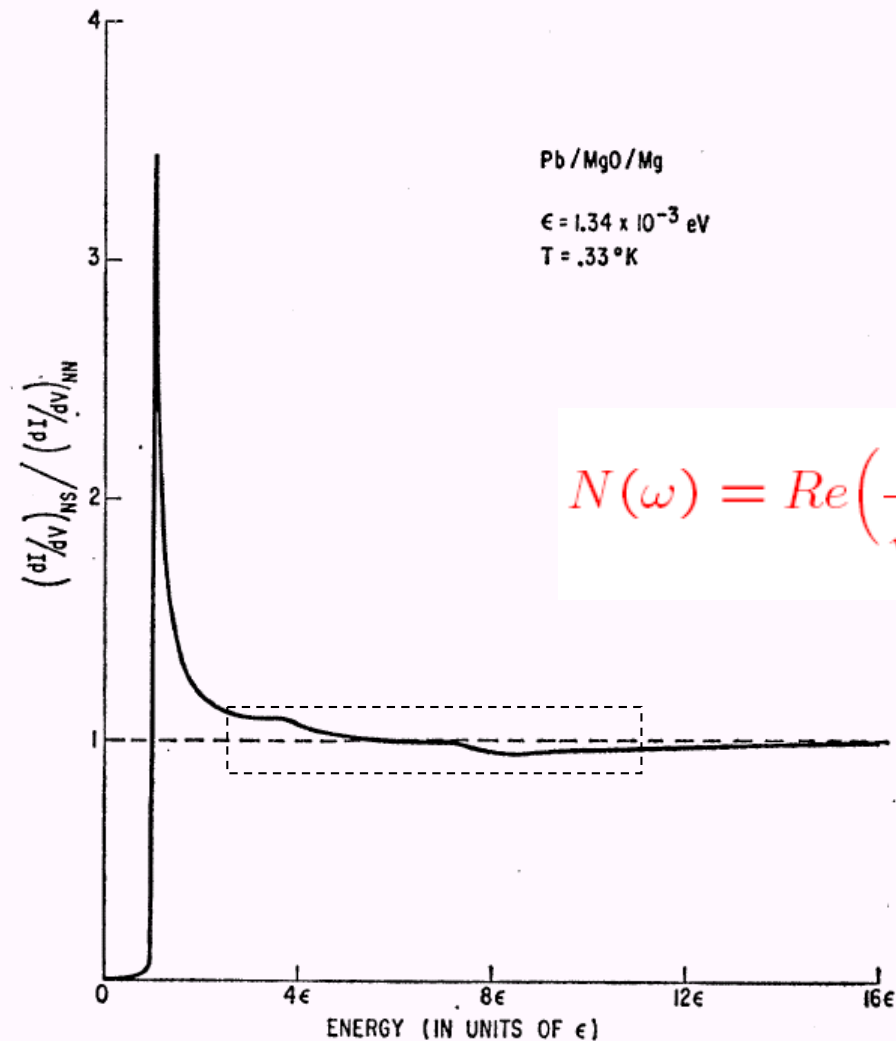


A functional of the interaction

Question: Can we invert the theory to extract the potential uniquely from a knowledge of $\Delta(\textcolor{red}{k}, \textcolor{blue}{\omega})$?

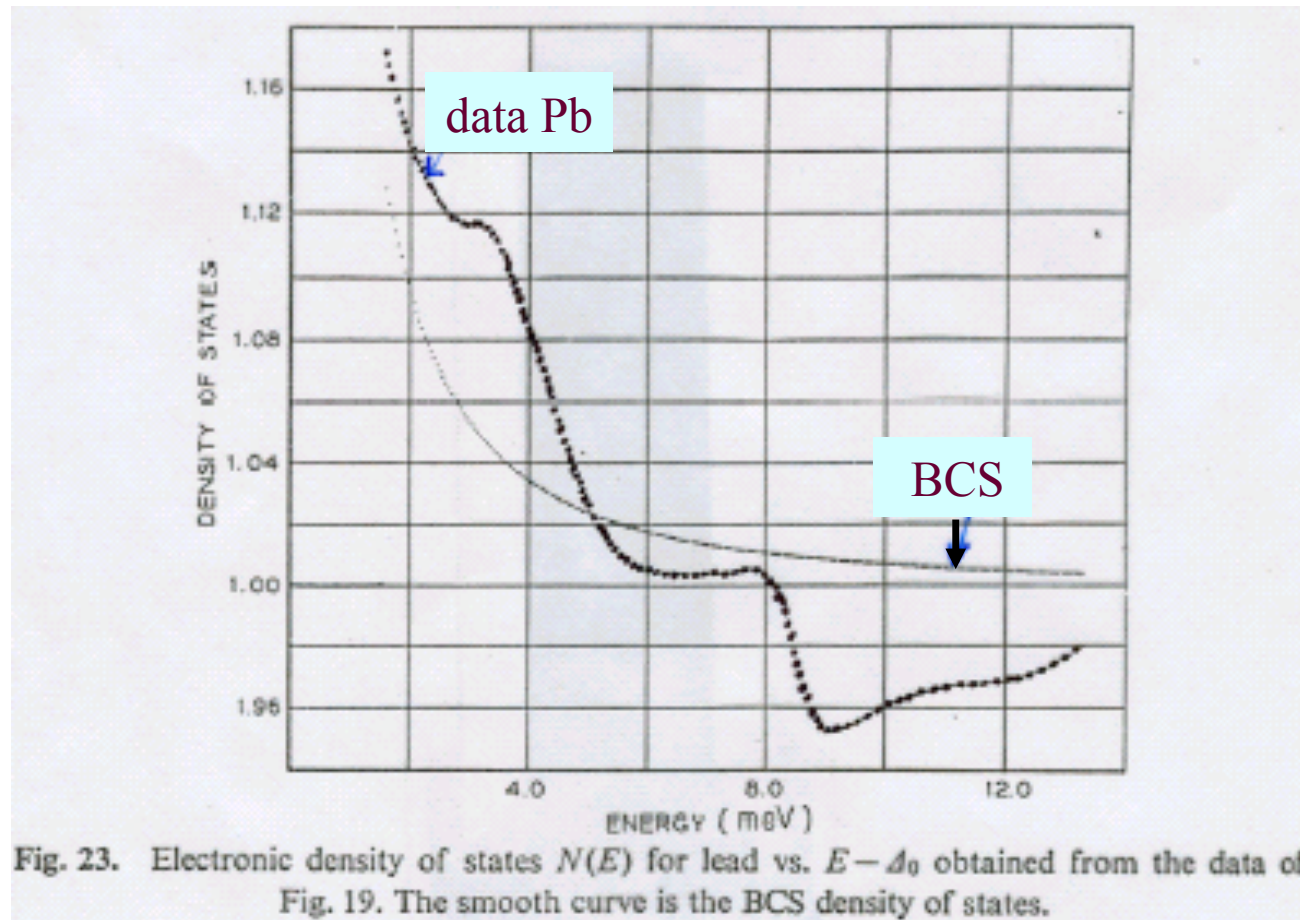
I. Giaever, H.R. Hart, Jr., and K. Megerle, PRB 126, 941 (1962)

$$\frac{dI}{dV} \sim N(\epsilon)$$



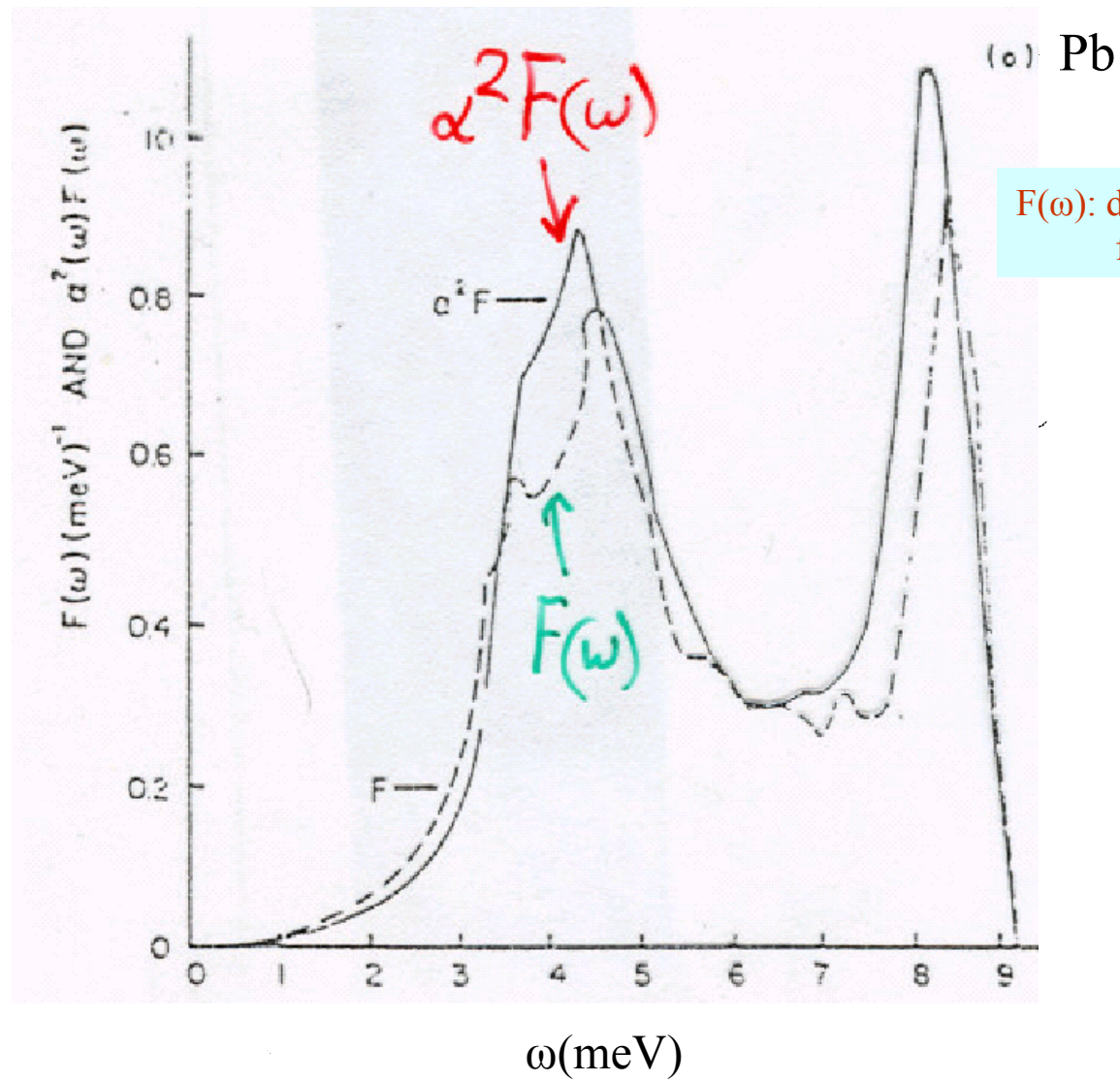
$$N(\omega) = \text{Re} \left(\frac{\omega}{\sqrt{\omega^2 - \Delta^2(\omega)}} \right)$$

FIG. 10. The relative conductance of a Pb-MgO-Mg sandwich plotted against energy. At higher energies there are definite divergences from the BCS density of states as can be seen from the bumps in the experimental curve. Note that the crossover point corresponds in energy to the Debye temperature.



requires Eliashberg theory:

- phonon dynamics (retardation) taken into account $[\alpha^2 F(\Omega)]$
- gap is a function of $\Delta(\omega) = \mathcal{F}[\{\alpha^2 F(\Omega)\}, \mu^*]$
- density of state $\frac{dI}{dV} \propto N(\omega) = N(\epsilon_F) \text{Re}\left\{\frac{\omega}{\sqrt{\omega^2 - \Delta^2(\omega)}}\right\}$



$F(\omega)$: density of phonon states
from neutron scattering

$$\alpha^2(\omega) \equiv \frac{\alpha^2 F(\omega)}{F(\omega)} \sim \text{constant}$$

Measurement of $\alpha^2F(\omega)$

- 1) measure structure in dI/dV accurately
- 2) “guess” $\alpha^2F(\omega)$
- 3) compute, using Eliashberg theory, $\frac{dI(\omega)}{dV}$
- 4) correct trial $\alpha^2F(\omega)$, using functional derivatives
- 5) iterate until calculated dI/dV agrees with experimental one

- structure beyond phonon region
- agrees fairly well with phonon density of states
- gap ratio comes out right
- mass enhancement comes out right
- agrees with thermodynamics

BUT, complexity of Coulomb repulsion is buried in one number, μ^*

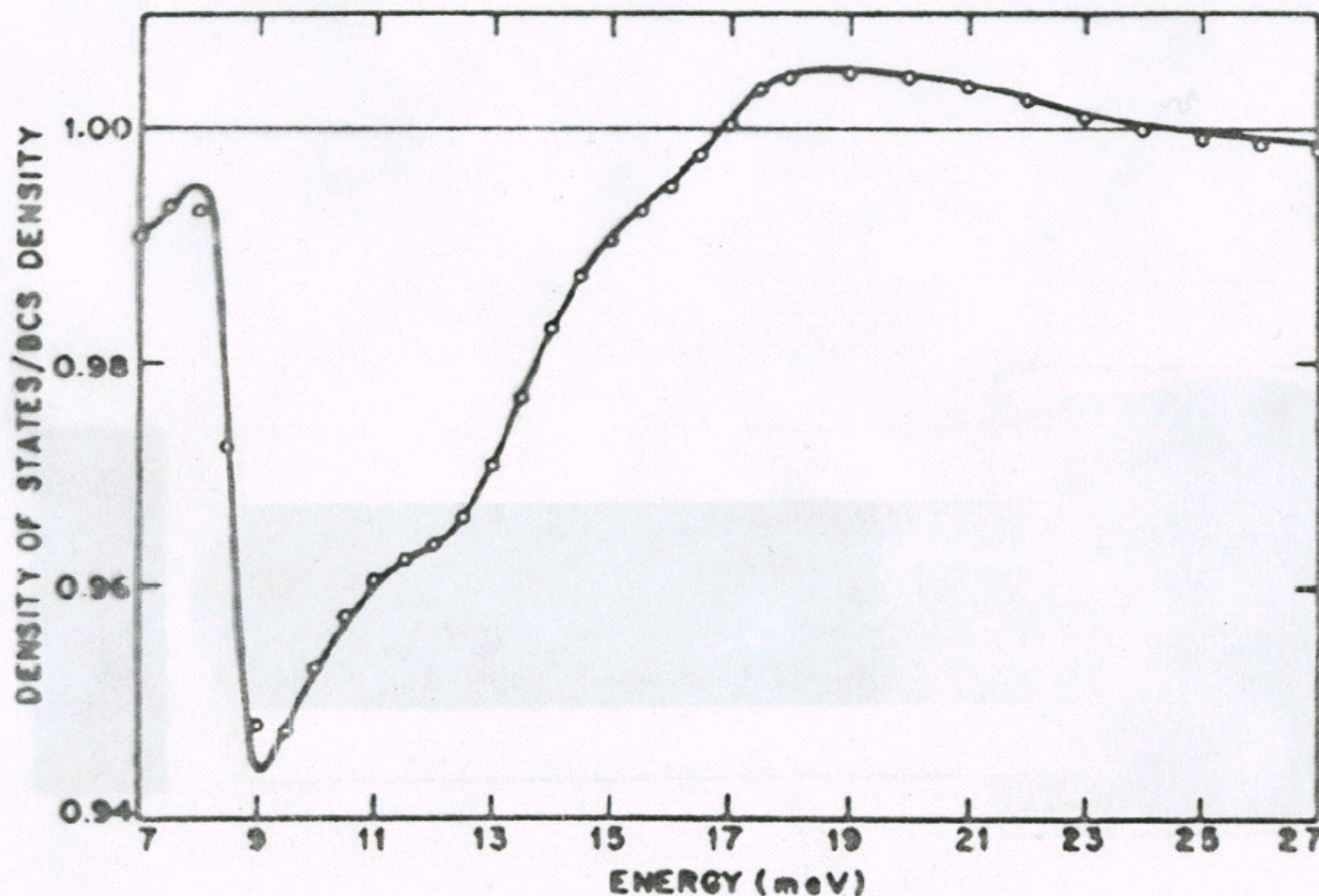


Fig. 32. Calculated (—) and measured (○○○) electronic density of states $N(E)$ for Pb normalized by the BCS density of states vs. $E - \Delta_0$. The measured density of states for $E - \Delta_0 > 11$ meV was not used in the fitting procedure and a comparison of theory and experiment in this “multiple-phonon-emission” region is a valid test of the theory. In the experiment the sharp drop near 9 meV is affected by thermal smearing.

Direct measurements of the *L*-gap surface states on the (111) face of noble metals by photoelectron spectroscopy

F. Reinert,* G. Nicolay, S. Schmidt, D. Ehm, and S. Hüfner

Photoemission

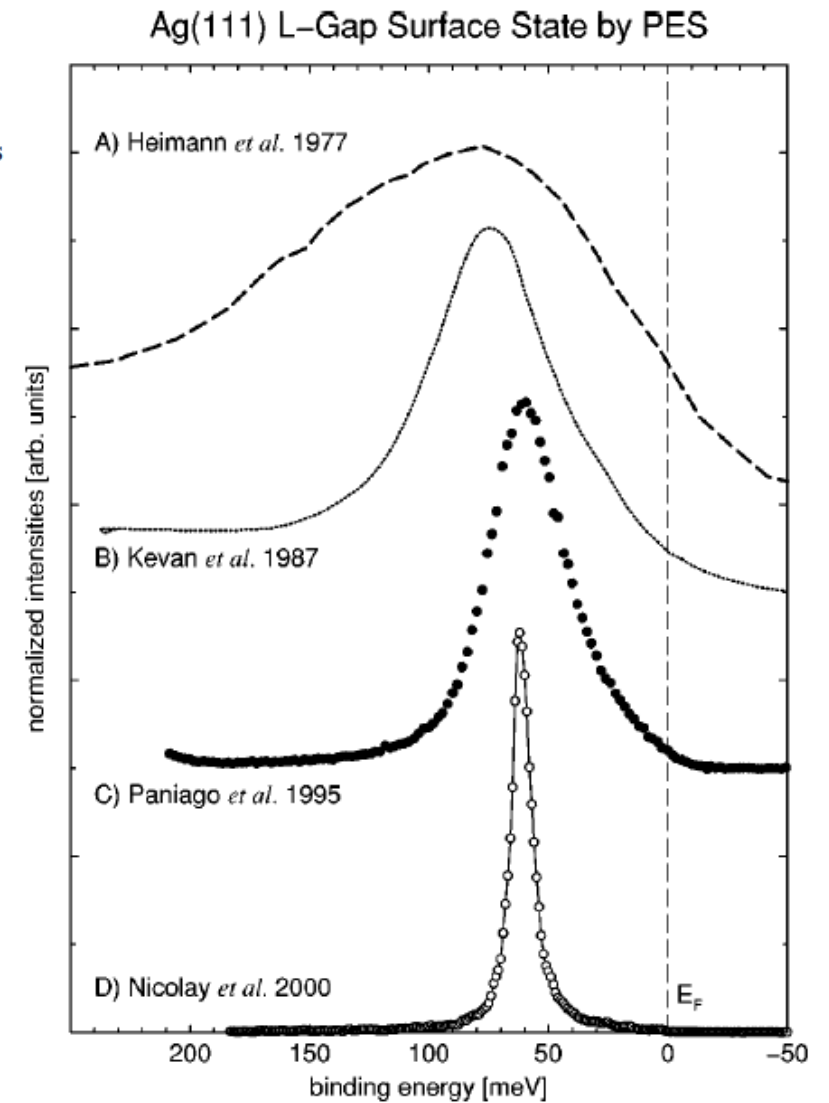
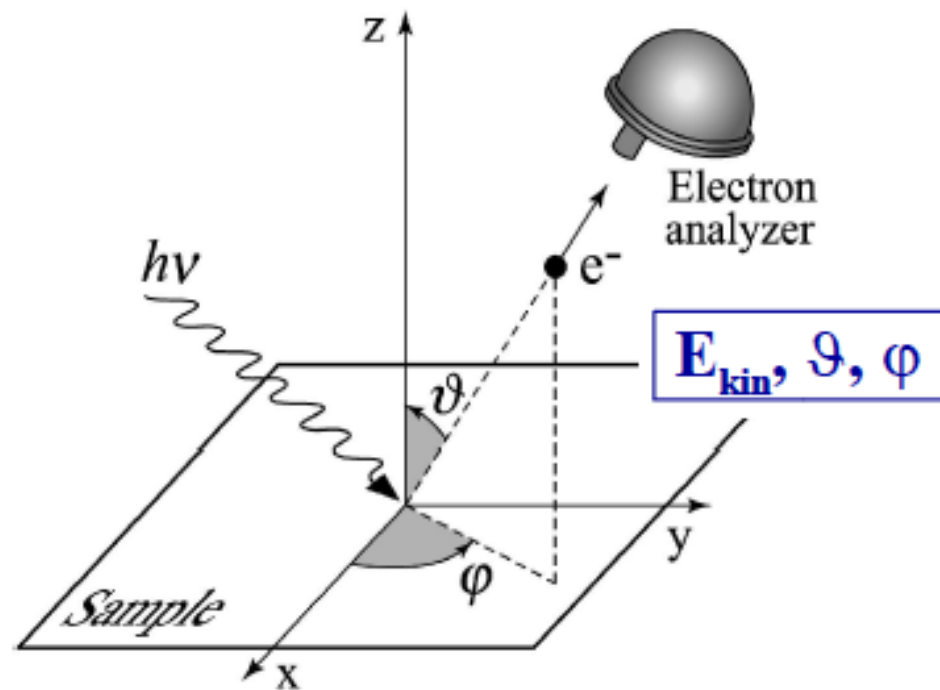
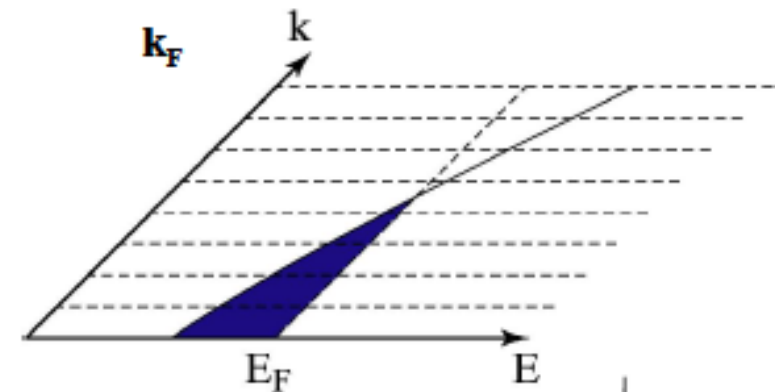


FIG. 1. Technological development in PES since the first observation of the Ag(111) surface state in photoemission spectra: (A) from Ref. 2 measured at room temperature (RT) with Ar I ($h\nu = 11.83$ eV), angular integrated; (B) from Ref. 30 at RT with $h\nu = 13$ eV, $\Delta E \approx 60$ meV and $\Delta\theta = 1^\circ$; (C) from Ref. 13 at $T = 56$ K with Ar I, $\Delta E = 21$ meV, and $\Delta\theta = 0.9^\circ$; (D) present data at $T = 30$ K with He I ($h\nu = 21.23$ eV), $\Delta E = 3.5$ meV and $\Delta\theta = \pm 0.15^\circ$.

Angle-Resolved Photoemission Spectroscopy



Electrons in Reciprocal Space



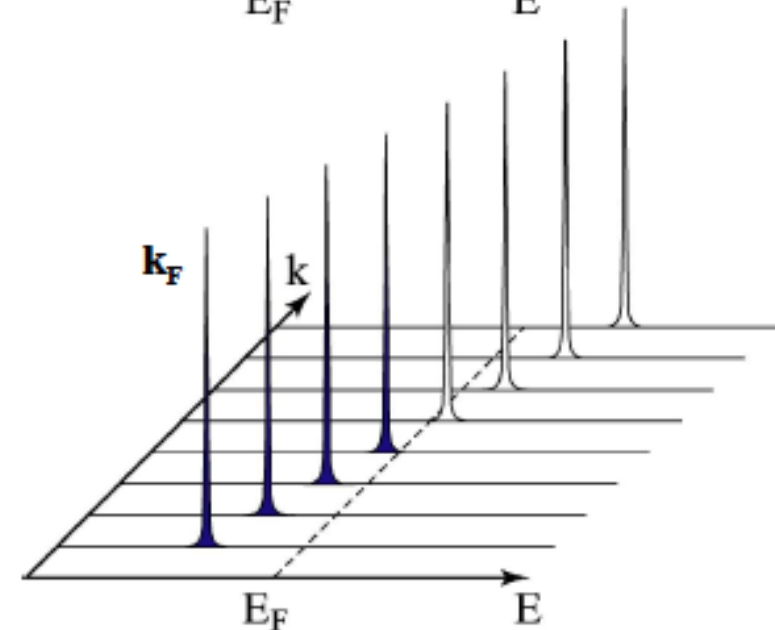
Energy Conservation

$$E_{kin} = h\nu - \phi - |E_B|$$

Momentum Conservation

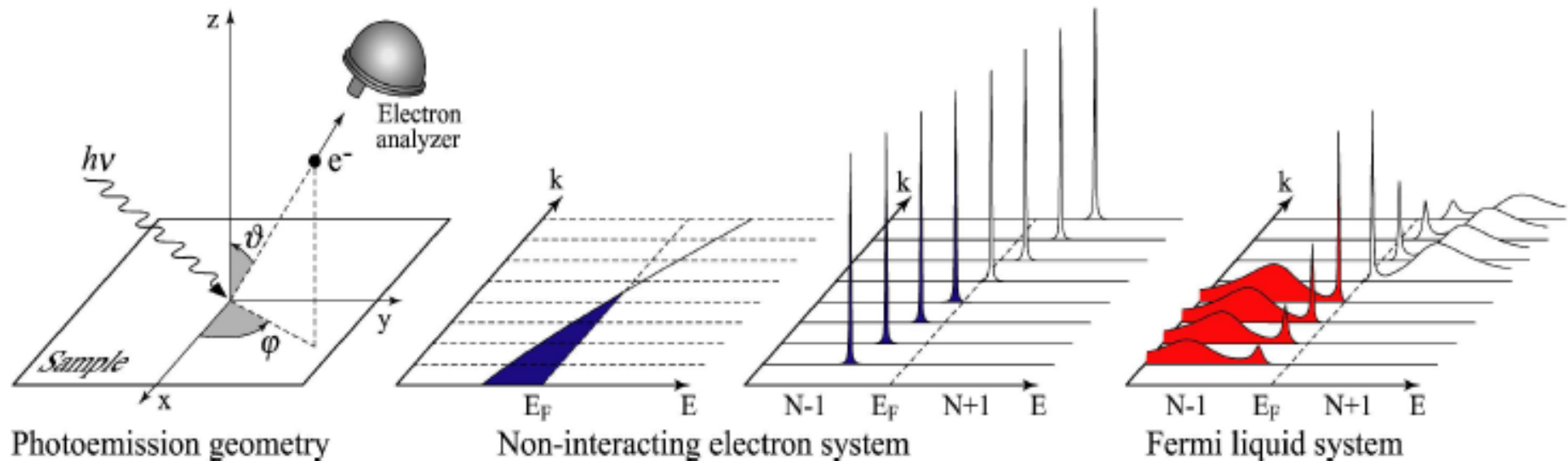
$$\mathbf{p}_{||} = \hbar \mathbf{k}_{||} = \sqrt{2m E_{kin}} \cdot \sin \theta$$

Damascelli (CIFAR Lectures)



Angle-Resolved Photoemission Spectroscopy

Damascelli (CIFAR Lectures)



Photoemission intensity: $I(k, \omega) = I_0 |M(k, \omega)|^2 f(\omega) A(k, \omega)$

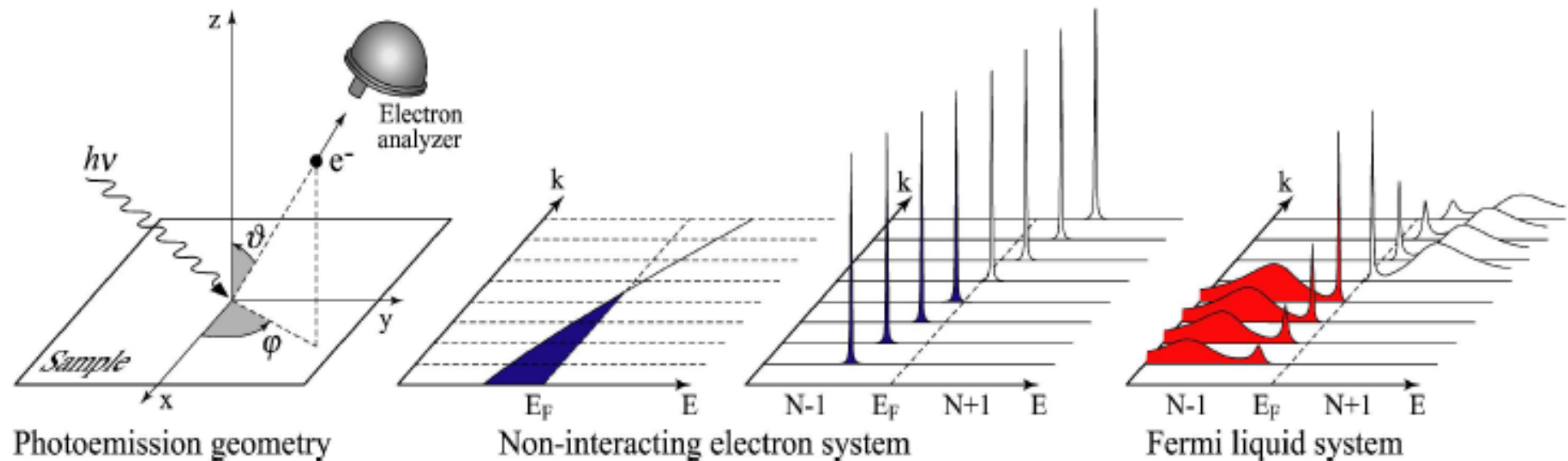
Single-particle spectral function

$$A(\mathbf{k}, \omega) = -\frac{1}{\pi} \frac{\Sigma''(\mathbf{k}, \omega)}{[\omega - \epsilon_{\mathbf{k}} - \Sigma'(\mathbf{k}, \omega)]^2 + [\Sigma''(\mathbf{k}, \omega)]^2}$$

$\Sigma(\mathbf{k}, \omega)$: the “self-energy” - captures the effects of interactions

Angle-Resolved Photoemission Spectroscopy

Damascelli (CIFAR Lectures)



Photoemission intensity: $I(k, \omega) = I_0 |M(k, \omega)|^2 f(\omega) A(k, \omega)$

Non-interacting

$$A(\mathbf{k}, \omega) = \delta(\omega - \epsilon_{\mathbf{k}})$$

No Renormalization

Infinite lifetime

Fermi Liquid

$$A(\mathbf{k}, \omega) = Z_{\mathbf{k}} \frac{\Gamma_{\mathbf{k}}/\pi}{(\omega - \epsilon_{\mathbf{k}})^2 + \Gamma_{\mathbf{k}}^2} + A_{inc}$$

$$m^* > m \quad |\epsilon_{\mathbf{k}}| < |\epsilon_{\mathbf{k}}|$$

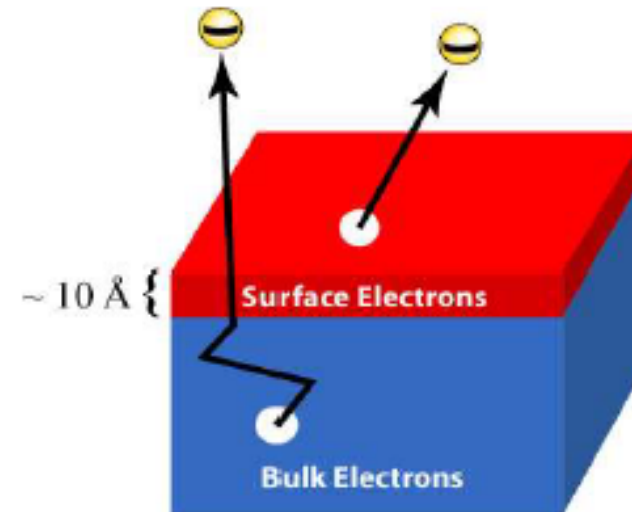
$$\tau_{\mathbf{k}} = 1/\Gamma_{\mathbf{k}}$$

ARPES: advantages and limitations

Advantages

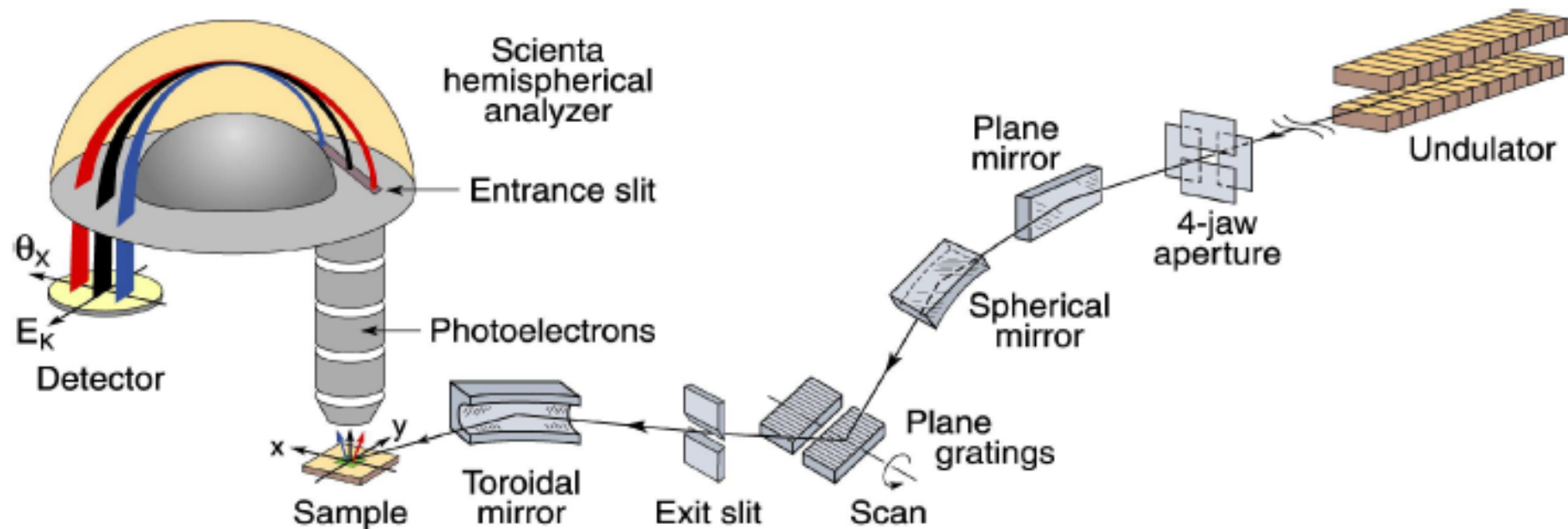
- **Direct information about electronic states!**
- Straightforward comparison with theory - little or no modelling.
- High-resolution information about **BOTH energy and momentum**
- **Surface-sensitive probe**
- Sensitive to “many-body” effects
- Can be applied to small samples (100 μm x 100 μm x 10 nm)

Limitations



- **Not bulk sensitive**
- Requires clean, atomically flat surfaces in **ultra-high vacuum**
- Cannot be studied as a function of pressure or magnetic field

Angle-Resolved Photoemission Spectroscopy

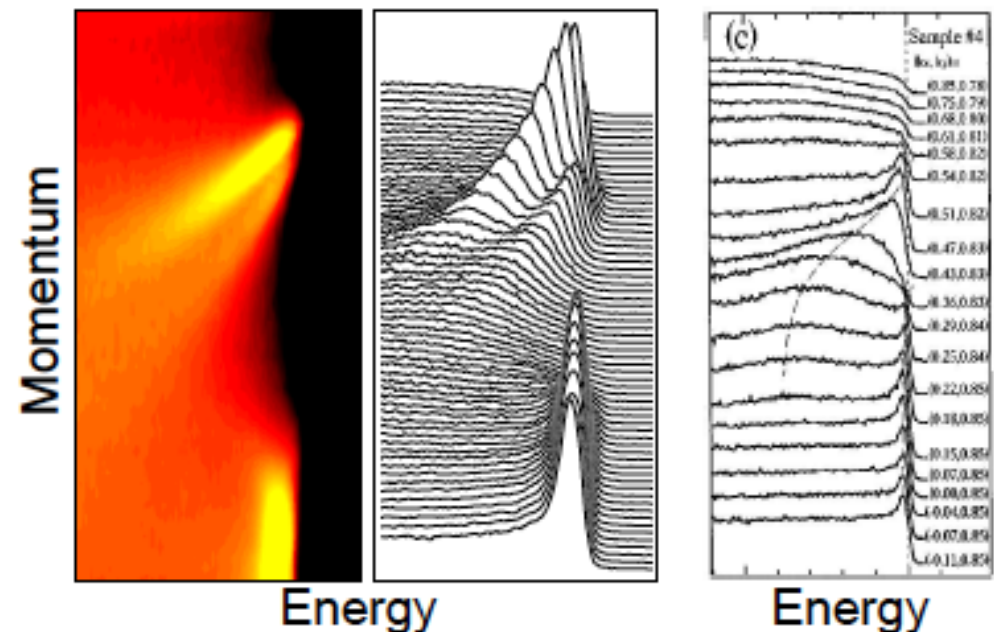


Parallel multi-angle recording

- Improved **energy resolution**
- Improved **momentum resolution**
- Improved **data-acquisition efficiency**

	ΔE (meV)	$\Delta \theta$
past	20-40	2°
now	2-10	0.2°

Damascelli (CIFAR Lectures)



Laser Based Angle-Resolved Photoemission, the Sudden Approximation, and Quasiparticle-Like Spectral Peaks in $\text{Bi}_2\text{Sr}_2\text{CaCu}_2\text{O}_{8+\delta}$

J. D. Koralek,^{1,2,*} J. F. Douglas,¹ N. C. Plumb,¹ Z. Sun,^{1,3} A. V. Fedorov,³ M. M. Murnane,^{1,2} H. C. Kapteyn,^{1,2} S. T. Cundiff,² Y. Aiura,⁴ K. Oka,⁴ H. Eisaki,⁴ and D. S. Dessau^{1,2,†}

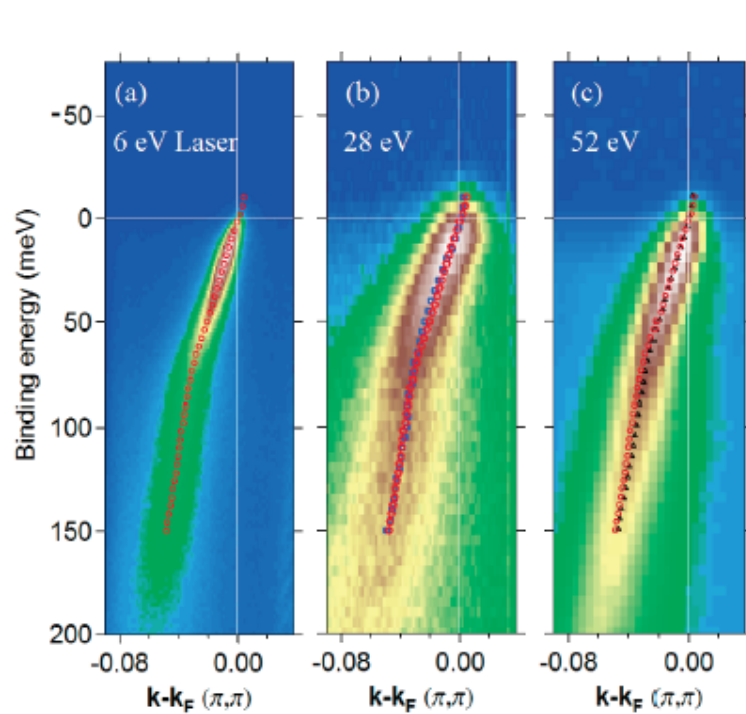


FIG. 1 (color). Comparison of ARPES along the node in near-optimally doped Bi2212 using (a) 6 eV laser photons at $T = 25$ K, (b) 28 eV photons at $T = 26$ K, and (c) 52 eV photons at $T = 16$ K. The images are scaled identically in E and \mathbf{k} , and all three contain MDC derived dispersion for the laser data (red circles). Additionally, the dispersions for the data of panels (b) and (c) are shown as blue squares and black triangles, respectively.

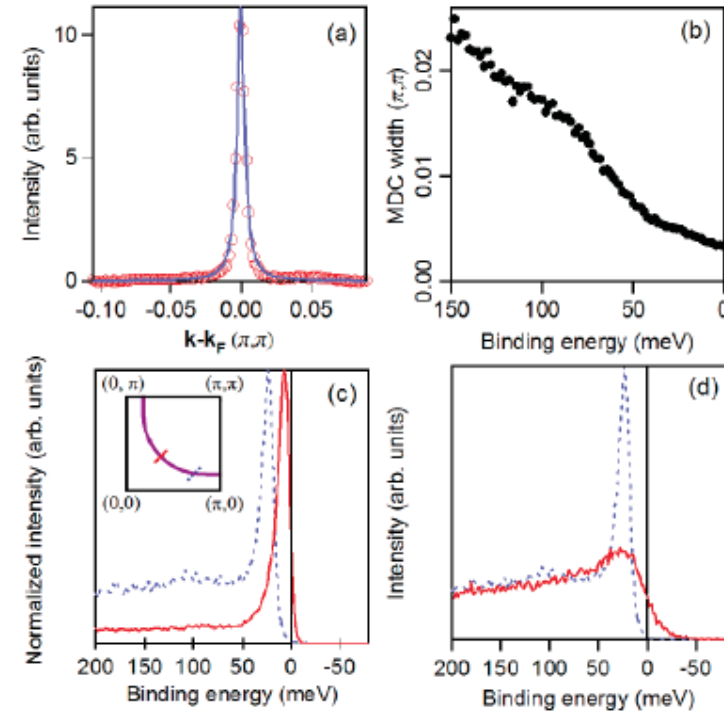


FIG. 2 (color). (a) The MDC at the Fermi energy (red circles) is shown along with a Lorentzian fit (blue line). (b) Lorentzian MDC half-widths from the 25 K laser ARPES data of Fig. 1(a). (c) Comparison of nodal (solid red line) and off-nodal (dotted blue line) laser ARPES in the superconducting state. The location of the cuts in the first Brillouin zone are shown in the inset. (d) Comparison of the off-nodal cut from (c) in the normal (solid red line) and superconducting (dotted blue line) states.

LETTERS

Superconductivity at 43 K in an iron-based layered compound $\text{LaO}_{1-x}\text{F}_x\text{FeAs}$

Hiroki Takahashi¹, Kazumi Igawa¹, Kazunobu Arii¹, Yoichi Kamihara², Masahiro Hirano^{2,3} & Hideo Hosono^{2,3}

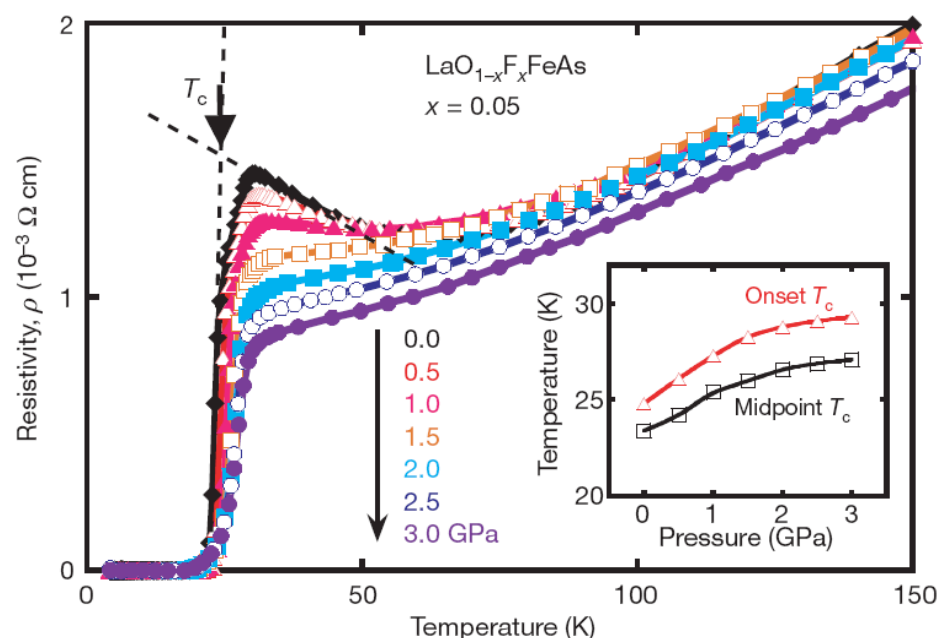
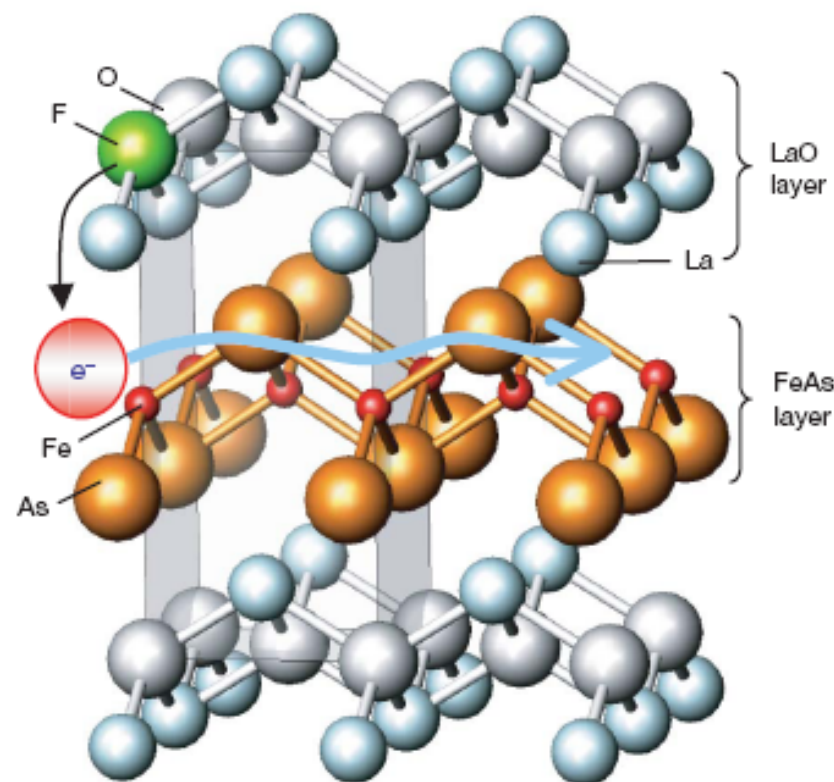
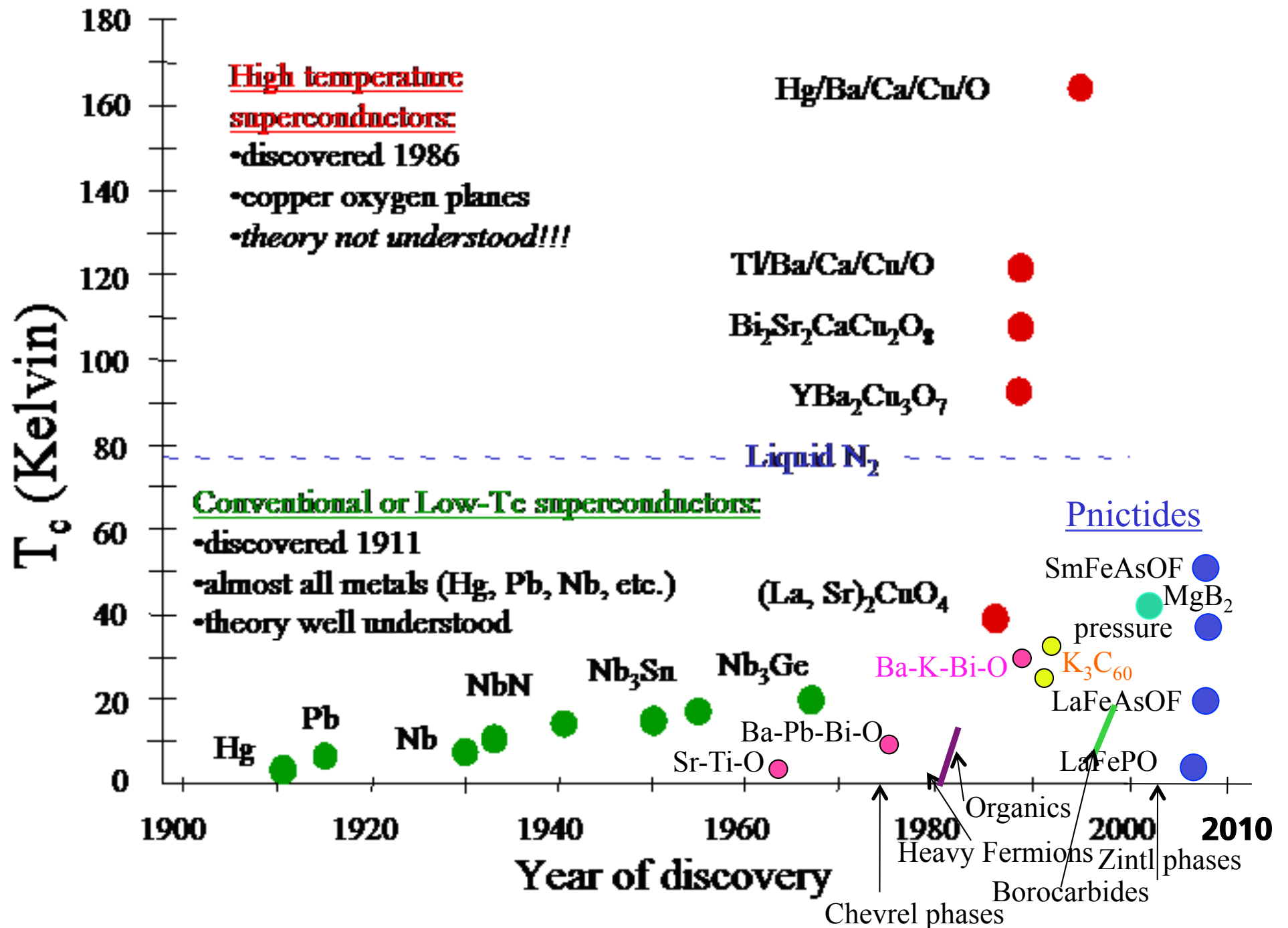


Figure 3 | Temperature dependence of the electrical resistivity of $\text{LaO}_{0.95}\text{F}_{0.05}\text{FeAs}$ below 3 GPa, using the piston–cylinder device. The inset shows the pressure dependence of the onset and midpoint T_c s. The onset T_c increases with increasing pressure, with an initial slope of 2.0 K per GPa.





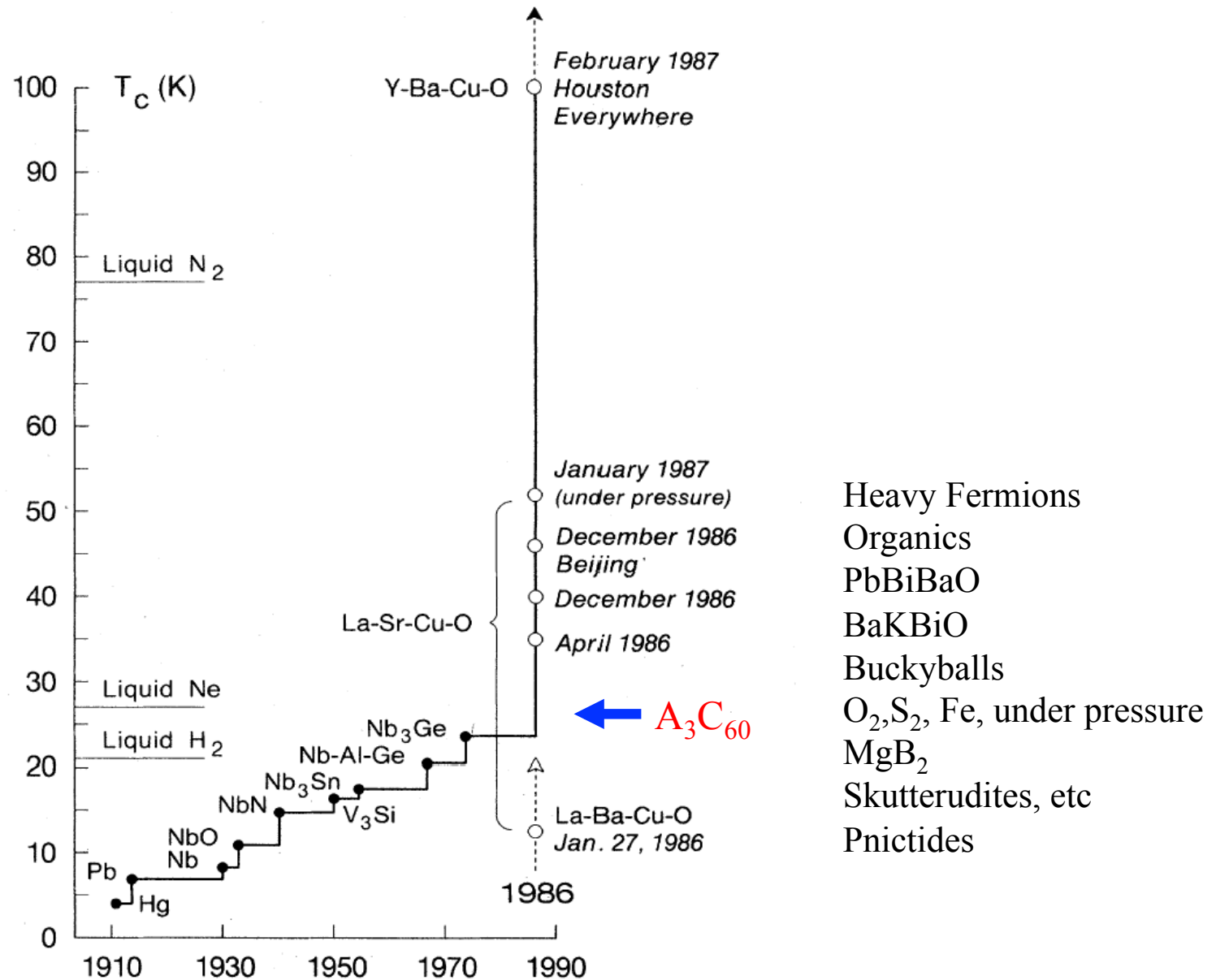


FIG. 13. Evolution of the superconductive transition temperature subsequent to the discovery of the phenomenon. From Müller and Bednorz (1987), © 1987 by the American Association for the Advancement of Science.

www.usatoday.com



Sports

SECTION C

Thursday, May 13, 2004

Sportsline

Baseball/American League

Coverage, 2-4C

Kansas City 4, Toronto 3	Cleveland 6, Boston 4
Texas 9, Tampa Bay 8	Oakland 2, Detroit 1
Baltimore at Chicago (ppd.)	Anaheim 11, New York 2
Minnesota 4, Seattle 3	

National League

Coverage, 3, 6C

Pittsburgh at Colorado (ppd.)	St. Louis 5, Atlanta 2
Milwaukee 4, Montreal 3	Florida 5, Houston 2
New York at Arizona	Cincinnati at San Diego
Chicago at Los Angeles	Philadelphia at San Francisco

Basketball/NBA playoffs

Coverage, 10C

Miami 100, Indiana 88	Minnesota at Sacramento
-----------------------	-------------------------

'Boss' buys tickets for military personnel

New York Yankees owner George Steinbrenner purchased 350 tickets for tonight's Game 2 of the NHL's Eastern Conference final between the Philadelphia Flyers and Tampa Bay Lightning for military personnel stationed at MacDill Air Force Base in Tampa. He also donated them to some of the families of servicemen and servicewomen fighting the war in Iraq. Steinbrenner also had donated more than 700 tickets for Game 2 of Tampa Bay's semifinals match-up against the Montreal Canadiens on April 25. Steinbrenner, who has a suite at the Ritz-Carlton, said he was proud to support the military.



Reuters

Steinbrenner, who has a suite at the Ritz-Carlton, said he was proud to support the military.



By Joseph Kaczmarek, AP

Big number: Little Matth Man, led by groom Maria Alvarez, is the longest of the long shots at 50-1. The draw and odds, 3C

Latest on Preakness

Derby winner Smarty Jones is the favorite, The Cliff's Edge might not run and Imperialism almost didn't come. Preakness news: In focus, 3C

LAKERS 2. SPURS 2. GAME 5 TONIGHT!



BCS formula up for tweaking

Stoops wants votes made public

By Steve Wieberg
USA TODAY

Architects of the Bowl Championship Series are close to drawing up a simpler and, they say, more fail-safe formula for selecting two teams to play for college football's national title.

The revisions won't be announced until next month. But Big East Conference Commissioner and outgoing BCS coordinator Mike Traghese said Wednesday that they'll likely streamline a convoluted mathematical formula, essentially giving one-third weight to the Association Press media poll, one-third to the USA TODAY/ESPN Coaches' Poll and a final one-third to a composite computer rating.

It no longer would include a separate strength-of-schedule rating, an escalating penalty for losses and probably bonuses for "quality" wins. A final determination is awaiting analysis by an outside mathematician.

The modifications, Traghese said, should avert a repeat of last year's messy split-championship outcome, which saw Southern California ranked No. 1 in the voting polls but left out of the BCS' championship game because of lower computer and strength-of-schedule ratings.

All three of the coaches involved in that controversy — USC's Pete Carroll, LSU's Nick Saban and Oklahoma's Bob Stoops — endorsed a change. "It was obvious after last year that a hard look was needed," Carroll said Wednesday.

Stoops, pointing to what would be an increased emphasis on the media and coaches' rankings, called for yet another change: publicizing ballots cast in both polls, something coaches in particular have balked at doing because of

the potential for offending opponents. "If you can't make it public, then you'd better know the coaches' poll out," he said. "There needs to be more accountability. If there's not, then that isn't any better than what we've had."

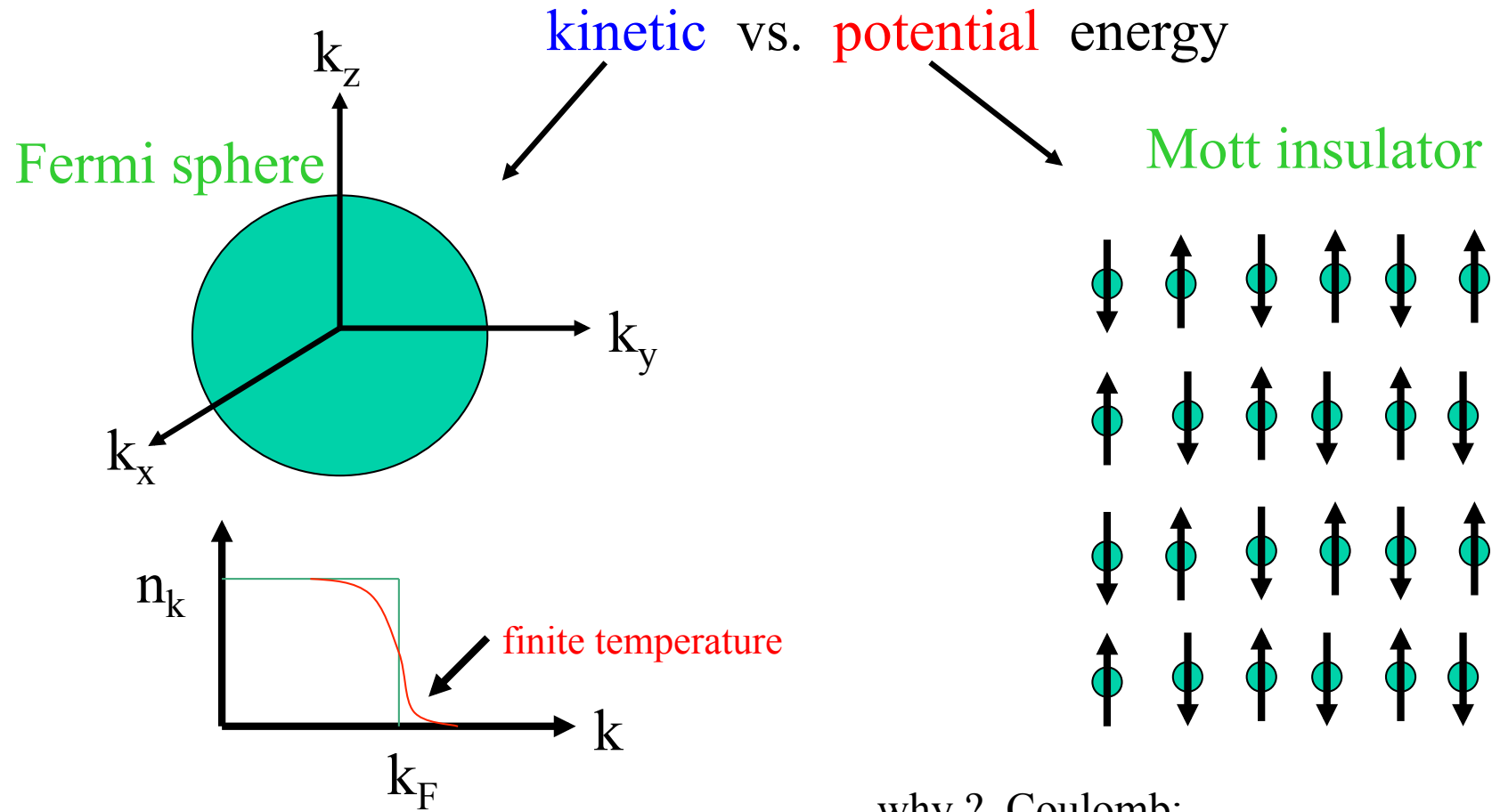
Traghese and the commissioners of the other five conferences that run the BCS met Wednesday in Chicago, along with those from the NCAA's five other major football-playing leagues. They're also weighing the BCS' long-term format, having largely committed to an additional, fifth BCS game and studying the feasibility of a new, stand-alone championship game matching the two highest-ranked winners.



Heat stay hot at home

Game 4 win evens series,

Electrons in solids



$$E_{\text{kin}} = 2 \sum \epsilon_k n_k$$

why ? Coulomb:
keep electrons away from one another !

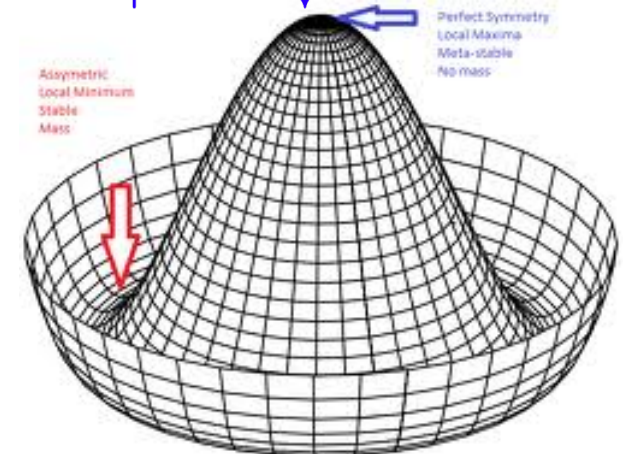
The conventional scenario: BCS



J. Bardeen L.N. Cooper J.R. Schrieffer

$$\psi_{\text{BCS}} = \prod_{\mathbf{k}} (u_{\mathbf{k}} + v_{\mathbf{k}} c_{\mathbf{k}\uparrow}^{\dagger} c_{-\mathbf{k}\downarrow}^{\dagger}) |0\rangle$$

$$\psi_{2\nu} = \int_0^{2\pi} \frac{d\theta}{2\pi} e^{-i\nu\theta} \prod_{\mathbf{k}} (u_{\mathbf{k}} + e^{i\theta} v_{\mathbf{k}} c_{\mathbf{k}\uparrow}^{\dagger} c_{-\mathbf{k}\downarrow}^{\dagger}) |0\rangle$$



It's all about pairs...

In Ogg's theory it was his intent
That the current keep flowing, once sent;
So to save himself trouble,
He put them in double,
And instead of stopping, it went.

George Gamow

**Bose-Einstein Condensation of Trapped Electron
Pairs. Phase Separation and Super-
conductivity of Metal-Ammonia
Solutions**

RICHARD A. OGG, JR.
Department of Chemistry, Stanford University, California
March 2, 1946

...Cooper pairs

The conventional scenario: BCS



J. Bardeen L.N. Cooper J.R. Schrieffer

$$\psi_{\text{BCS}} = \prod_{\mathbf{k}} (u_{\mathbf{k}} + v_{\mathbf{k}} c_{\mathbf{k}\uparrow}^{\dagger} c_{-\mathbf{k}\downarrow}^{\dagger}) |0\rangle$$

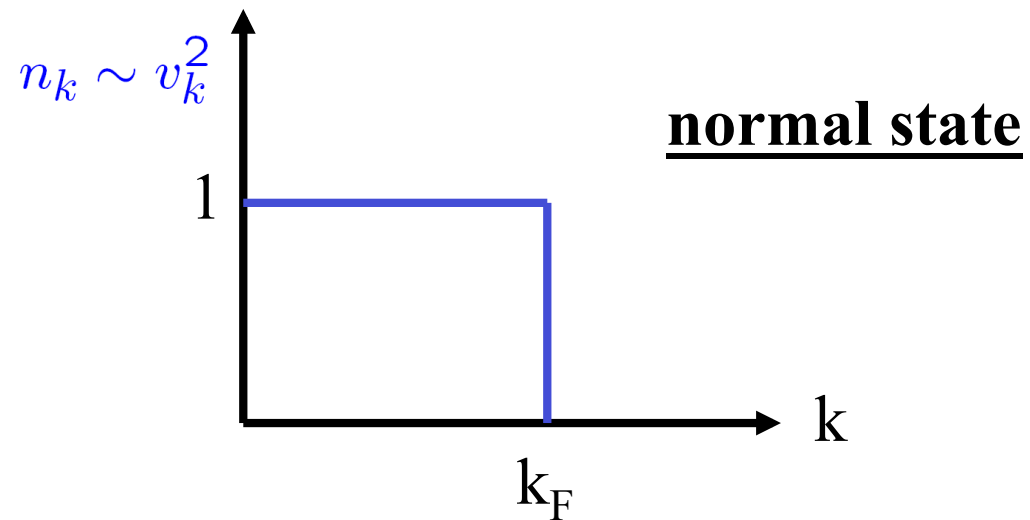
↑
all \mathbf{k} 's !! --- occupation is controlled by $u_{\mathbf{k}}$ and $v_{\mathbf{k}}$.

order parameter ($\Delta_{\mathbf{k}}$) becomes non-zero, so, e.g.

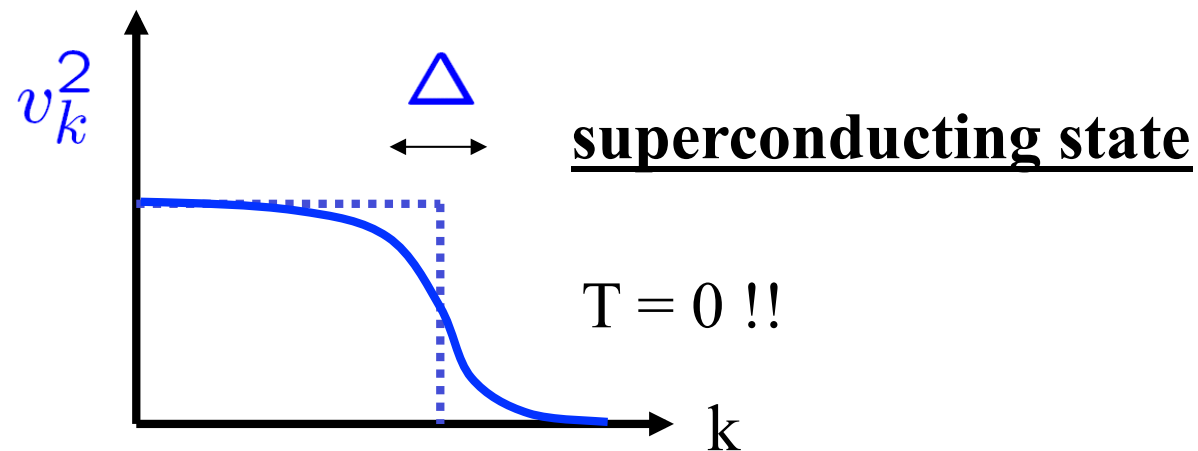
$$v_{\mathbf{k}}^2 = \frac{1}{2} \left(1 - \frac{\epsilon_{\mathbf{k}}}{E_{\mathbf{k}}} \right) \quad \text{where} \quad E_{\mathbf{k}} = \sqrt{\epsilon_{\mathbf{k}}^2 + \Delta_{\mathbf{k}}^2}$$

$$\sim 1 \quad \text{for} \quad \epsilon_{\mathbf{k}} < 0$$

$$\sim 0 \quad \text{for} \quad \epsilon_{\mathbf{k}} > 0$$



why sacrifice
kinetic energy ?

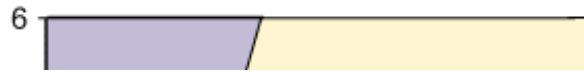


Ans: gain
potential energy

remember,
$$v_k^2 = \frac{1}{2} \left(1 - \frac{\epsilon_k}{\sqrt{\epsilon_k^2 + \Delta_k^2}} \right)$$

Supersolid Helium

Supersolid phase in He⁴?



PRL 109, 155301 (2012)

PHYSICAL REVIEW LETTERS

week ending
12 OCTOBER 2012

Absence of Supersolidity in Solid Helium in Porous Vycor Glass

Duk Y. Kim and Moses H. W. Chan*

Department of Physics, Pennsylvania State University, University Park, Pennsylvania 16802, USA

(Received 24 July 2012; published 8 October 2012)

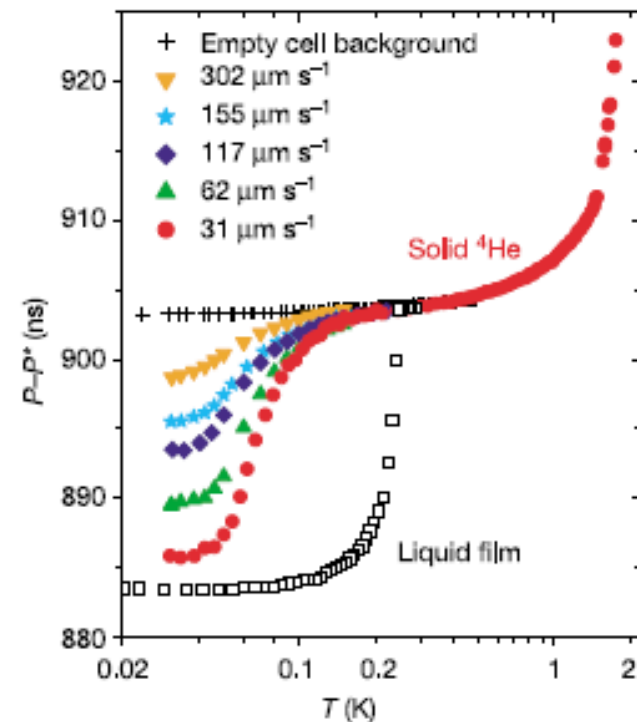
In 2004, Kim and Chan carried out torsional oscillator measurements of solid helium confined in porous Vycor glass and found an abrupt drop in the resonant period below 200 mK. The period drop was interpreted as probable experimental evidence of nonclassical rotational inertia. This experiment sparked considerable activities in the studies of superfluidity in solid helium. More recent ultrasound and torsional oscillator studies, however, found evidence that shear modulus stiffening is responsible for at least a fraction of the period drop found in bulk solid helium samples. The experimental configuration of Kim and Chan makes it unavoidable to have a small amount of bulk solid inside the torsion cell containing the Vycor disk. We report here the results of a new helium in Vycor experiment with a design that is completely free from any bulk solid shear modulus stiffening effect. We found no measurable period drop that can be attributed to nonclassical rotational inertia.

Probable observation of a supersolid helium phase

E. Kim & M. H. W. Chan

Department of Physics, The Pennsylvania State University, University Park, Pennsylvania 16802, USA

When liquid ^4He is cooled below 2.176 K, it undergoes a phase transition—Bose–Einstein condensation—and becomes a superfluid with zero viscosity¹. Once in such a state, it can flow without dissipation even through pores of atomic dimensions. Although it is intuitive to associate superflow only with the liquid phase², it has been proposed theoretically^{3–5} that superflow can also occur in the solid phase of ^4He . Owing to quantum mechanical fluctuations, delocalized vacancies and defects are expected to be present in crystalline solid ^4He , even in the limit of zero temperature. These zero-point vacancies can in principle allow



news and views

intein that can have such a domain consists of 134 amino acids^{5,6}. So it is unlikely that the events described by Hanada *et al.* are regulated in the same way. More similar is the process, seen in jack beans, of enzyme-mediated protein splicing — the ligation of polypeptide stretches to result in a functional protein⁷. In addition, protease enzymes, which generally slice up proteins, have been engineered to work in reverse⁸. Whatever

Condensed-matter physics

Supersolid helium

John Beamish

Superfluids flow without resistance. It's hard to imagine, but quantum mechanically possible, that solids should do the same at low enough temperatures. Helium-4 might be the first known 'supersolid'.

actual period P and $P^* = 971,000$ ns.

. The
s of the
insition
depends
insition
d of an
xor, are
carried
pty cell
if the

LETTERS

Low-temperature s and connection to s

James Day¹ & John Beamish¹

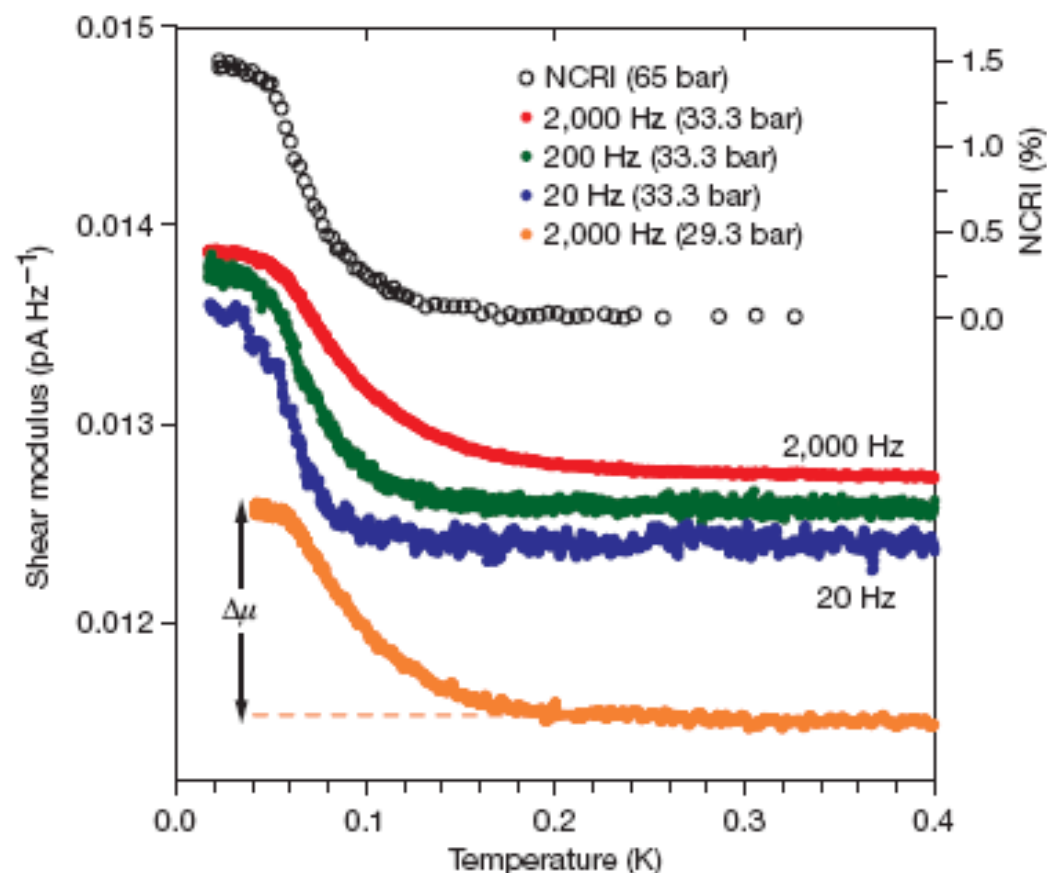


Figure 1 | Shear modulus of solid ^4He at strain $\varepsilon = 2.2 \times 10^{-8}$ as a function of temperature. Shear modulus is given as I/f , where I is the measured current and f is the frequency; data have been offset for clarity. Bottom (orange) curve, μ at 2,000 Hz in a 29.3 bar sample. Middle three curves, μ at 2,000 Hz (red), 200 Hz (green) and 20 Hz (blue) in a 33.3 bar sample. Top curve (open circles, right axes), typical NCRI fraction from a torsional oscillator measurement¹ in a 65 bar sample.

Topological Superconductivity

See http://www.princeton.edu/~psscmp/ss2010/Lecture_Notes_files/Lecture3.pdf

(Charlie Kane)

Cold Atoms and Optical Lattices

BCS-BEC Crossover